NASA Technical Memorandum 58256

(NASA-TM-58256) HIGH ALTITUDE AERODYNAMIC PLATFORM CONCEPT EVALUATION AND PROTOTYPE ENGINE TESTING (NASA) 124 p HC A06/MF A01 CSCL 21E

N84-16182

Unclas
G3/07 11488

High Altitude Aerodynamic Platform Concept Evaluation and Prototype Engine Testing

J. W. Akkerman

January 1984

National Aeronautics and
Space Administration

NASA Technical Memorandum 58256

High Altitude Aerodynamic Platform Concept Evaluation and Prototype Engine Testing

J. W. Akkerman
Lyndon B. Johnson Space Center
Houston, Texas

January 1984

CONTENTS

TABLES

FIGURES

ABSTRACT

A design concept has been developed for maintaining a 150-pound payload at 60,000 feet altitude for about 50 hours. A 600-pound liftoff weight aerodynamic vehicle is used operating at speeds just sufficient to overcome prevailing winds and powered by a turbocharged four-stroke-cycle gasoline-fueled engine. Endurance of 100 hours or more appears to be feasible with hydrogen fuel and a lighter payload.

A prototype engine has been tested to 40,000 feet simulated altitude. Mismatch of the engine and the turbocharger system flow and problems with fuel/air mixture ratio control characteristics prohibited operation beyond 40,000 feet. But the concept could reasonably be developed to function as analytically predicted.

INTRODUCTION

High altitude flight continues to be of increasing interest among both civilian and military organizations. Most high altitude vehicles have been developed for the purpose of transportation. Also, there are needs for high altitude surveillance, communications relays, and certain scientific applications including atmospheric monitoring and earth resources. These later needs have been met for the most part with transportation vehicles. Rockets and balloons have been used in some cases.

Studies at NASA Edwards Flight Research Center in the mid-1970's indicated that the technology in low-speed airfoils and lightweight structures could be used to fly at extremely high altitudes and at relatively low speeds. This technology has the potential of satisfying many of the high-altitude flight requirements at relatively low cost. It offers a combination of high altitude capability and maneuverability not available in transportation vehicles and reusability not feasible with balloons or rockets.

Previous work at JSC has supported a vehicle conceived at the Dryden Flight Research Center (DFRC) to take high altitude air samples (Mini Sniffer) (ref. 1). This vehicle supported a short-term mission and used a non-air-breathing engine. More recent applications are aimed at long-term operation supporting a communication relay station.

Various concepts have been proposed of airplanes and balloons in combination with solar cells/batteries, remote microwave power, fuel cells, solar cells/regenerative fuel cells, piston engine with various fuels, etc. Studies have indicated that all of these are technically feasiblle with varying requirements for system development and operational characteristics.

The central issue at this point is the cost of the concept, both in the development phase and its potential low cost in the operational phase. The solar concept (ref. 2), whether applied to a balloon or an airplane, awaits the evolution of low-cost solar cells before it can become economically viable. Also, for any significant duration, it will require development of an energy storage system for nighttime operations. The microwave-energy-powered balloon or airplane (ref. 3) will require the further development of a microwave power transmission system and an antenna which is steerable to the degree required.

Its operational cost would be strongly influenced by the efficiency of the energy transfer system as well as its capital cost.

A primary issue is on-station flight duration. Some candidate concepts could conceivably fly indefinitely (microwave) and, therefore, minimize the handling costs and hazards involved with frequent flight up and down through low altitudes. However, ground turnaround operations and associated equipment will still be necessary and will have to be accounted for.

An aircraft system, using two or three vehicles, could maintain a continuous service with the convenience of easy access for maintenance of the vehicle and the payload system (fig. 1). "On-station" redundancy could be maintained. The issue of low-altitude flight of this airplane could be managed with a variable geometry wing, using a low performance/high strength configuration through the turbulent atmosphere, and the high performance/lower strength configuration on-station at high altitude. Studies at JSC have focused on this approach.

The author wishes to acknowledge and thank Dr. Kraft for his decision to fund this activity. Also, the many individuals throughout JSC are to be commended for their support during the testing, analysis, and data reduction. The patience of management personnel in supporting an activity so far removed from the areas of responsibility and expertise in which they are officially involved is acknowledged.

CONCEPT ANALYSIS

The configuration concept in figures 2, 3, and 4 show the basis of the work reported herein. The concept has a wing which potentially folds to form a triangular truss to provide a higher strength configuration during low-level flights. At about 40,000 feet altitude or above, where gust loads are reduced, a winch system deploys the wing into the fully extended position for efficient operation during the on-station cruise part of the flight mission. Figure 4 (HAAP 3) is for a fixed wing version for concept evaluation. The concept was presented in November 1979 at a workshop session held at Langley Research Center (LRC). Since then, LRC personnel have verified the estimates of structural weight and aerodynamic efficiency (ref. 4). They have suggested the addition of a controllable flap on the trailing edge of the outboard wing section to provide lift in the folded configuration. Recent JSC studies have focused on the system engineering aspects to understand better what the primary cost drivers are. Table 1 shows design features for each of four variations of the baseline vehicle, plus a configuration conceived by Dr. Paul McCready. The preliminary cost sensitivity results are shown in table 2. The sensitivity study (appendix A) was performed using a computer to calculate performance and total program costs. As shown in table 1, a baseline has been established which is in the middle of the range of estimates of performance for the primary elements -- engine, propeller, structure, and aerodynamics. This baseline was then changed by 10 percent for each of the variables to assess their effects on the life cycle costs. The results are shown in figure 5. As one might expect, aerodynamic efficiency and weight are the major drivers. Also, the analysis predictably shows that lower operational altitudes are less expensive, within wind limitations and communications requirements.

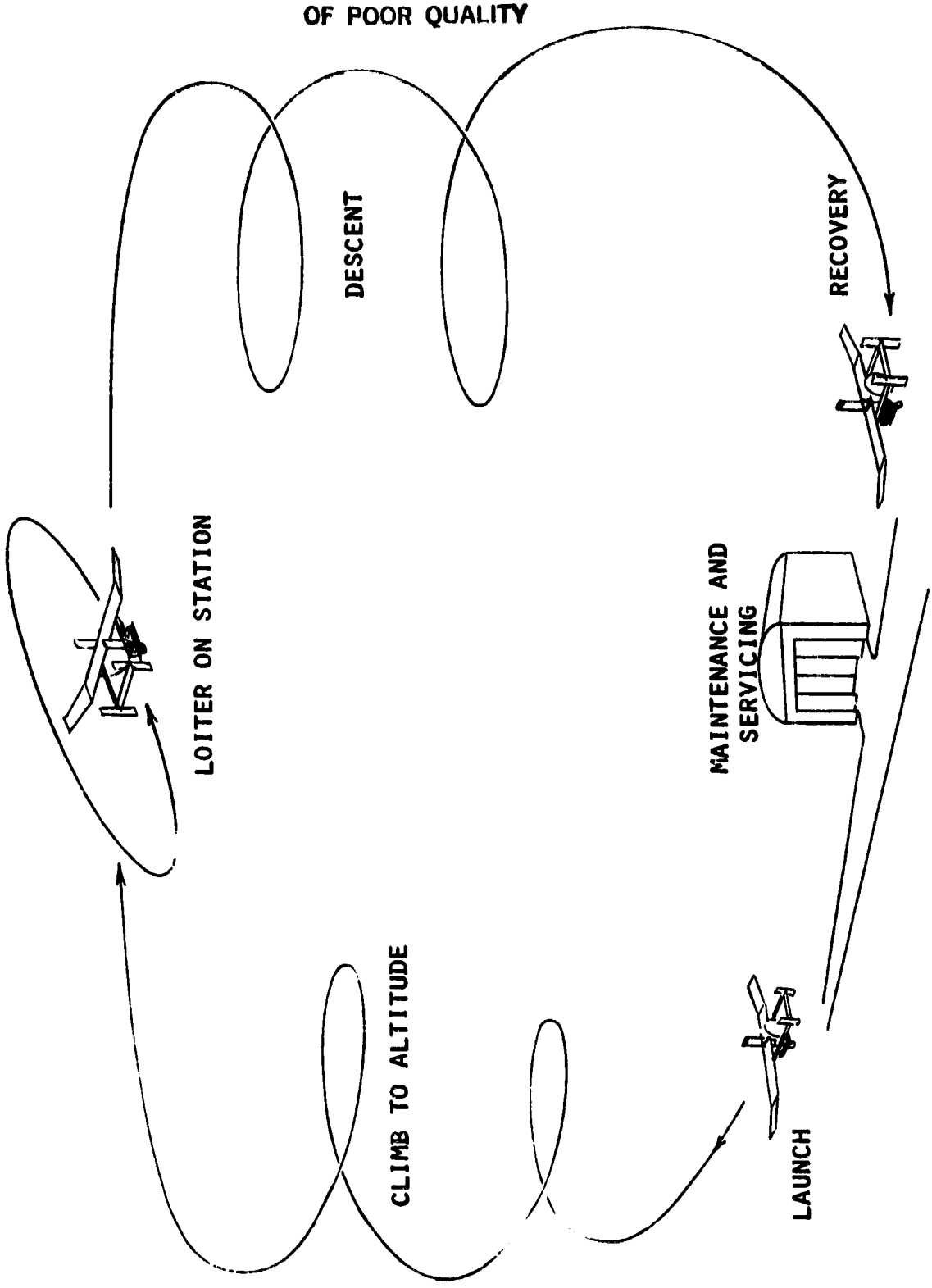

Figure 1. - Operational concept.

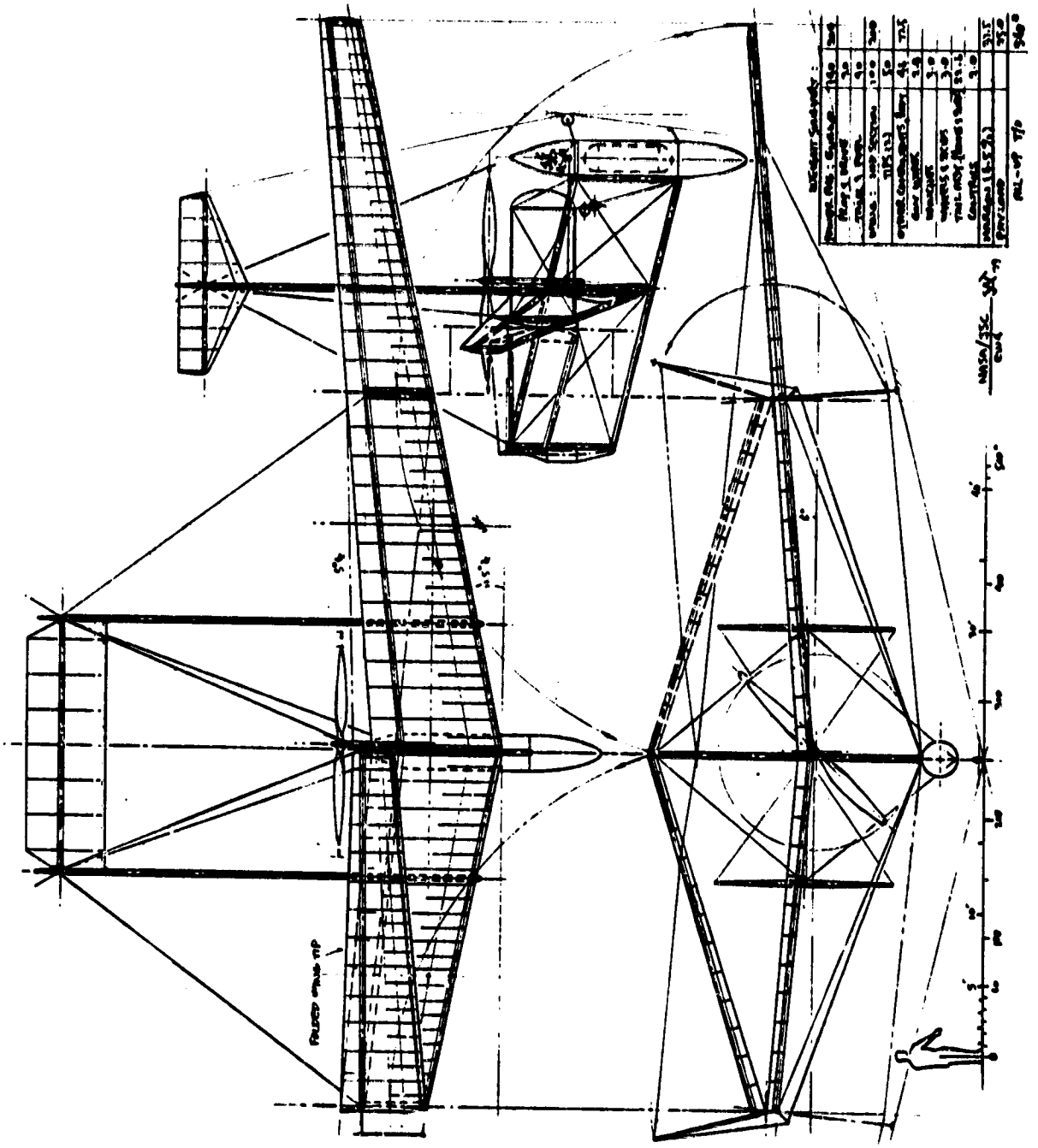

Figure 2.- Early vehicle concept.

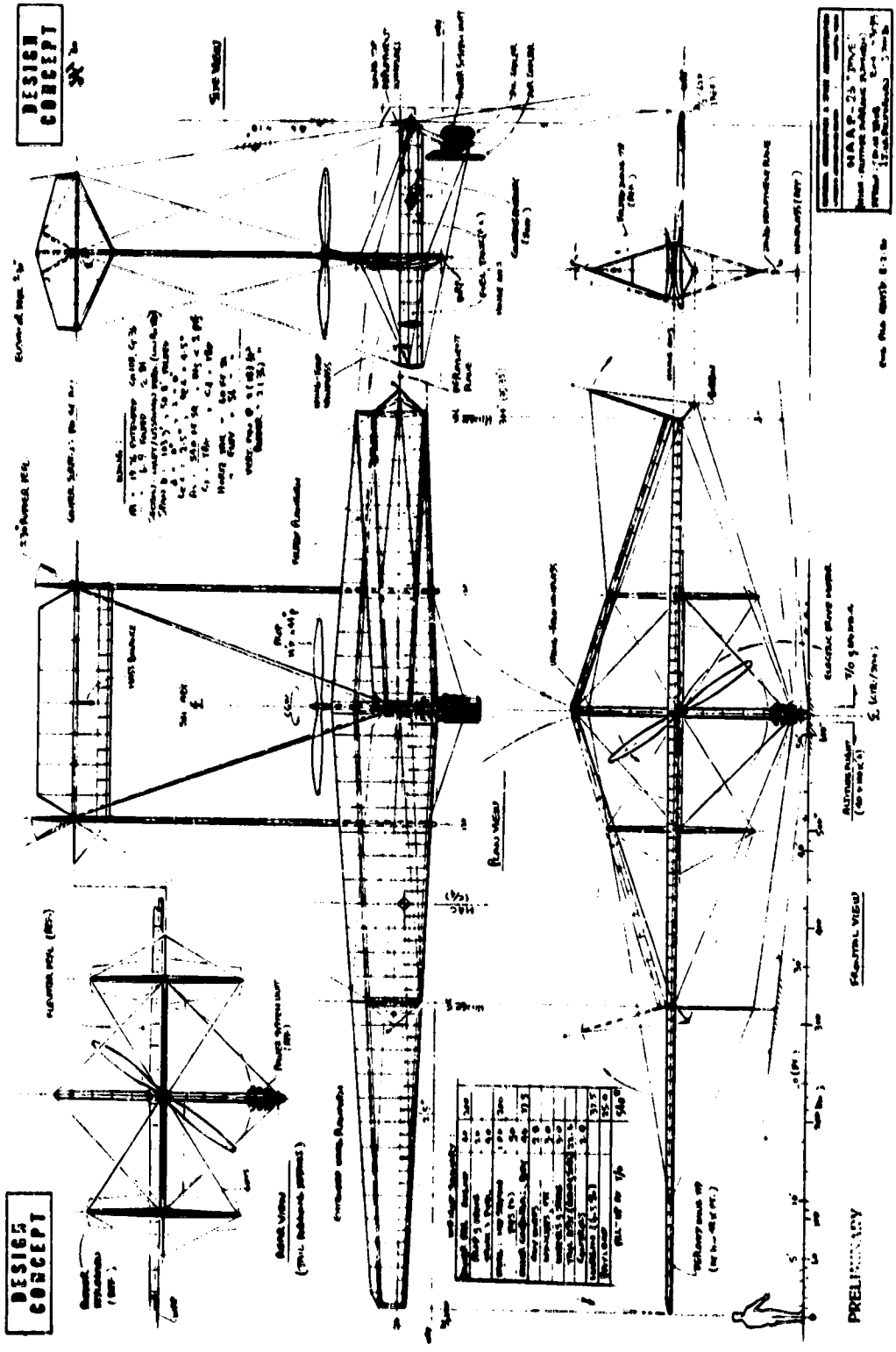

Figure 3 - Vehicle concept 2.

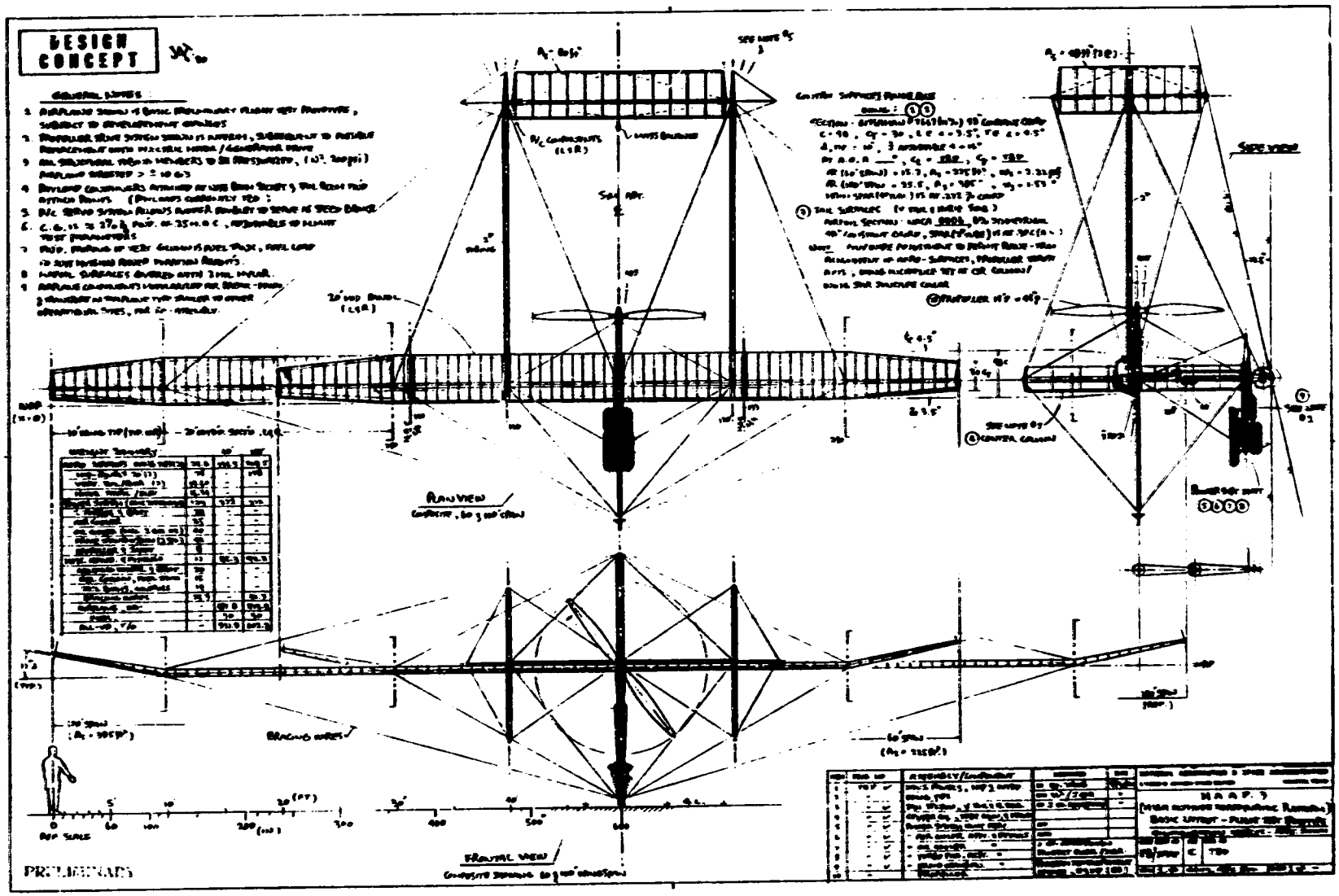

Figure 4.- Vehicle concept HAAP3.

TABLE 1. - DESIGN FEATURES

Parameter	Worst	Baseline	Best	Military	McCready
Fuel cost, dol/lb	.20	.20	.20	5.00 (H2)	.20
Fuel weight, lb	81	150	350	110 (TX+H2)	36
Payload weight, lb	81	150	350	5	1
Total weight, lb	540	775	1400	300	237
Cruise power, hp	11	15	17.5	20 (20 KPT)	11
Cruise altitude, ft. . . .	60,000	60,000	60,000	90,000	60,000
Wing area, ft^2	540	540	540	540	260
Clift-cruise	.8	1.0	1.3	1.3	1.0
L/D	15	20	25	25	25
η Propeller	.7	.8	.85	.85	.75
η Drive	.85	.9	.96	.96	.9
S.F.C., lb/hp hr	.360	.394	.45	.14 (H2)	.36
Climb time, hr	7.04	2.40	5.06	1.39	.787
Cruise time, hr	12.66	34.72	49.06	174.52	34.78
Operating costs, dollars. .	200	150	100	250	150
Facility cost, dol/hr . . .	.30	.25	.20	.25	.25
Overhead factor	2.5	2.0	1.5	2.0	2.0
Life on-station, percent. .	40	50	80	50	-
Vehicle life, yr	4	5	6	5	-
Cost effectiveness, dol/hr	.6685	.1029	.0206	2.80	-

TABLE 2. - LIFE CYCLE COSTS

[Dollar Value of 10% Parameter Design Improvement of One Base Vehicle Lifetime]

Parameter	Delta, 10 percent	Vehicle lifetime cost savings (compared to "baseline")
Lift coefficient	+0.1	$31,229.00
Cruise altitude	-6,000 ft	29,585.00
Vehicle empty weight	-54 lb	27,942.00
Fuel specific energy	+1,800 BTU/lb fuel	25,311.00
Specific fuel consumption	0.04 lb fuel/hp-hr	23,011.00
Drag coefficient	-0.005	21,367.00
Propeller efficiency	+8%	21,367.00
Operations cost	-$15.00/flight	18,737.00
Wing area	: 54 ft^2	9,862.00
Fuel cost	$.02/lb-fuel	3,287.00
Climb horsepower	+2.1 hp	3,287.00

Basic Vehicle Cost - $50,000.00
Vehicle Life: 5 Years, 20,000 Hrs -Operation
Total Operations Cost: $86,900
Total Lifetime Cost: $308,700.00

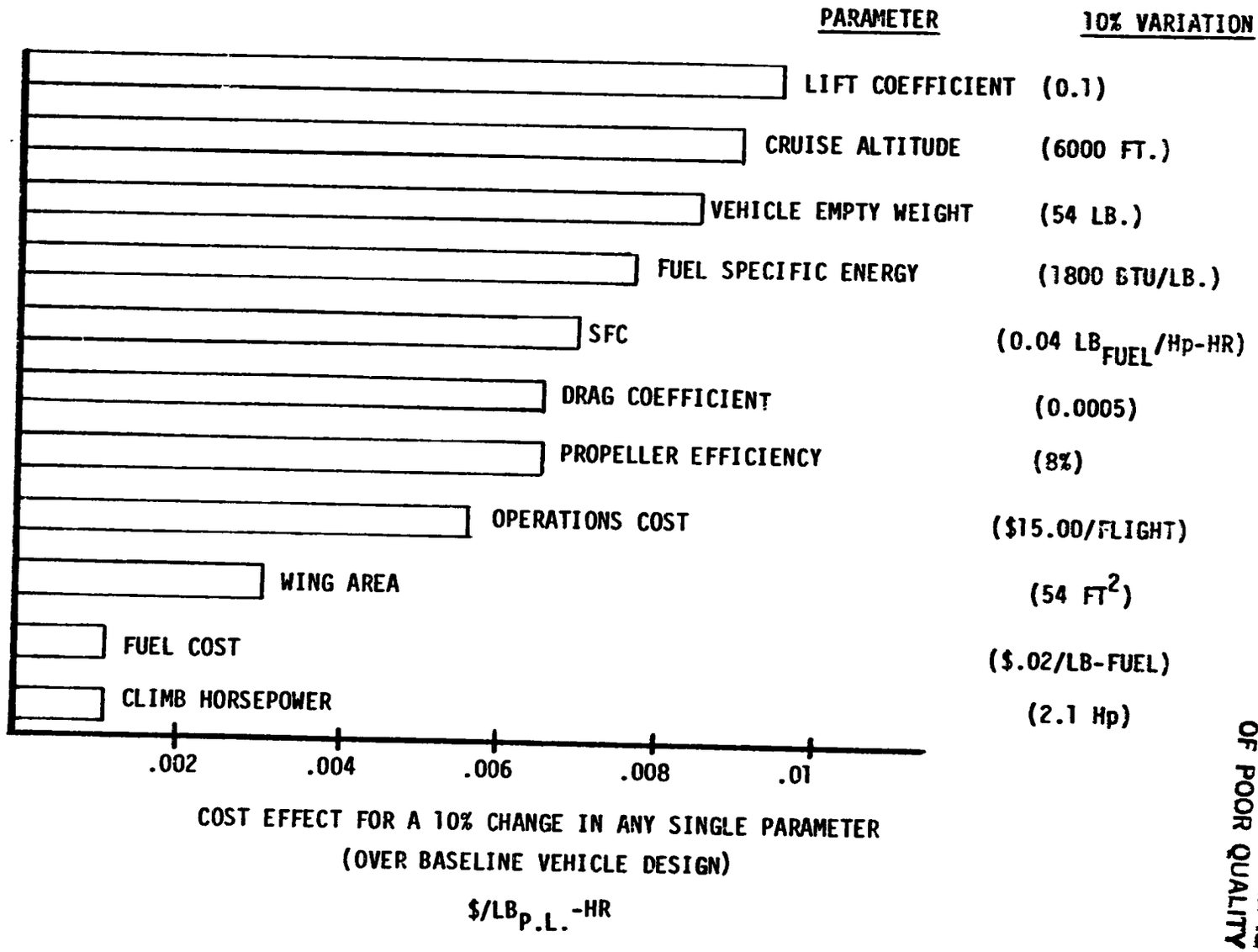

Figure 5. - Cost sensitivity.

Studies of winds aloft (ref. 5) indicate that the choice of an operational altitude is strongly influenced by winds. The results are shown graphically in figure 6. Since the forward speed required is a major influence on power and energy required, there will be an advantage in operating at the altitude of "minimum wind," which varies with season and latitude. It might prove cost-effective to operate with different aerodynamic configurations during different times of the year. All our studies have been based upon the assessment of operations at 60,000 feet. However, operational costs would be lower if the altitude could be reduced. Work should continue to improve the math model and further refine the concept.

There are, however, definite limitations to the analysis. Specifically, there is presently a serious shortage of aerodynamic performance data on vehicles operating at low velocity at very high altitudes. These data will likely not become available in the near future because of the lack of facilities for this kind of testing. Another source of potential uncertainty is in weight estimating. The accuracy to which weights can be predicted varies with the accuracy to which loads are known. In vehicles of the type involved here, where structural flexibility will interplay with the aerodynamic loads, prediction by analysis is difficult.

These issues, along with the relatively low cost of the vehicle involved, indicate that the best progress might be made by moving from the purely analytical approach for vehicle design into hardware testing in a real operational environment. Early vehicles could use the payload capacity for data-gathering on well instrumented, lightly loaded vehicles. Each flight could serve to further optimize the vehicle and its operations, leading to an early definition of an operational configuration. Seemingly minor improvements can result in significantly lower costs as shown in the sensitivity cost delta estimates in table 2. This kind of payoff could justify a fairly rigorous effort for vehicle optimization even with a limited projected fleet size.

Because of this and the fact that an early demonstration seems important to some potential users, a flight test program probably should be the next step. A review of potential flight test vehicles indicates that McCready's solar powered airplane (see fig. 7) is suitable, within certain limitations, and could have early availability. It is a lightweight vehicle with low power requirements. The only serious compromise when compared to the "baseline" vehicle design is its frailty due to its fixed wing. Test operations would have to be limited to fair weather. Dryden Flight Research Center (DFRC) is in the process of constructing a similar vehicle, but metal is being used instead of the lightweight plastics. This vehicle is also a good candidate for demonstration tests. Some lightweight sailplanes would also be acceptable. Any of these vehicles can potentially be used to test any or all of the presently envisioned power systems -- solar cell/battery, microwave, and piston engine. Also, any of these power system alternatives can be configured to provide power for an electric drive propeller.

Early flight tests for evaluation of aerodynamics could be balloon-lofted and released for simple glide testing, with the later addition of batteries and a motor to extend the test time and raise the structural loads to operational levels. As candidate power systems become available, they could be added to extend the flight time and/or increase the payload carrying capacity. A test system of this type should provide adequate concept verification and

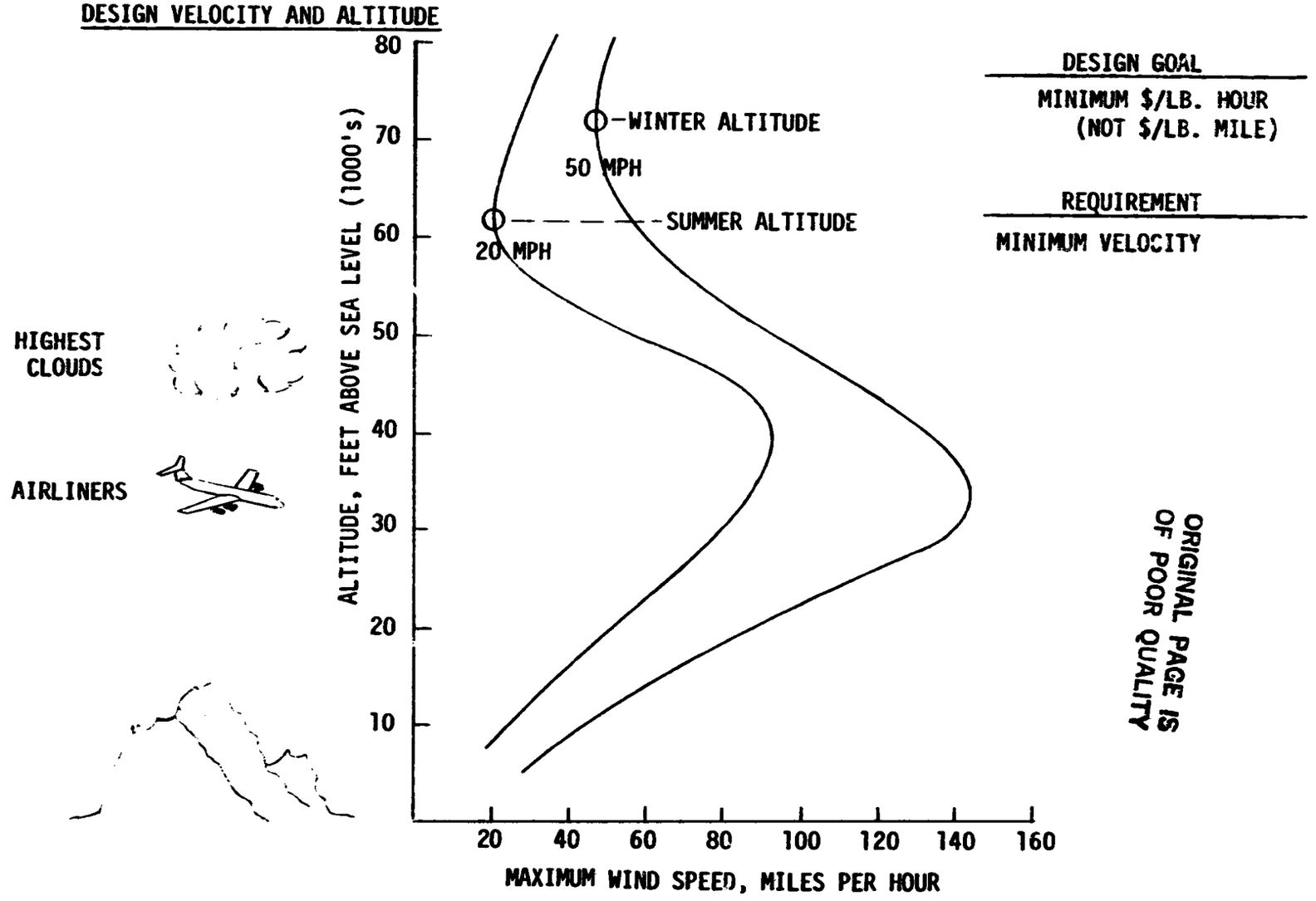

Figure 6.- Winds at altitude.

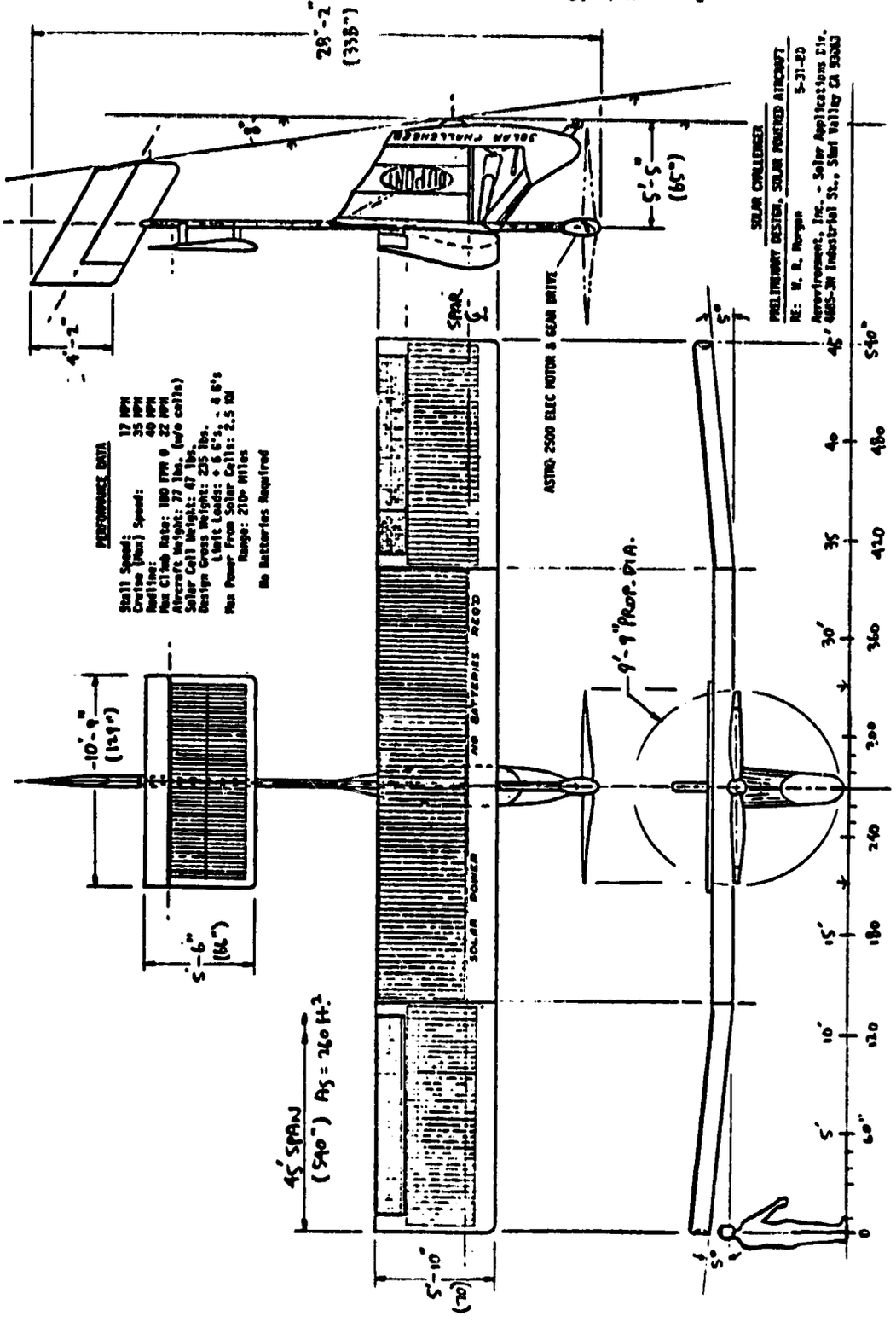

Figure 7.- Solar challenger.

demonstration at a relatively low cost. Such a flight test program in a real environment could conceivably provide a high fidelity test of a power system at a much lower cost than a test cell under simulated conditions operating on the ground. The operational handling experience and derived vehicle flight data would be valuable "extra" benefits.

PROTOTYPE POWER SYSTEM DEFINITION

The early design concepts of figure 2 were discussed at the November 1979 meeting at LRC. The power system schematic is shown in figure 8. The early design is shown in figures 9, 10, and 11. The turbocharger assembly is shown in five views in figure 12. The early configuration was tested using a stock OMC model 200 engine and two Schweitzer turbochargers, a model 2LM243 for the first stage and a model S6-200 for the second stage (close to the engine). Both turbochargers used identical turbines, the only difference being the choice of housings for the two units. The housing selection is discussed in the testing section.

These two turbochargers were later changed to use a unit by Rayjay for a first stage and IHI as a second stage with much improved results. Figure 13 shows the original two stage concept schematically along with the instrumentation points.

A second basic configuration was assembled using three stages of turbochargers as shown schematically in figure 14. The all-up engine assembly is shown in figures 15, 16, 17, and 18. Early tests were performed using the stock configuration engine. Later, the cam was modified to give less valve overlap and earlier exhaust valve opening (see fig. 19). The compression ratio was also increased from about 6:1 to 11:1 using a piston cap attachment as shown in figure 20. As discussed in the test section, the final configuration was restricted to operation with reduced manifold pressure to avoid preignition and/or detonation.

The interstage cooling between compressors consists of seven stainless steel tubes of the bellows type flowing in parallel. The material was supplied by the Anaconda Corporation and is normally used inside a braided steel wire cover to provide structural support. In this case, however, the pressure is low enough not to require external support. The first stage compressor discharges into seven 1-inch inside diameter tubes, the second stage into seven 3/4-inch inside diameter tubes, and the third stage into seven 1/2-inch inside diameter tubes. The first stage is cooled by ambient air in the test cell while the other two bundles of seven tubes are covered with a large flex tube and water is circulated between the tubes for cooling. In a flight configuration, the outer shell would be omitted. Inside each of the seven air tubes, in each heat exchanger, a thin strip of stainless steel (.020-inch thick) is twisted about five times per foot. This causes spiral flow in the tubes to promote heat transfer. Four of the spirals in each heat exchanger are left hand and three right hand. The end fittings are fastened and sealed with epoxy. Silicone rubber (RTV) is used to seal the ends onto the turbochargers. Set screws provide mechanical attachment.

The innerconnecting fittings on the exhaust side of the turbocharger serve as structure to hold the turbocharger package together and to serve as

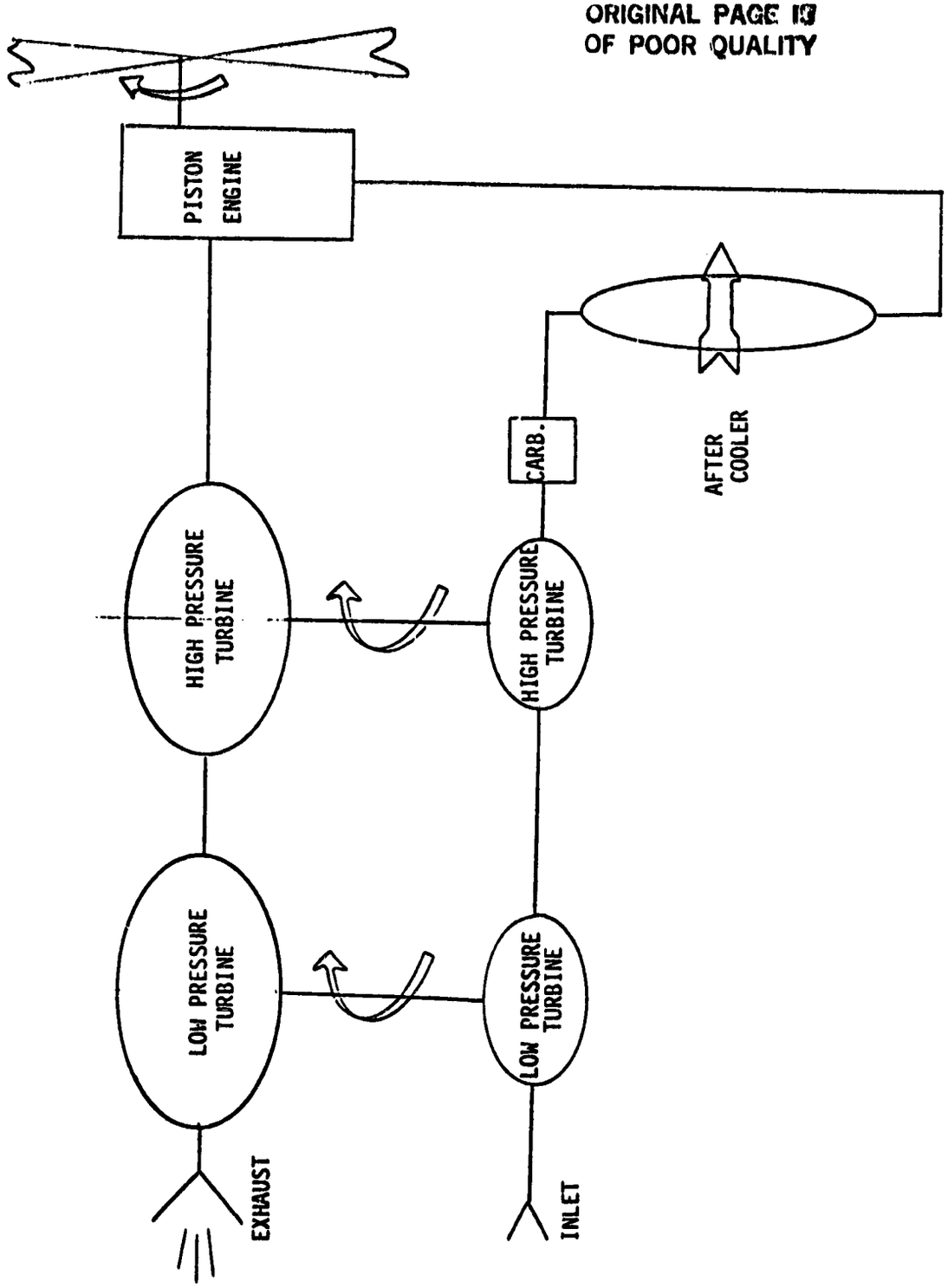

Figure 8.- Original power system schematic.

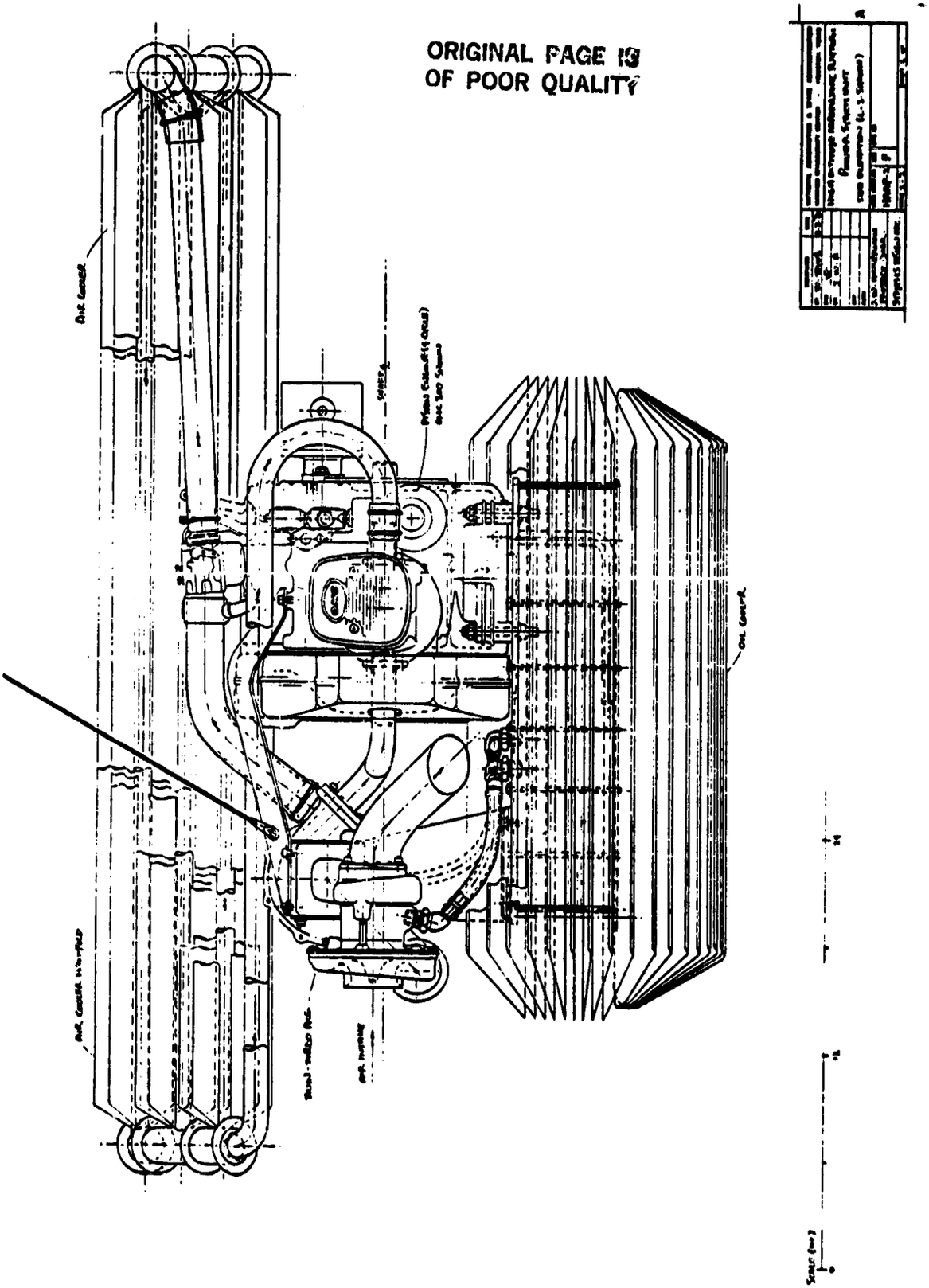

Figure 9.- Engine side view.

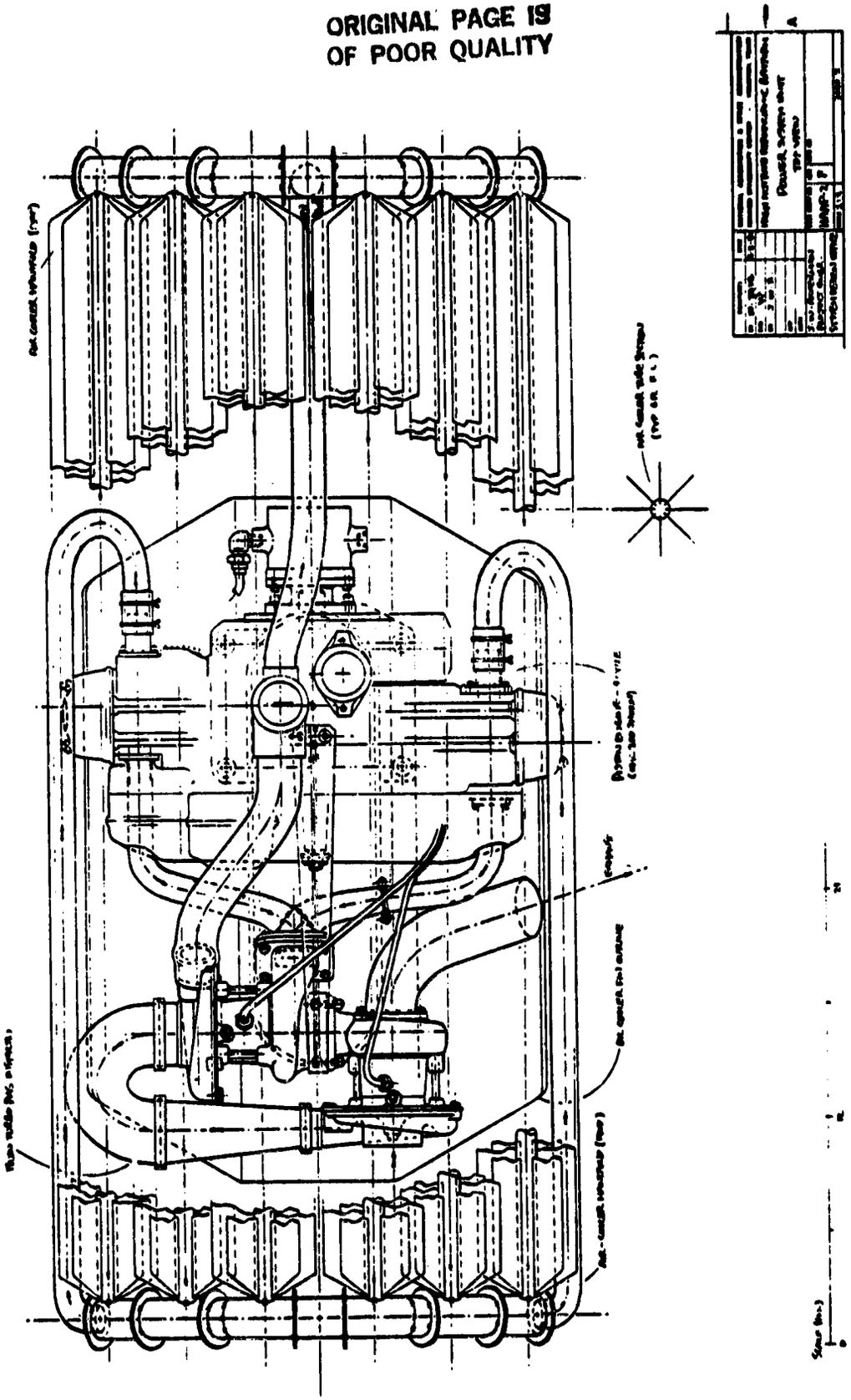

Figure 10. - Engine top view.

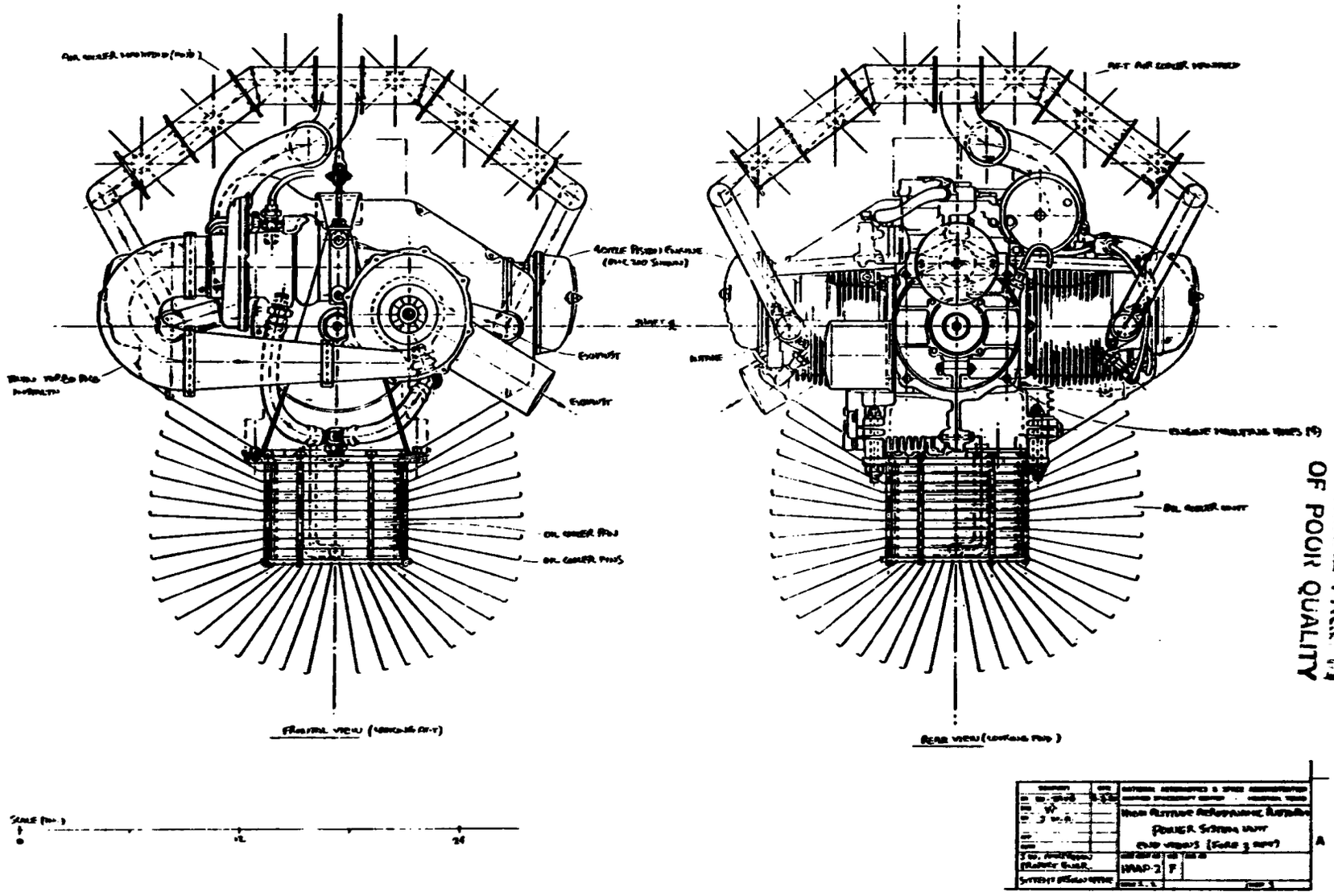

Figure 11.- Engine fore and aft views.

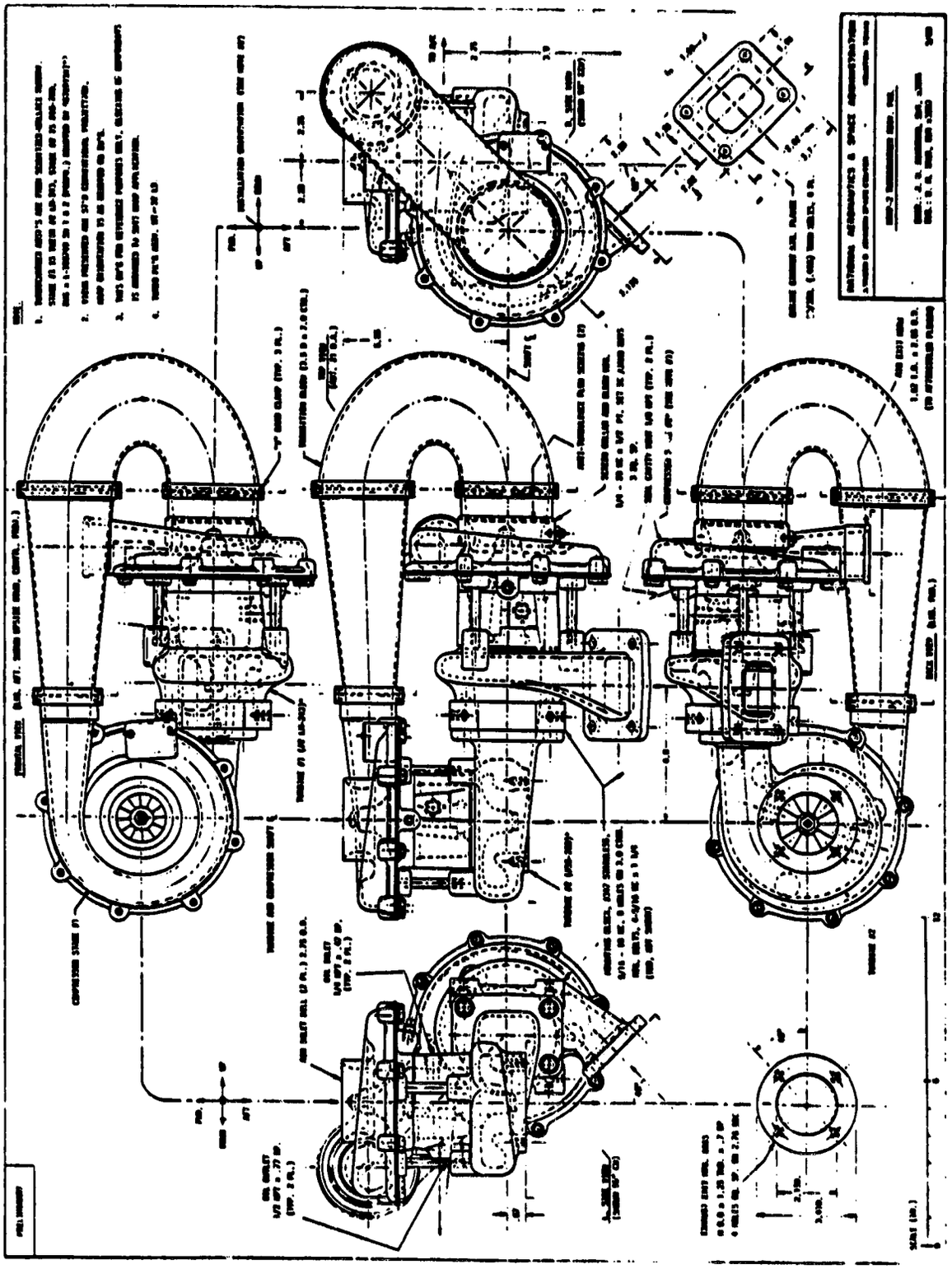

Figure 12.- Turbocharger detail.

HAAP POWER SYSTEM SCHEMATIC

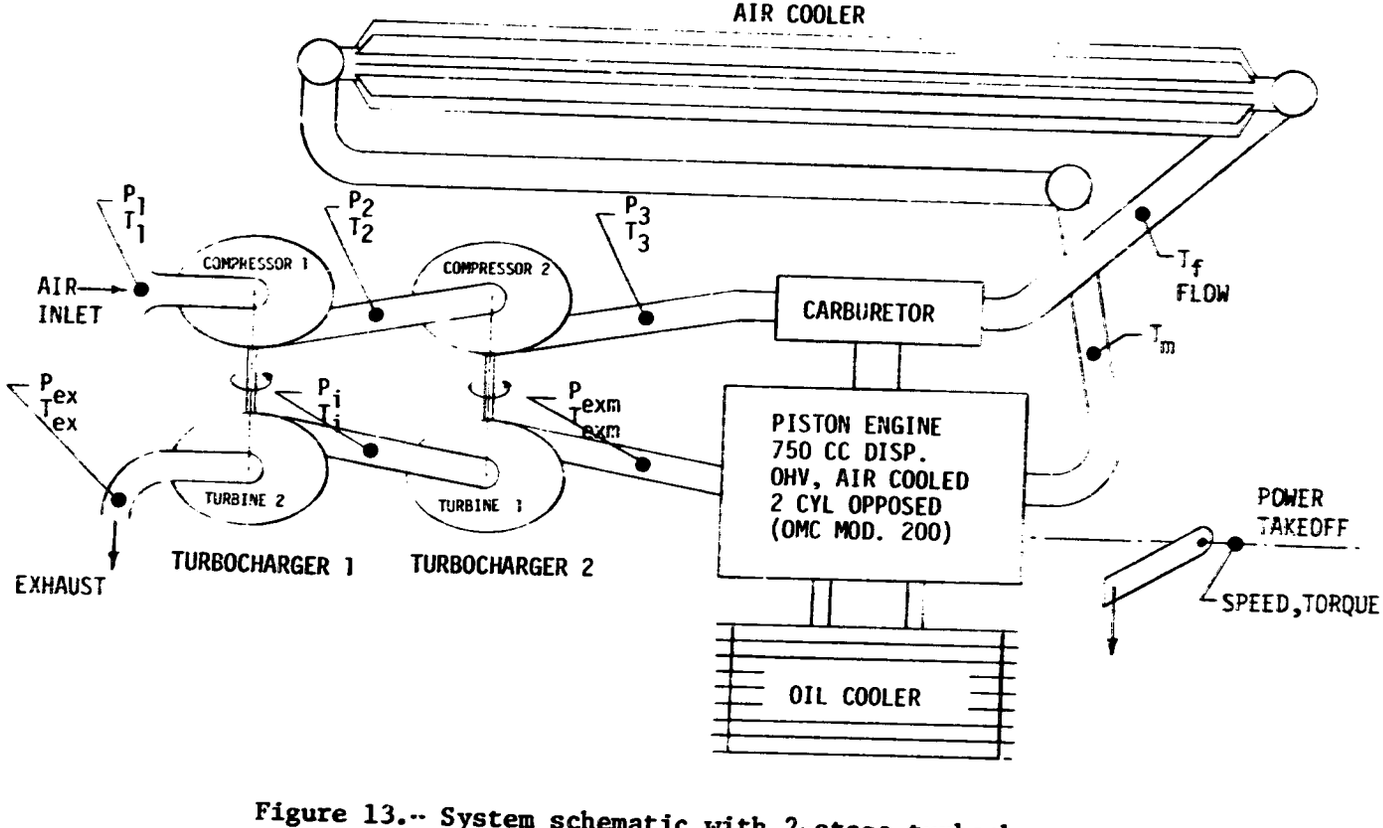

Figure 13.-- System schematic with 2-stage turbocharger

HAAP POWER SYSTEM SCHEMATIC

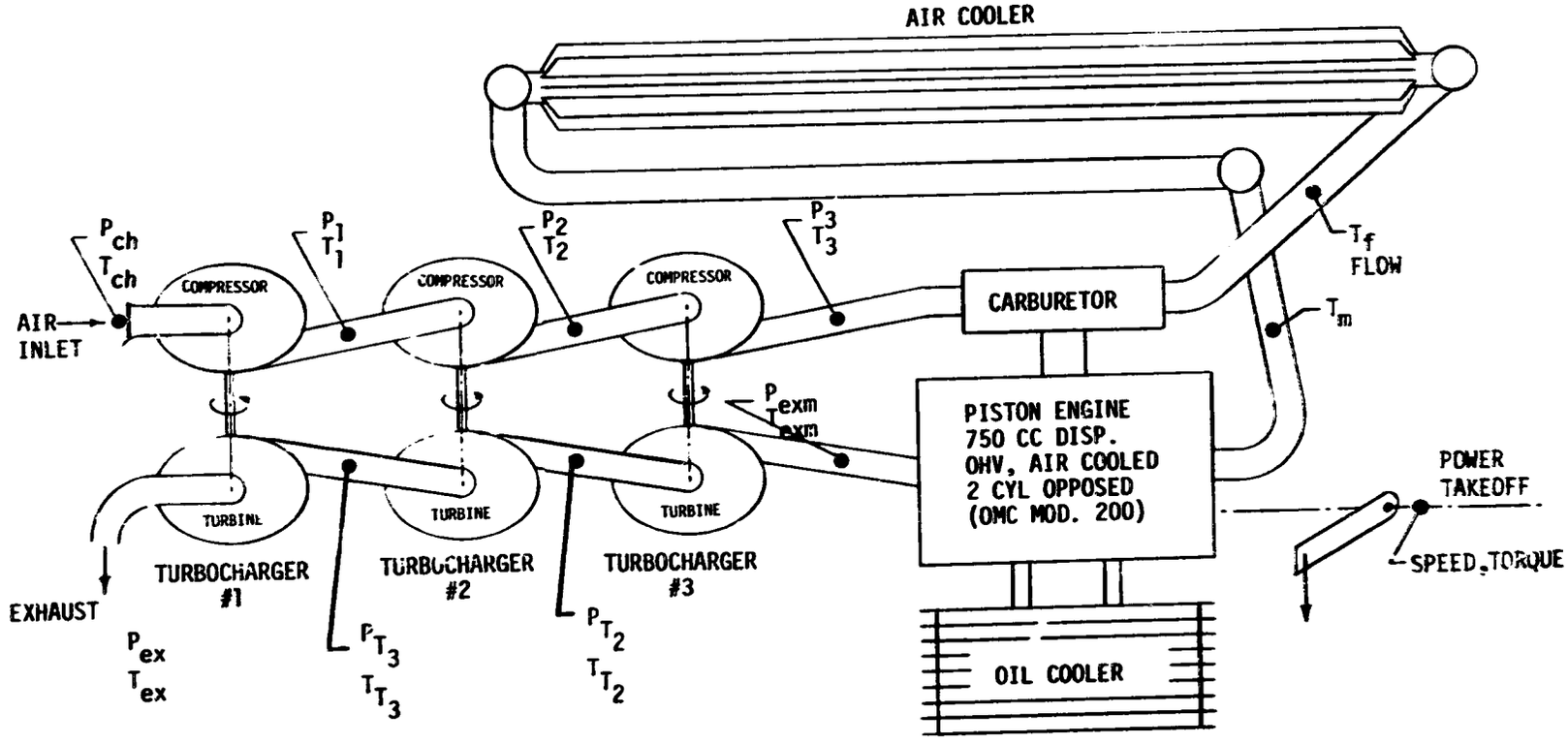

Figure 14.- System schematic with 3-stage turbocharger

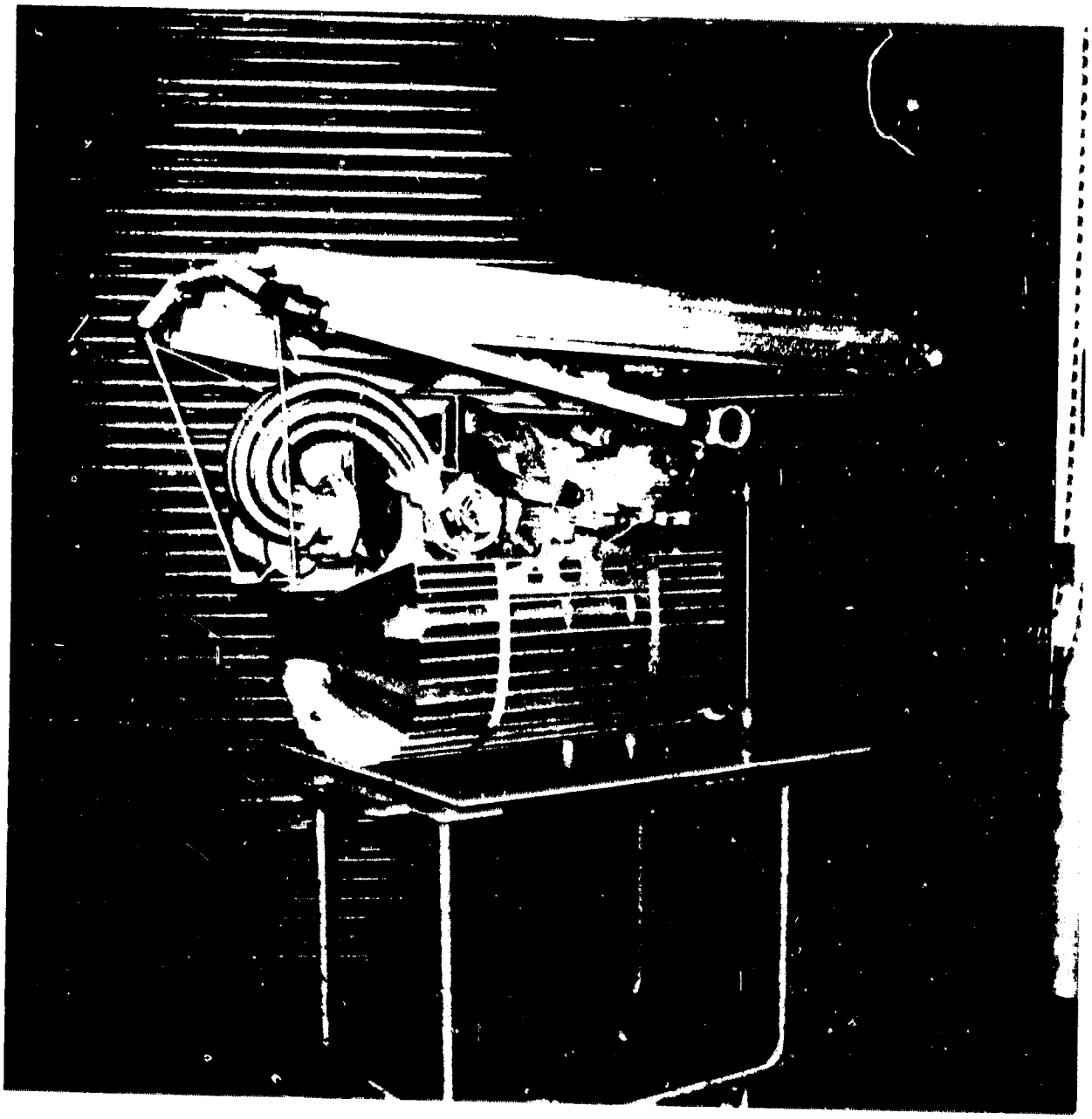

Figure 15. - Engine assembly, front quarter view

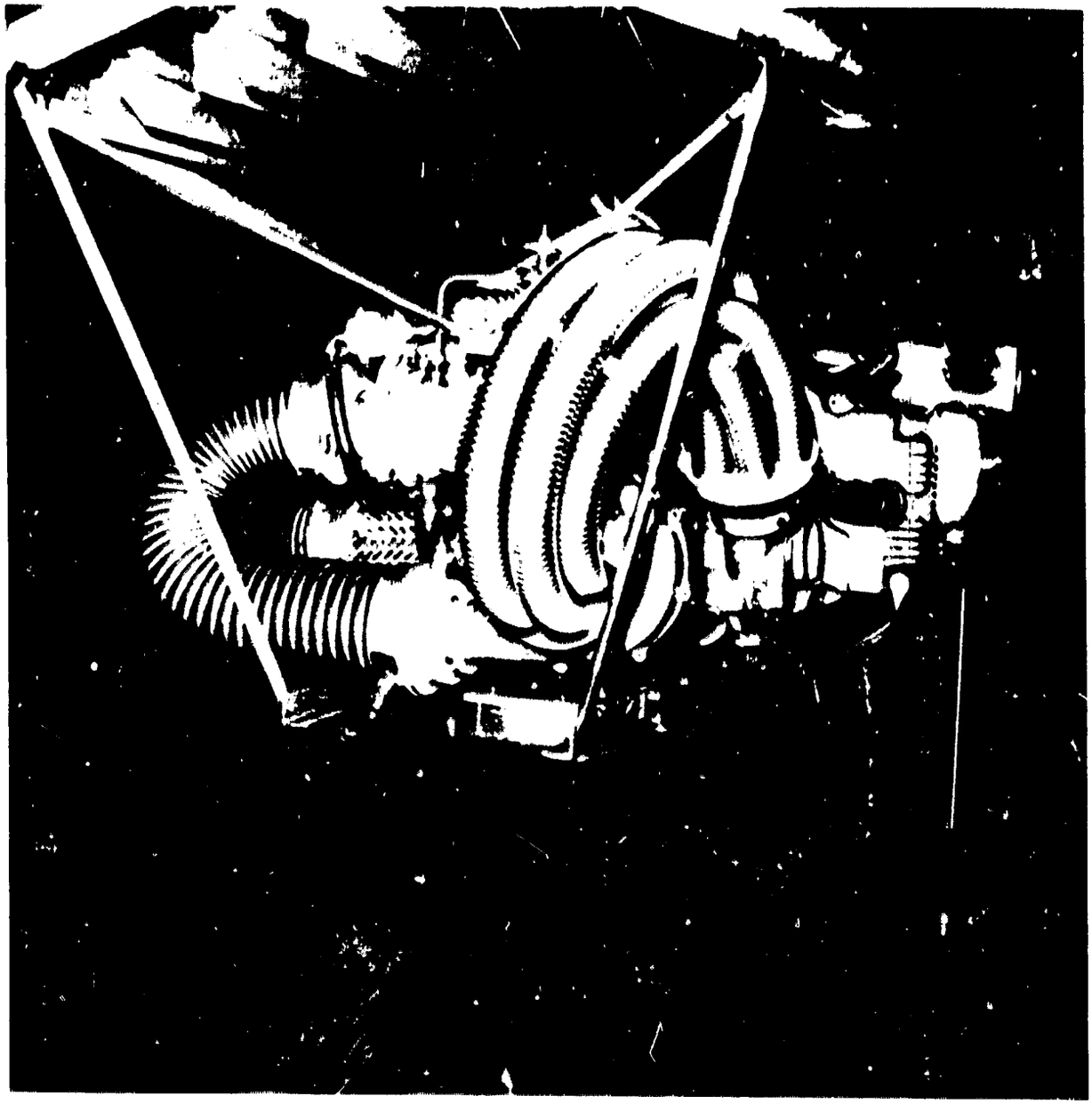

Figure 16. - Engine assembly, front view

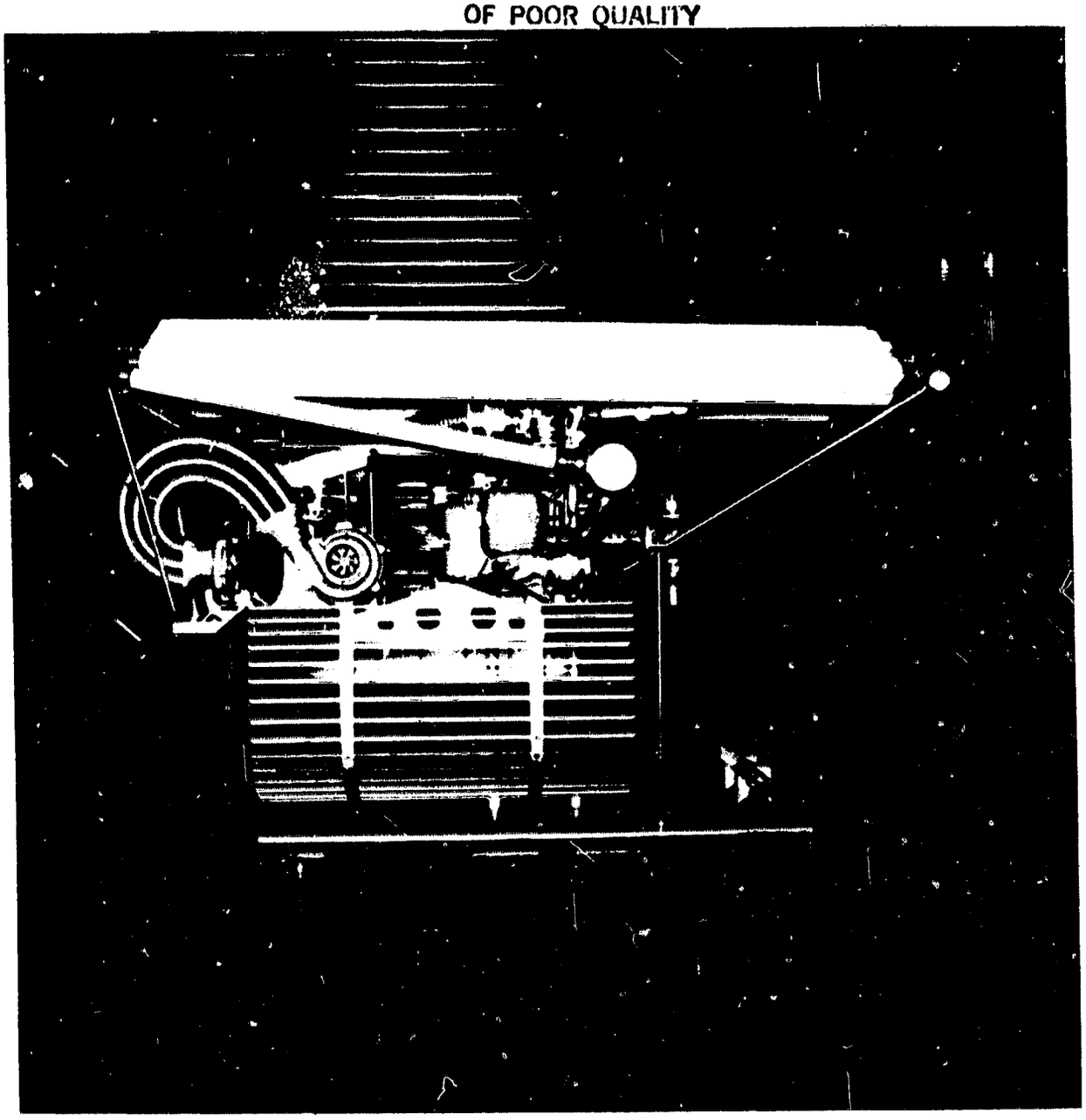

Figure 17. - Engine assembly, right view

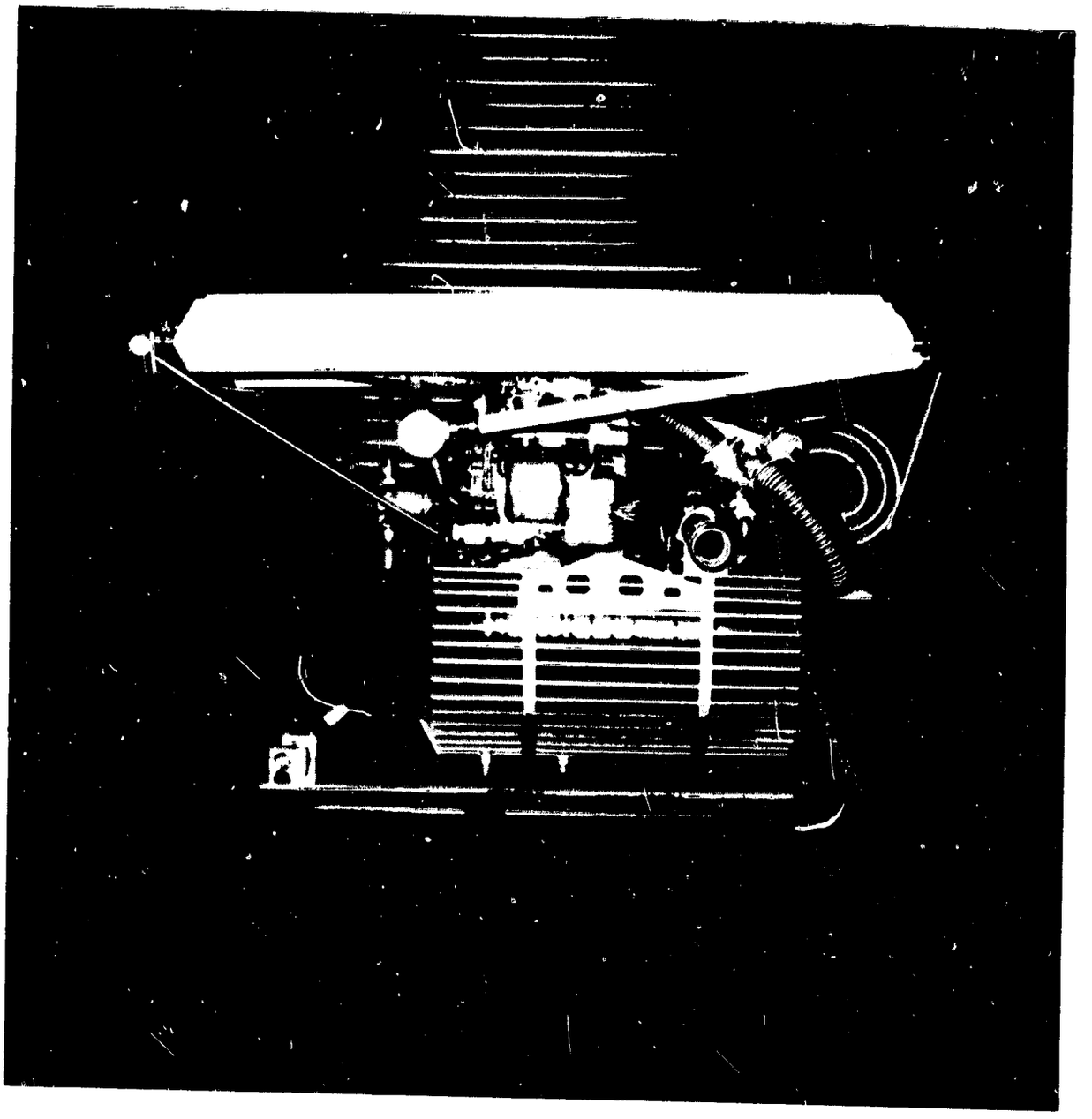

Figure 18. - Engine assembly, left view

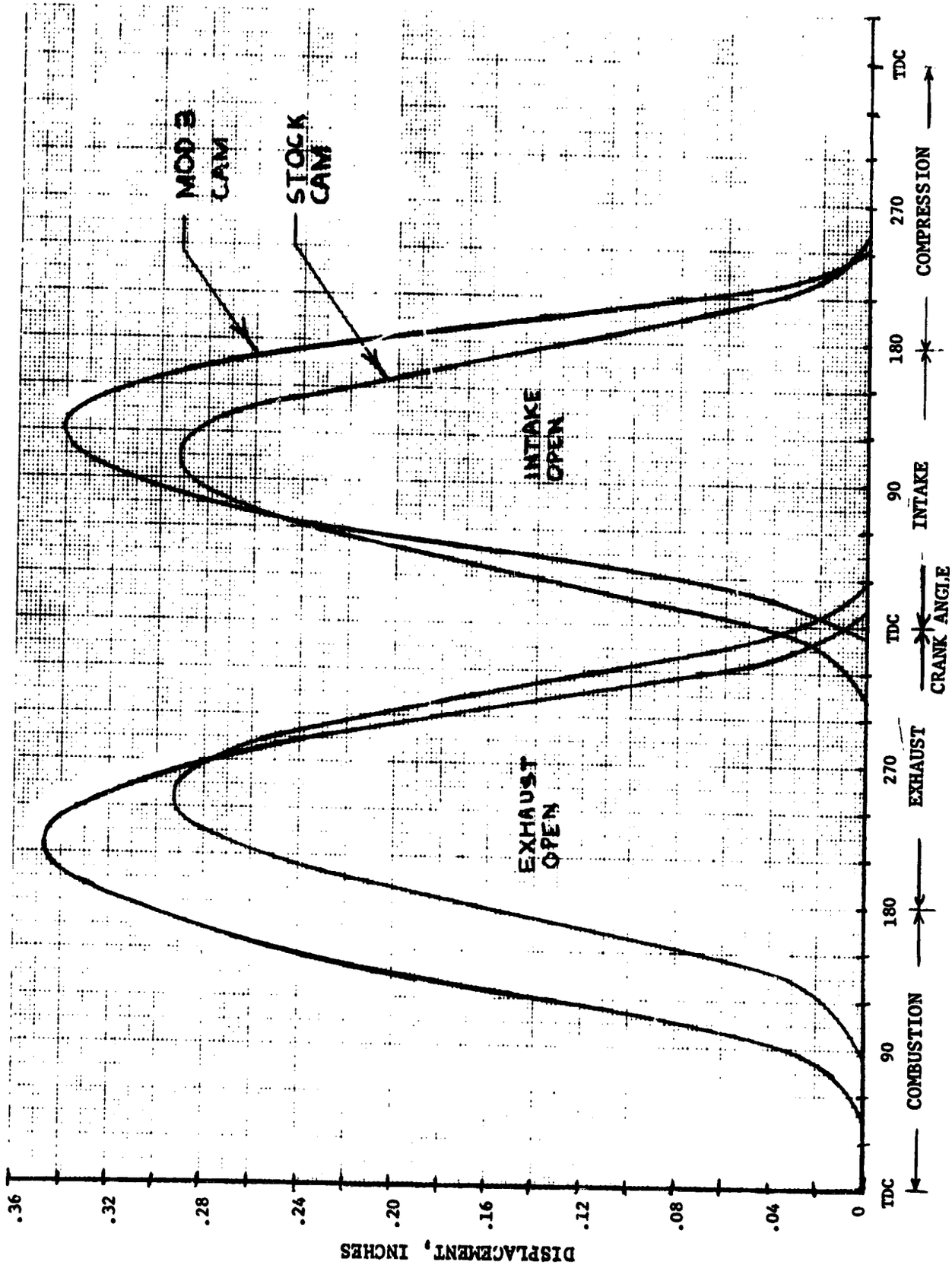

Figure 19.- Stock and modified valve motion.

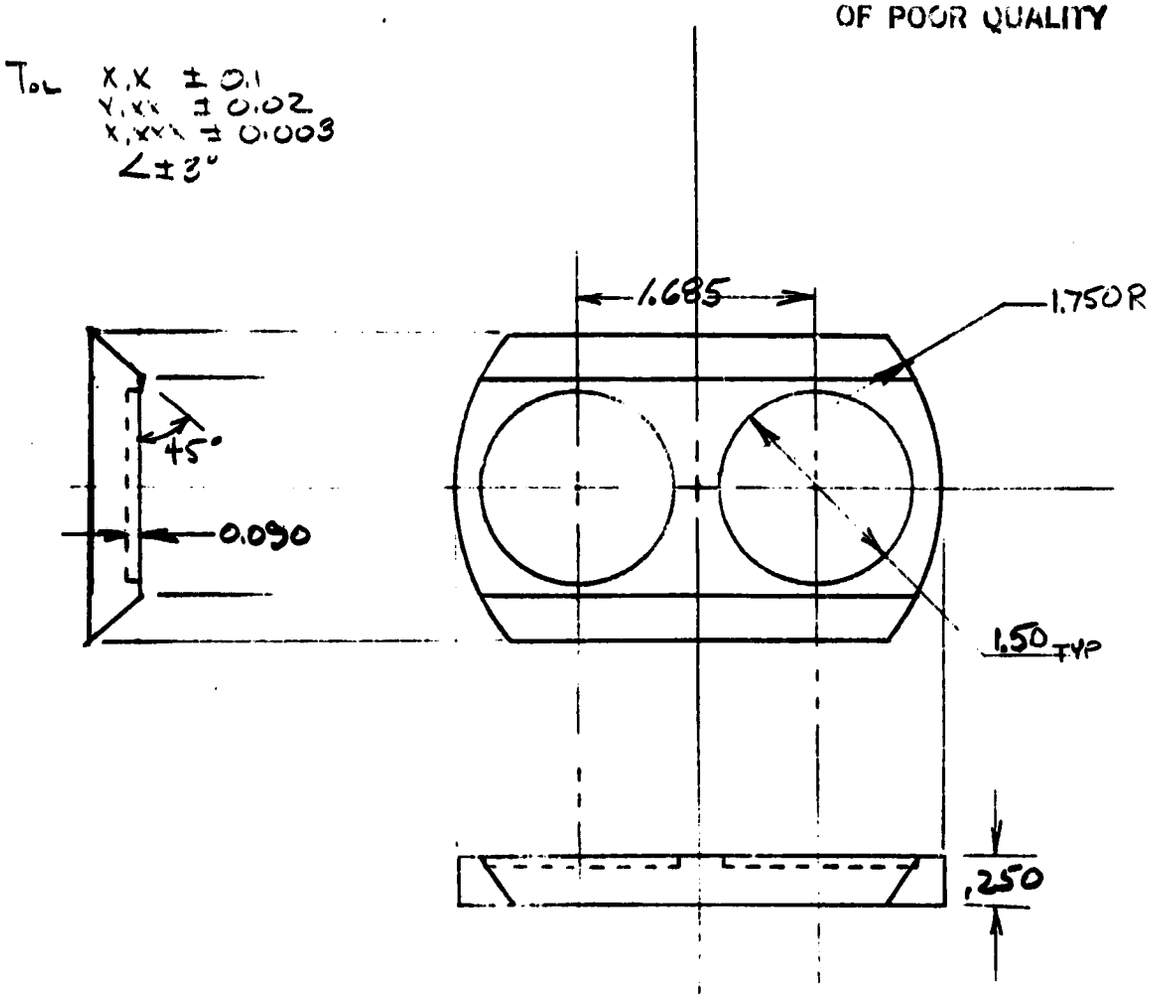

Figure 20.- Piston cap

mounting. In each case, flanges were fabricated for the end connections, then a pipe was fitted to connect the flanges as required.

The air aftercooler is fabricated of heat exchanger tube normally used to vaporize liquid nitrogen. It was chemically etched from .095-inch thickness to .030-inch thickness for weight reduction and to provide more flow area. It has eight external radial fins 2 inches long, eight internal radial fins 1/4 inch long, all on a basic 1-inch tube. The material is 5052 T4 aluminum. Six of these tubes, 5 feet long, are manifolded in parallel. The oil cooler/reservoir is fabricated of ten 0.025-inch thick sheets 2 feet wide and 4 feet long. They are bent to maximize the air spacing and spaced 1/2 inch apart by an O-ring sealed hoop 6 inches wide and 24 inches long. The assembly is clamped together between two 3/8-inch plates with 20 number 10x32 bolts 6 inches long. The oil pickup port for the engine oil pump is ducted to the middle of the bottom of the reservoir with a 3/4 inch by .062-inch wall aluminum tube. The oil returns from the turbochargers, the valve covers and the crankcase vent with 3/4-inch hose to the collector at the center of the top of the reservoir. The crankcase PCV valve is connected to the intake manifold. Later tests used a separate oil supply for the turbochargers and simply pressurized it to the first stage compressor discharge pressure. The crankcase of the engine was left connected to the intake manifold. See the oil circuit schematic, figure 21.

The prototype test system included several variations in mechanical details as will be discussed in the section on results. One major change from the schematic of figure 14 was the relocation of the carburetor to include two carburetors mounted directly on the cylinders. This and the shift to three turbos were the only major changes made. An effort was made to increase the displacement of the engine by increasing the stroke, thereby increasing the engine flow, but little success was achieved because of mechanical problems. No test results of that configuration were recorded. Space limits in the crankcase required a pressed-together assembly, making the modified crankshaft difficult to work on. Some success with camshaft variations caused the emphasis to shift so that the approach involving increased displacement was set aside.

Other variations are mentioned in the section on "Other Observations." The drawings for each of the mechanical details are on file if they are needed.

ENGINE TESTING AND DEVELOPMENT

The testing was divided into three phases: (1) stock engine, (2) stock engine at altitude, and (3) prototype system tests. The results of phases 1 and 2 are shown in figures 22 and 23. Much experience was gained with the engine during these tests. In phase 1, the performance was measured with various ignition timing, lubricating oils, oil additives (molydisulphide), fuels (aircraft and automotive), ignition primary voltage, exhaust configurations, induction system configuration, etc., (tests A, B, C, D, E, and F of appendix A). None of these items affected the performance significantly except the ignition timing. (Nominal changes in the ignition timing consistently degraded the performance slightly.) The reason that the engine is so insensitive is not entirely clear, but is likely the result of a basically efficient mechanical design (as reflected by the insensitivity to lubricant selection) and the low compression ratio. The most curious phenomenon is the relatively good specific fuel consumption in spite of the low compression

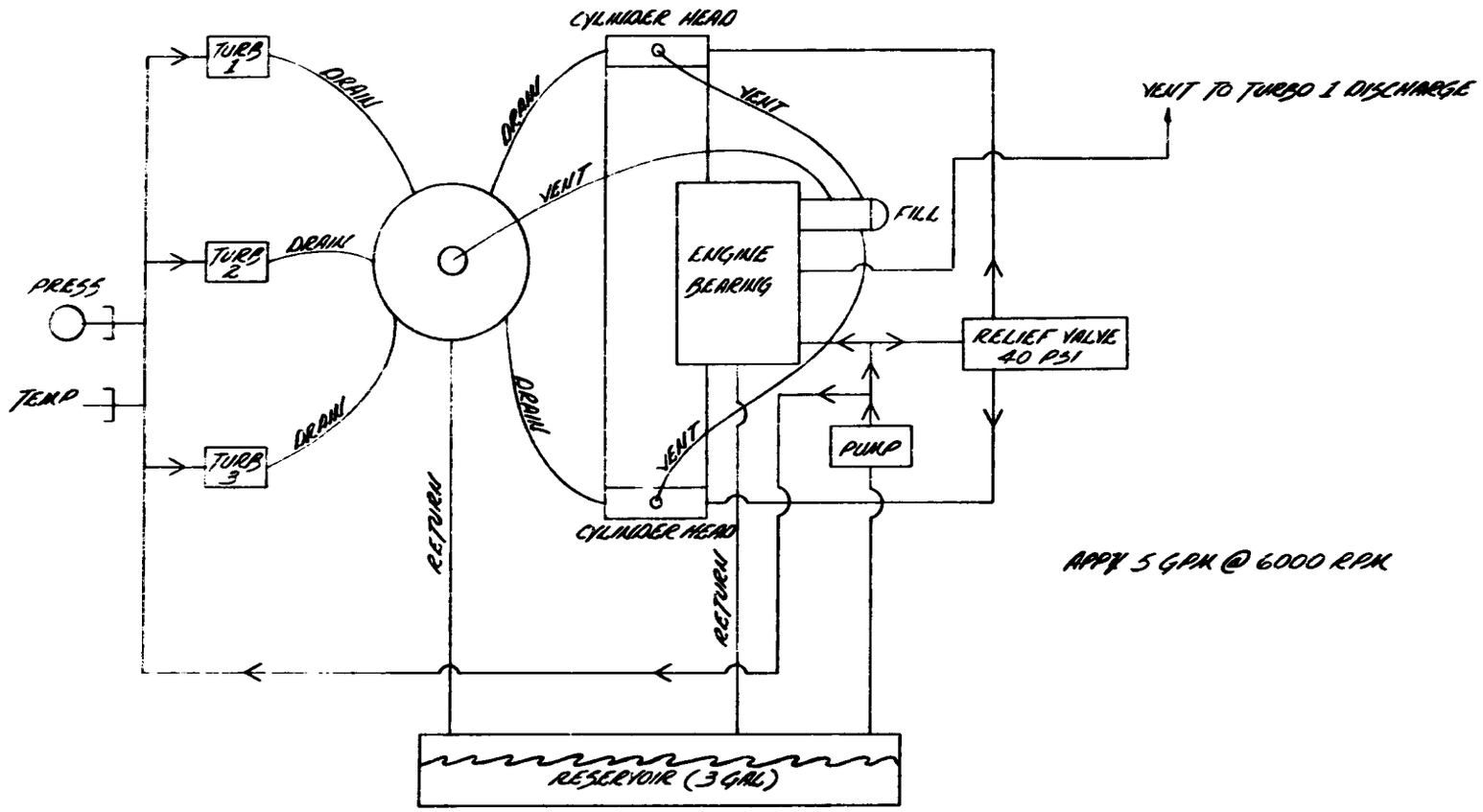

SIGNATURES	DATE	NATIONAL AERONAUTICS AND SPACE ADMINISTRATION
DR H Emanuel	1-4-83	LYNDON B. JOHNSON SPACE CENTER, HOUSTON, TEXAS
ENG		HHAP POWER SYSTEM SCHEMATIC (OIL)
CH		
APP		
AUTH		

CODE IDENT NO	SIZE	DWG NO	
21356	B	352-2013	A
SCALE N/A		SHEET 2 OF 12	

ORIGINAL PAGE IS
OF POOR QUALITY

Figure 21. - Oil circuit schematic.

STOCK OMC MODEL 200 ENGINE (2 CYL. OPP., OHV) - 43.2 CU. IN. DISPL.

- REGULAR GASOLINE FUEL (NO LEAD) 110 PSI COMPRESSION
- 85°F AMBIENT TEMP. - SEA LEVEL 7° BTDC IGN. TIMING (STATIC)

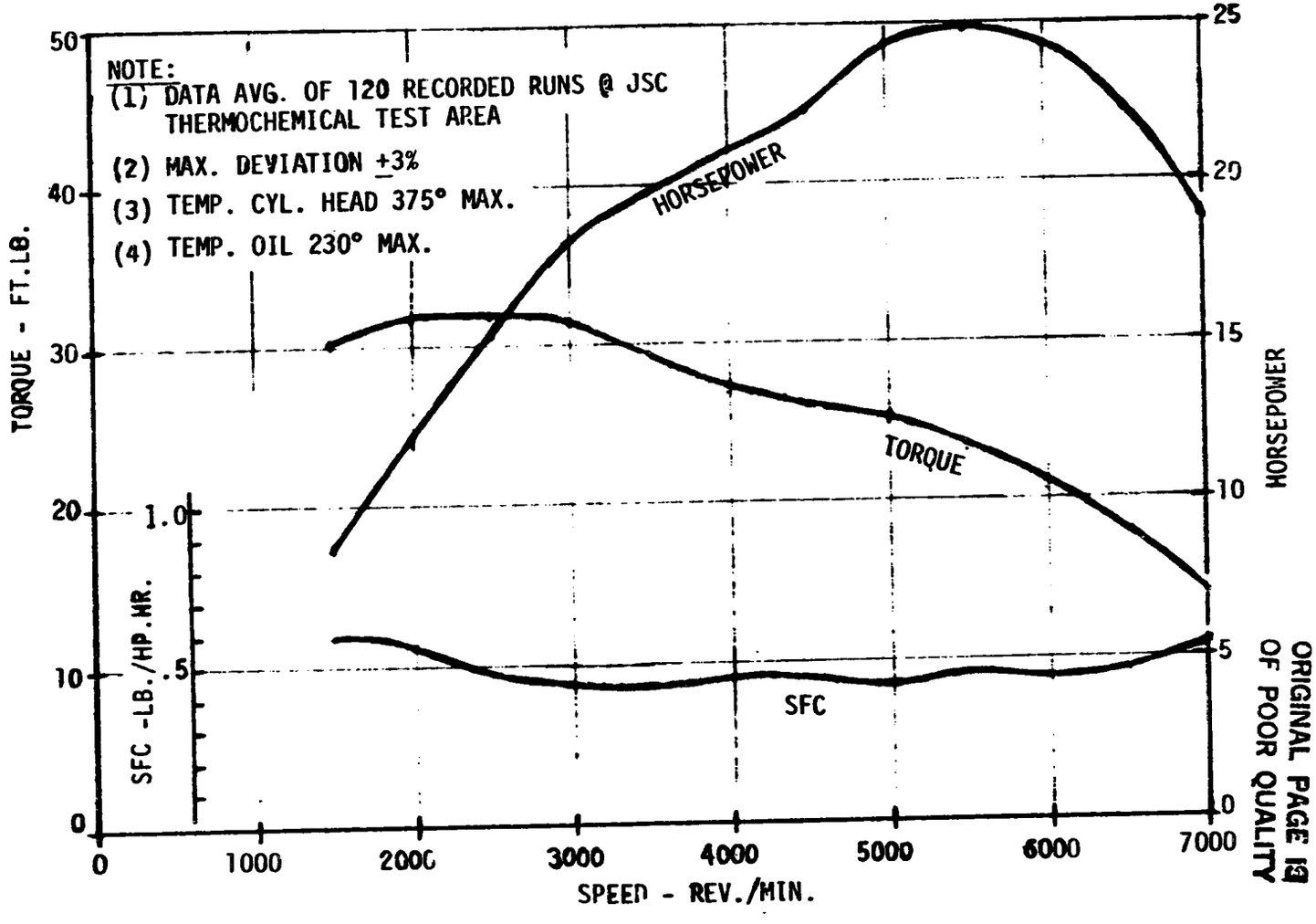

Figure 22.- Stock engine performance.

STOCK OMC MODEL 200 (2 CYL, OPPOSED, OHV) - 43.2 CU. IN. DISPL.
- REGULAR GASOLINE FUEL (NO LEAD) - 110 PSI COMPRESSION, 7° BTDC IGN. TIMING(STATIC)

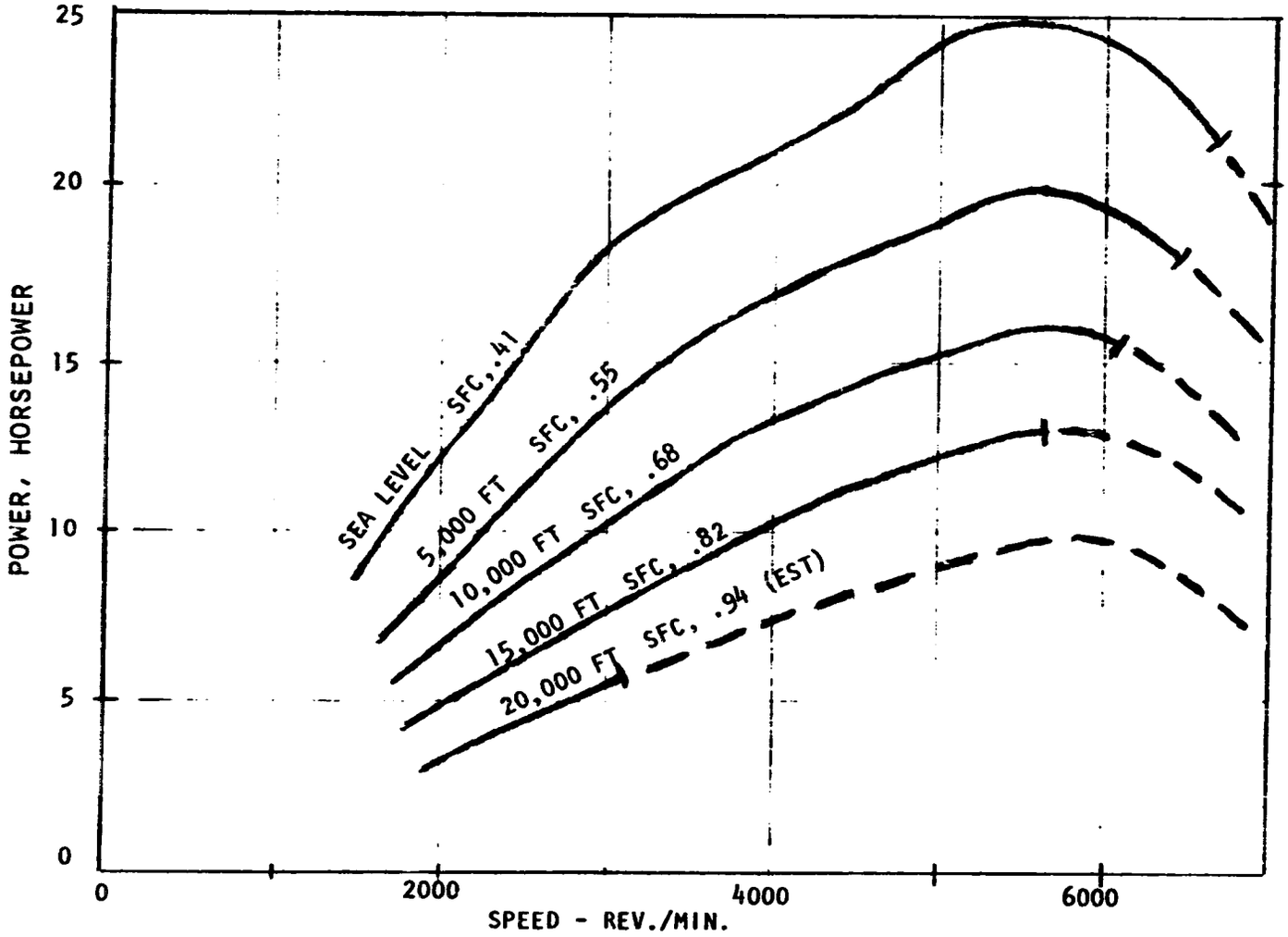

Figure 23.-Stock engine performance at altitude.

pressure (110 psi). The results of the tests of the stock engine were consistent with published manufacturers' data.

The phase 2 tests were limited at low power (high altitude) by the inability to reduce the load sufficiently. A smaller pump and a larger valve were used in the load circuit in the phase 3 tests.

Phase 3 testing began with the assembly of the prototype engine with two Schweitzer turbochargers and continued with various modifications. These are discussed in the "Prototype Power System Definition" and "Discussion of Results" sections of this report.

TEST SYSTEM

The initial test system consisted primarily of a hydraulic pump mounted directly to the engine crankshaft and a flow restricting throttle valve to control the load on the engine. A 1-foot long torque arm was mounted onto the pump and a load cell was used to measure the force generated. An electronic tachometer was used to measure engine speed. Oil temperature and cylinder temperatures were measured with thermocouples, and all the data were recorded on a paper tape in engineering units. A strip chart kept a record of oil pressure and engine speed. An automatic ignition cut off was used sensing low oil pressure (below 10 psi) and/or excess engine speed (above 7,000 rpm).

This test system was moved to the vacuum chamber and reassembled to do the initial altitude tests of the stock engine as recorded in tests G and H (appendix A). The test cell (vacuum chamber) is shown in the background of the photograph of figure 24. The schematics of the test system developed over a period of time on an as-needed basis and are shown in appendix B (Operating Procedure). Some special test systems were used on occasion and are discussed below in connection with the test results.

The data system is worthy of special mention. It required considerable innovation because of the remoteness of the engine (in altitude chamber) and the desire to be able to detect problems before damage occurred. The instrumentation list is shown in figure 25 along with the readout mode. The data logger proved to be a very convenient way of recording most of the data, recording the data on a paper tape in engineering units. The data program form is shown in figure 26 along with a typical data printout sheet in figure 27. Three strip charts provided quick access to the turbocharger boost pressures and the engine speed data. Six differential pressure gages were used to monitor pressure drops in the four heat exchangers, the carburetor and overall across the system from inlet to outlet (See the data sheet in figure 28). The speed pickups were a problem on occasion. Phototransistors were used in early attempts, but then magnetic washers were added to the shafts of the turbochargers to excite inductive pickups. Some problems were experienced with the pulse/analog conversion, but the system worked satisfactorily most of the time. The fuel consumption was measured with a calibrated volume in a sight glass using a stopwatch to measure time to deplete a known volume of fuel.

The vacuum system in the initial phase was a single 350 cfm piston-type pump. It was adequate for about 20,000 to 30,000 feet simulation when the engine was running about 4,000 rpm. A second vacuum pump with 850 cfm capacity

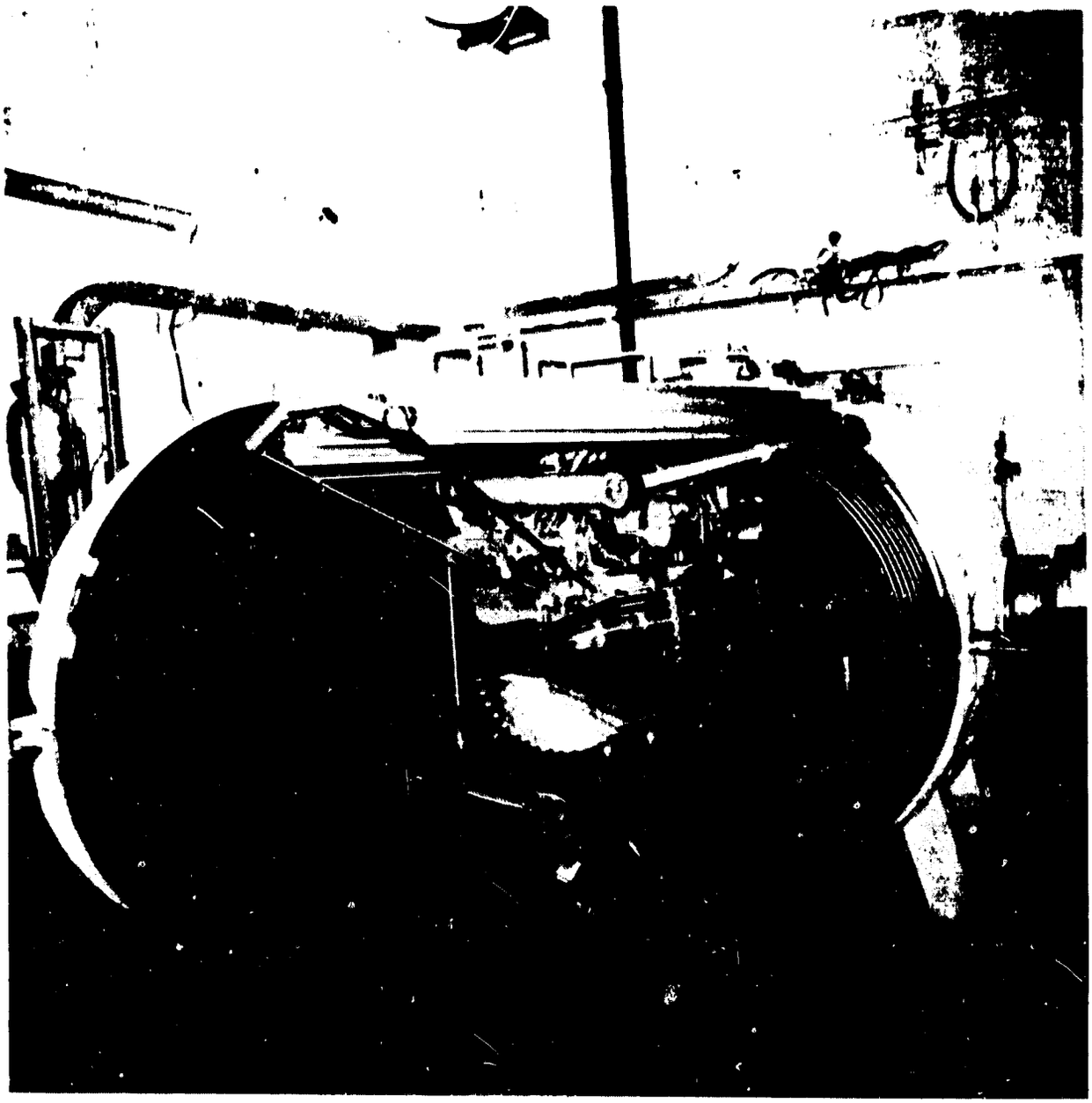

Figure 24.- Altitude test chamber.

1	Pressure	Compressor (1) Inlet	0-30 PSIA	(Data Logger
2	"	" (2) "	"	(Strip
3	"	" (3) "	"	Chart)
4	"	Carburetor Inlet	"	
5	"	Intake Manifold	"	
6	"	Turbine (1) Inlet	"	
7	"	" (2) "	"	
8	"	" (3) "	"	
9	"	" (3) Outlet	"	
10	"	Oil (Guage)	0-100 PSIA	
11	"	Dyno Load (Guage)	0-2000 "	
12	Torque,	Engine Output	0-50 Lb Force	
13	ΔPress.	HX 1	0-30 " H_2O	(Manometers)
14	"	HX 2	"	
15	"	HX 3	"	
16	"	Carburetor	"	
17	"	Flow Meter	"	
18		HX 4	"	
19	Air Flow	Carburetor Discharge	0-100 CFM Air @ 8 PSIA	
20	Speed Eng.	Engine (Meter)	0-10,000 RPM	
21	Turbo 1	Compressor (1)	0-200,000 RPM	
22	" 2	" (2)	"	
23	" 3	" (3)	"	
24	Temp.	Cylinder Head, West	0-500°F	
25	"	" , East	"	
26	"	Oil	"	
27	"	Compressor (1) Inlet	-70-4200°F	
28	"	" (1) Outlet	"	
29	"	" (2) Inlet	"	
30	"	" (2) Outlet	"	(Data Logger)
31	"	" (3) Inlet	"	
32	"	" (3) Outlet	"	
33	"	Carburetor Inlet	"	
34	"	" Outlet	"	
35	"	Aftercooler Outlet	"	
36	"	Turbine (1) Inlet	500-2000°F	
37	"	" (2) "	"	
38	"	" (3) "	"	
40	"	Exhaust Cooler Outlet	0-200°F	
41	"	Cooling Water Inlet	-60--+100°F	
42	"	" " Outlet	"	
43	"	Chamber Wall	"	
44	"	Cooling Shroud	-300--4100	
45	"	Cold Box Air Outlet (Meter)	-60--+100°F	

Figure 25.- Instrumentation list.

FLUKE 2240B PROGRAM FORM

FIRST CHANNEL _____ INTERVAL _____
LAST CHANNEL _____ FIXED DATA _____
MONITOR CHANNEL _____ SINGLE CHANNEL _____

TEST NO. _____
SH. _____ OF _____
DATE _____

CHANNEL PROGRAM

	CHANNEL ADDRESS	FUNCTION	ADDRESS LIMIT A (1-15)	ADDRESS LIMIT B (16-30)
	1	40 VDC RPM		
	2	T3 Oil Temp.		
	3	T3 Head Temp. West		
	4	T3 Head Temp. East		
	5	T3 Air Inlet Temp.		
	6	T3		
	7	T3 Carburetor Inlet		
	8	T3 Compressor #? Inlet		
	9	T3 1st Stage Discharge		
	10	T2 Exhaust Temp.		
	11	T2 Turbine #2 Temp.		
	12	T2		
	13	T2 Free Air Temp. West	Turbo Oil Temp. 6/30/82	
	14	T2 Turbine #3 Temp.		
	15	T2		
P60205	16	400 MV Oil Pressure		
	17	T2 Turbine #1 Temp.		
	18	T2		
	19	T2		
	20			
P60384	21	40 MV Load Press.		
P11098	22	400 MV Torque		
P60113	23	40 MV Compressor #1 Inlet Press.		
P60127	24	400 MV Compressor #2 Inlet Press.		
P60140	25	400 MV Compressor #3 Inlet Press.		
P60138	26	400 MV Compressor #3 Discharge Press.		
	27	40 V ENg.-RPM #2		
	28	4 V 4 VDC UEL Inside Chamber		
	29	4 V 4 VDC UEL Outside Chamber		
	30			
	31	4 V Turbine #1 Speed RPM		
	32	4 V Turbine #2 Speed RPM		
	33	4 V Turbine #3 Speed RPM		
P60605	34	400 MV Accumulator Press.		

LIMIT A PROGRAM

LIMIT ADDRESS	SENSE (HI/LO)	VALUE AND POLARITY
1		
2		
3		
4		
5		
6		
7		
8		
9		
10		
11		
12		
13		
14		
15		

LIMIT B PROGRAM

LIMIT ADDRESS	SENSE (HI/LO)	VALUE AND POLARITY
16		
17		
18		
19		
20		
21		
22		
23		
24		
25		
26		
27		
28		
29		
30		

Figure 26.- Data program.

FLUKE 2240B PROGRAM FORM

FIRST CHANNEL _____ INTERVAL _____ TEST NO. _____
LAST CHANNEL _____ FIXED DATA _____ SH _____ OF _____
MONITOR CHANNEL _____ SINGLE CHANNEL _____ DATE _____

CHANNEL PROGRAM

	CHANNEL ADDRESS	FUNCTION	ADDRESS LIMIT A (1-15)	ADDRESS LIMIT B (16-30)
P60058	35 - 400 MV Turbine #1 Press.			
P60069	36 - 400 MV Turbine #2 Press.			
P60004	37 - 400 MV Turbine #3 Press.			
P60275	38 - 400 MV Exhaust Press.			
	39 - 4 V Air Turbine			
	40 - T3 Compressor #2 Inlet Temp.			
	41 - T3 3rd Stage Discharge Temp.			
	42 - T3 2nd Stage Discharge Temp.			
	43 - T3 Shroud Temp.			
	44 - T3 Chamberwall Temp.			
	45 - T3			
	46 - T3 Air Turbine Flowmeter Temp.			
	47 - T3 Accumulator Temp.			

LIMIT A PROGRAM

LIMIT ADDRESS	SENSE (HI/LO)	VALUE AND POLARITY
1		
2		
3		
4		
5		
6		
7		
8		
9		
10		
11		
12		
13		
14		
15		

LIMIT B PROGRAM

LIMIT ADDRESS	SENSE (HI/LO)	VALUE AND POLARITY
16		
17		
18		
19		
20		
21		
22		
23		
24		
25		
26		
27		
28		
29		
30		

Figure 26. - Concluded

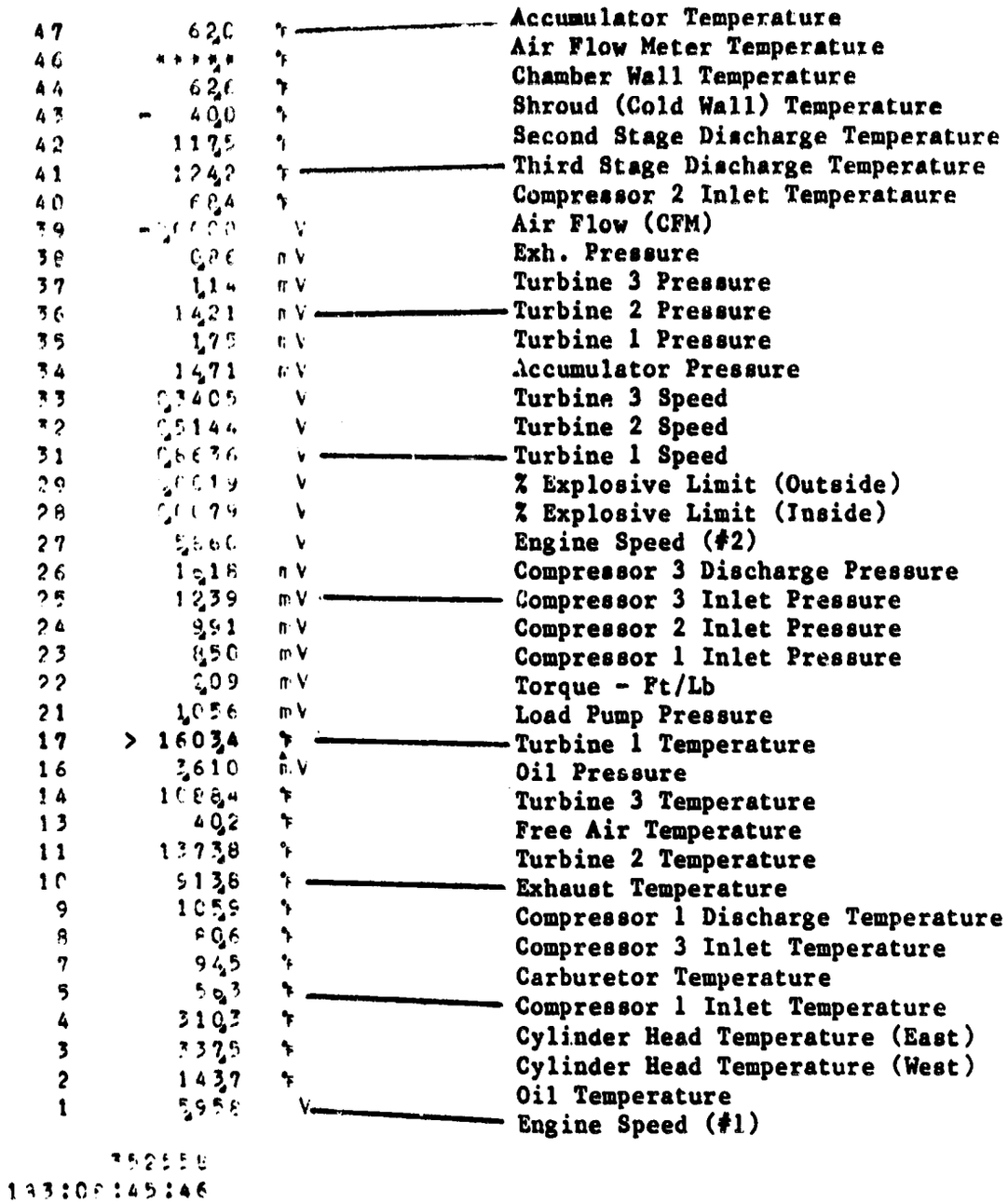

Figure 27.- Data printout.

HAAP POWERPLANT TEST

RUN# TIME DATE

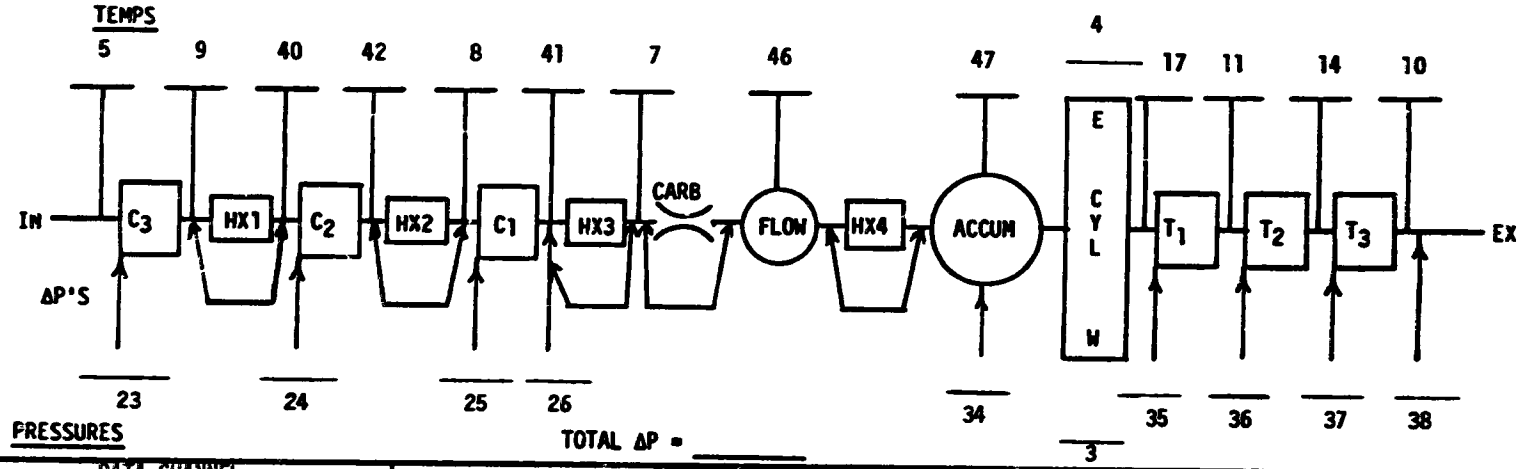

PRESSURES TOTAL ΔP = _____

	DATA CHANNEL
RPM =	1, 27
FLOW =	39
MASS FLOW =	
LOAD PR =	21
TORQUE =	22
OIL TEMP =	2
OIL PR=	16
DENS. ALT. =	
HP =	
FUEL FLOW TIME =	
SFC =	
N_{VOL} =	

TURBOCHARGERS

COMP. RATIOS:

1 =

2 =

3 =

NET =

TURBINE RATIOS:

1 =

2 =

3 =

NET =

TURBOCHARGER	HOUSING	COMPRESSOR
1.		
2.		
3.		

		DATA CHANNEL
SPEEDS:	1 =	31
	2 =	32
	3 =	33
TURBO EFFICIENCY.	1 =	
	2 =	
	3 =	
	NET =	

Figure 28.- Data sheet.

was added along with a better exhaust cooling unit. Adequate flow was available to keep the test cell purged with fresh inbleed air.

A unit was added for cooling and dehumidifying the inbleed air. This unit consisted of two aluminum 3- by 5-ft cold plates attached to a spacer framework, mounting the two cold plates about 6 inches apart. A series of aluminum strips about 6 inches apart between the plates forced the air coming in at the top to flow back and forth as it progressed through to the outlet at the bottom. The entire unit was covered with foam insulation. Liquid nitrogen was used in the cold plates. This unit kept the cold wall in the chamber from being covered over with frost so quickly and gave better temperature control in the test cell.

The only real problem with the test system was the inconvenience of its access after installation in the test cell. With seven fans for air circulation, the test chamber was essentially "filled." Any work required removal of several fans and, in most cases, the large aftercooler heat exchanger on top of the engine.

The test procedure (appendix B) outlines the operation of the system and the many safety features.

DISCUSSION OF RESULTS

This report presents almost 3 years of activity concerning demonstration of an operational assembly of hardware for powering a vehicle at 60,000 feet altitude. The purpose is to aid those who may continue the effort to avoid the same problems. A chronology of the major events is summarized in figure 29. A more detailed chronology is shown in appendix C, which includes 76 tests, 92 engineering orders, 57 purchases, 49 correspondences, six meetings, three analyses, and five drawings. Each is documented in the files and may be reviewed by interested individuals.

The simplest summary of the results is as follows:

1. The goal of demonstrating 60,000 feet operation was not achieved - only about 40,000 feet on two occasions.

2. While the particular combinations of hardware selected for test did not function as desired, there seems to be no basic reason why the concept cannot be made to work.

The significance of the decision concerning compression ratio was revealed early in the project. In the beginning, considerable effort was involved with making the clearance volume in the engine automatically variable, to obtain the best possible combination of efficiency and power output. However, as the analysis of the overall concept was being completed, it became apparent that a controllable clearance volume did not offer a significant benefit. It was dropped for the time being, because other factors were more important in the cost realm (see appendix A). The choice of a "fixed" clearance volume continues to be a major factor in the engine design. It affects exhaust gas temperature, overall efficiency turbocharger effectiveness, volumetric efficiency, and ultimately the turbocharger compressor size. It also affects maximum allowable manifold pressure which limits power output. These factors should be related to

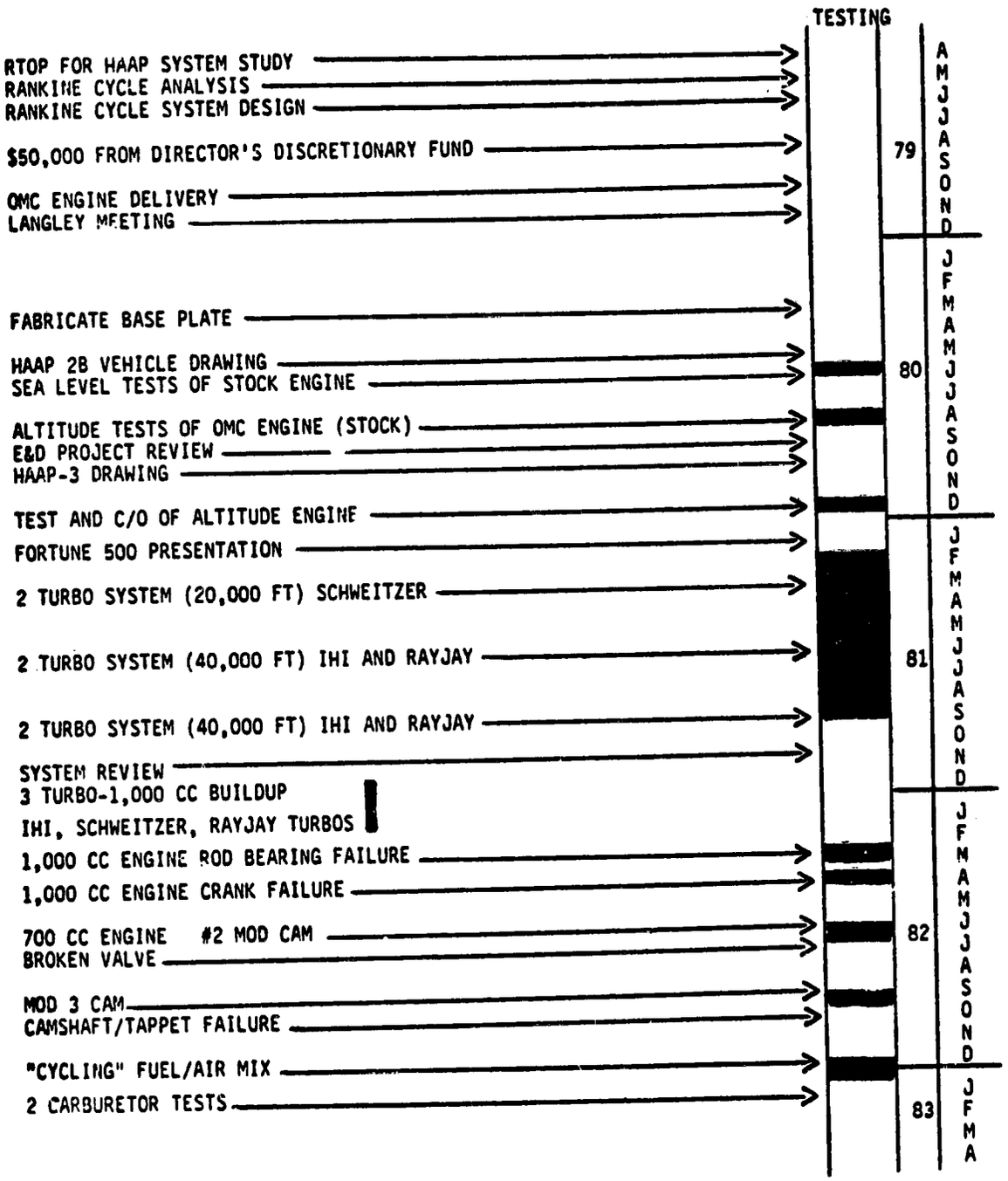

Figure 29. - Project chronology summary.

one another and included in the math model outlined in appendix A for an adequate understanding of the need for a variable compression ratio.

A natural initial choice is operation at the smallest possible clearance volume that will avoid detonation with the fuel being used and allow adequate manifold pressure for sufficient climb power. But that requires early exhaust valve opening to maintain exhaust gas temperature at reasonable levels for sufficient turbine power. To get the best engine efficiency, the turbocharger size selection is driven toward very small units to function with low temperature exhaust gas.

As in any power plant, the major consideration is the combustion process which is primarily influenced by clearance volume. The combustion should occur in the best possible temperature, pressure, and turbulence environment to produce the most energy release.

Theoretical minimum clearance volumes for the engine are shown in figure 30. The actual clearance volume minimum limit that can be used is primarily a function of the chemical octane of the fuel. But the temperature, heat transfer, turbulence, ignition characteristics, basic combustion zone configuration, and fuel/air mixture characteristics also are influential. They are sometimes referred to as "mechanical" octane of an engine. These factors must be determined by testing. But after the limit is established, the adiabatic compression temperature data (figure 30) can be used to make appropriate adjustments for inlet air temperature limits. Also, if a fuel is used with known different basic temperature limits, then adjustments in clearance volume can be made to run that new fuel. For example, the limit for 100-octane gasoline is about 1160° F. For 90 octane it is about 1,000° F. In operating at 560° R (100° F) the difference is 2.5 to 3.5 $in.^3$, a difference of 40 percent. This dramatically affects exhaust valve opening timing requirements and the resulting energy delivery to the crankshaft and to the turbocharger.

As discussed in appendix A, efficiency is paramount in this concept. The machinery must produce the most favorable situation possible for energy release and then convert that energy into useful work. In this example, the energy in the exhaust gas is used for air compression; therefore, the choice of exhaust valve timing is involved. This affects the expansion ratio of the gases in the engine and the relative amount of energy released to shaft work or to exhaust gas energy. Thus, as the exhaust valve is opened earlier, the shaft work goes down, lowering the efficiency of the engine but increasing the exhaust gas energy to power the compressors.

While the original plan for the project was to "match" the engine/turbocharger combination, little was understood of the complex interrelationship of the many factors which affect the results. Much could be done analytically, but there are some fundamental problems. Turbochargers are basically considered in the industry today as "volume" machines. Some of the older companies in the industry still consider the flow primarily on a mass basis because that relates well to the power involved in the machine. Of course both mass flow and volume must be considered in any analyses, but the difference is in the way of "thinking" about the situation. The volume basis relates well to various engine displacements and is used in most data for users, particularly in compressor selection. The turbines are somewhat flexible in their operation,

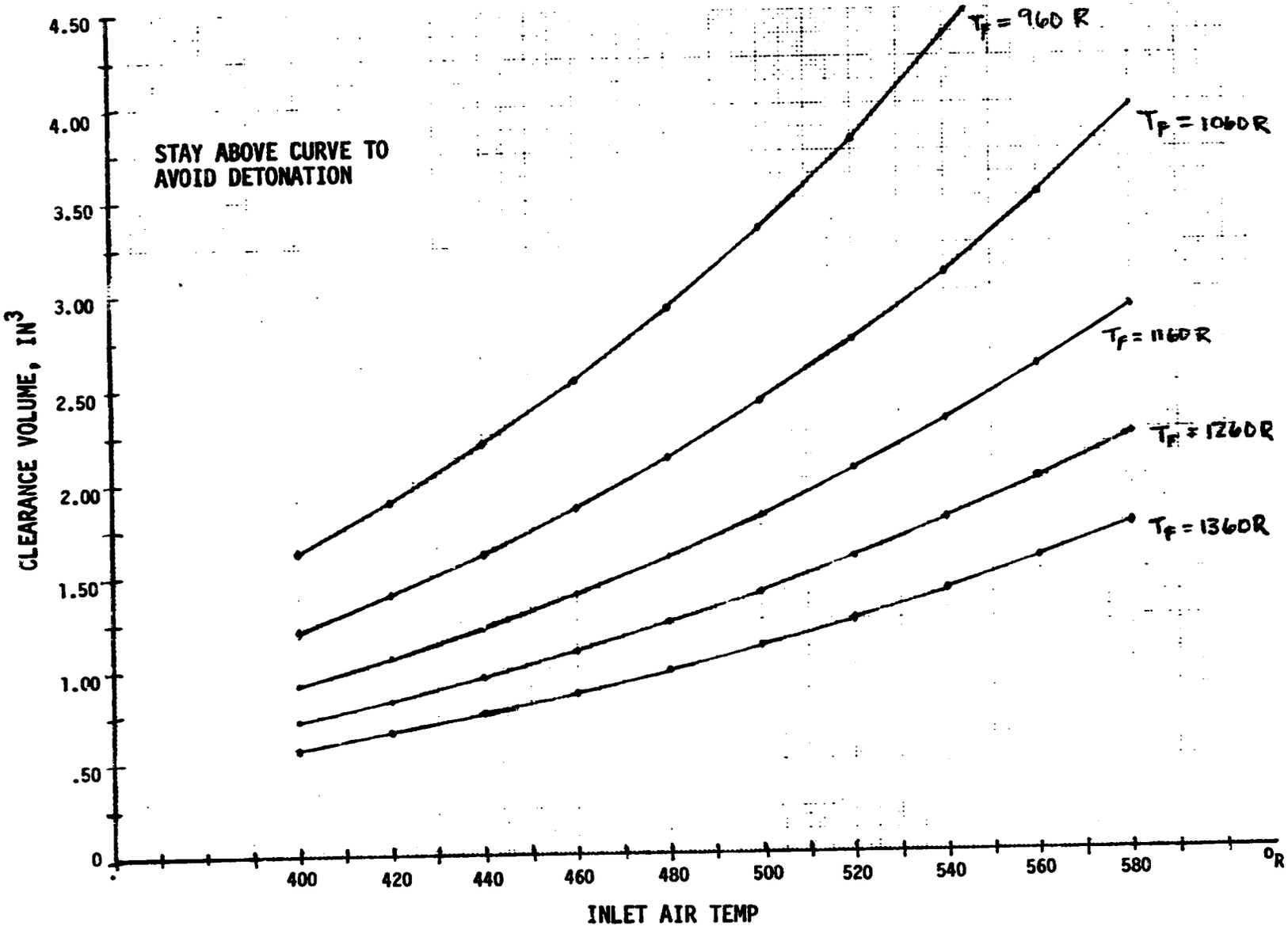

Figure 30. - Clearance volume limits.

and typically companies will base their entire turbocharger "family" around a single turbine. A series of housings (nozzles) is made available so that the user can power the compressor selected to whatever speed is needed to give the pressure ratio desired. Therefore, in a company's "line," there will be a particular combination of compressor and turbine housing that will give the desired result for a selected engine.

In past experiences, no turbine/housing data have been made available--only compressor data. The user selects a compressor to match the flow of the engine, and "tries" various turbine housings (nozzles) to get the unit to produce the boost in manifold pressure desired.

This situation is the primary reason that the project has extended so long. The only option was to "cut and try." The first try was to use the units built by Schweitzer. The results were very discouraging. Even with the smallest housings available, little speed could be attained. The turbine itself was basically too large - by at least a factor of 2 and very little boost was achieved. As the altitude was increased, the mass flow decreased, reducing the speed and power in the turbine even more. See figure 31 (tests 3, 4, and 5).

The next step was to look for the smallest possible turbine. The unit selected was the IHI model 51B used on the 500 cc displacement Honda motorcycle. This violated a basic groundrule of using American built equipment, but there was no alternative. The Schweitzer unit was the smallest available in the United States.

Early tests with the IHI turbocharger combined with the Schweitzer unit produced the results of tests 8, 10, and 11 (figure 31). With the additional flow induced by the IHI unit, the Schweitzer compressor was flowing in a very inefficient range, but the results were much better. Finally, a Rayjay unit was selected to better fit the compressor flow situation and runs 18 and 33 produced sea-level power output at 40,000 feet altitude.

Many "adjustments" were made in runs 19 through 32 attempting to increase the turbine speed and produce higher pressure ratios. Fuel mixture ratio (lean and rich) showed very little effect. Ignition timing diffrent from stock timing had only adverse effects. Probably the most discouraging effect was the changing of turbine housings. Smaller housings (nozzles) caused extra back pressure on the engine and reduced the volume flow of the engine so much that the net result was a lower boost. Larger housings reduced backpressure, and allowed higher volumetric efficiency of the engine, but the lower turbine speed produced lower pressures in the manifold and less boost.

It became obvious at that point that something different was necessary. The data showed (fig. 32) that increased mass flow gave better performance. Also, higher compression pressure gave higher exhaust temperatures. It became apparent that all three units tested had best efficiency in the range of about 2/1 compression ratio in each stage. A pressure ratio in the range of 2.8/1, needed for 1/2 atmospheric manifold pressure at 60,000 feet with two stages, required much more exhaust gas energy than three stages operating at 2/1.

It was decided that the system would work best if the engine flow could be increased as well as changing to three turbochargers. A 1000-cc engine was assembled, using a crankshaft with 1/2-inch extra throw. The initial test

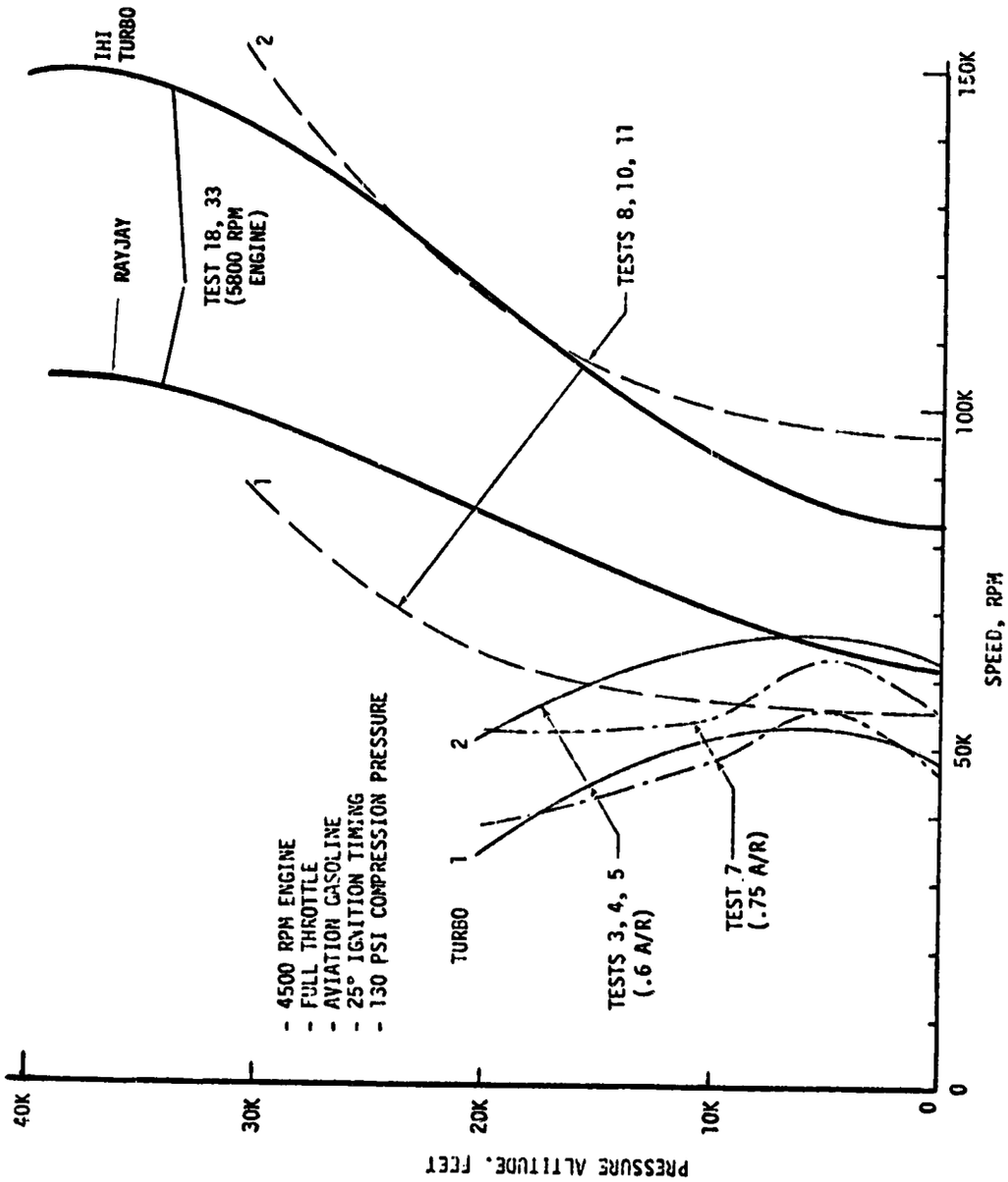

Figure 31. - Altitude/speed for various turbochargers.

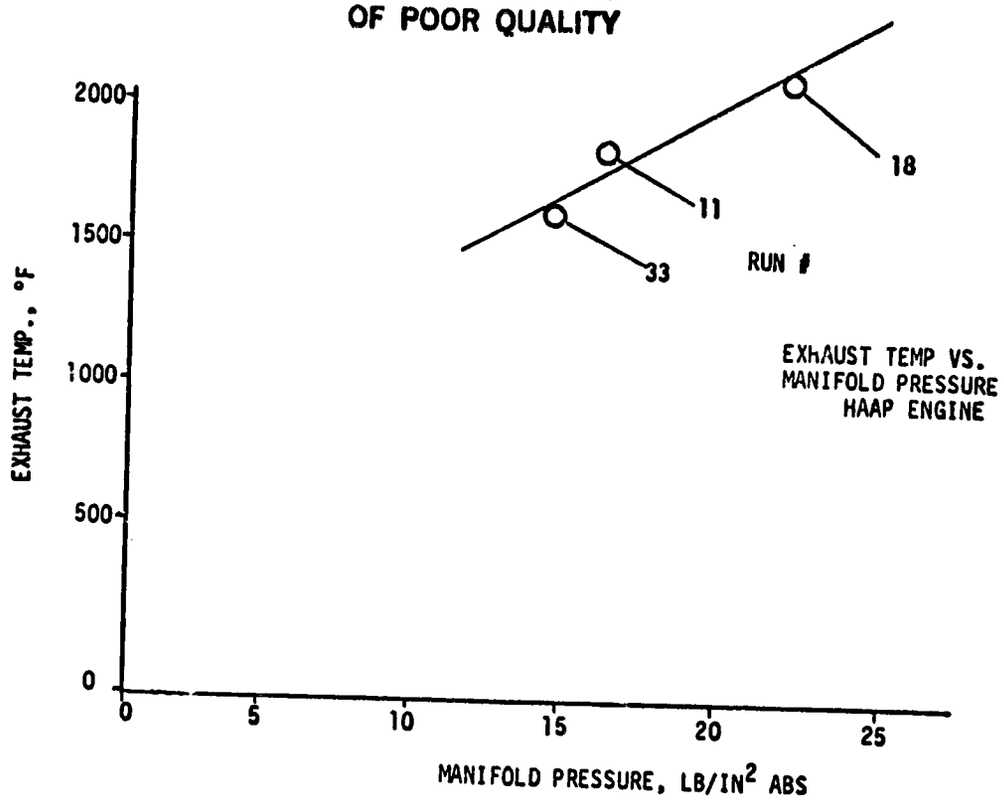

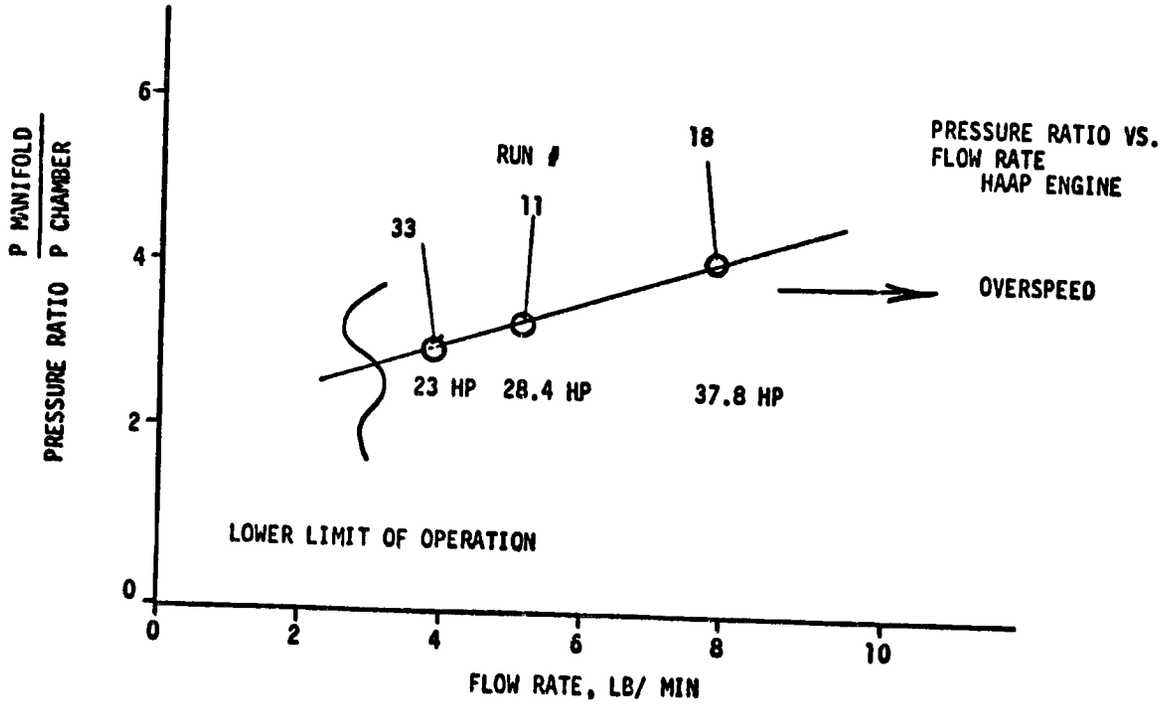

Figure 32. - Flow/pressure/temperature relationships.

experienced a rod bearing seizure - probably because of inadequate oil flow. A second test with larger oil holes, resulted in a "slip" of the pressed-together crank assembly. These results were discouraging because the crankshaft appeared to be the quickest and easiest way to significantly improve the flow. At that point, it seemed reasonable that the extra flow needed might well be produced with a camshaft modification to give essentially standard valve timing, but increased lift.

The stock crankshaft was reinstalled and tests continued, but with no improvement in attitude capability. The boost was always good at high flow rates but as the altitude was increased, the pressures decreased, the exhaust temperatures decreased, the boost reduced, and the system would consistently cease to function when the manifold pressure was below 14 psia. Finally, the exhaust valve broke on one cylinder when the system's rpm and temperatures became too high. It was believed that something must be done to increase the flow (i.e., the power to the turbines) to get the boost desired.

At the outset, it was recognized that the clearance volume must be reduced to get the best combustion efficiency at reduced manifold pressures. But that is a risky thing to do on an engine with potentially high manifold pressure. Reducing the clearance volume was postponed as long as possible in the hope that an adequate demonstration could be achieved without the risk. It became apparent that volumetric efficiencies of 60 percent typically would not suffice and that 80 percent was required. See the curves of figures 33 and 34. Another problem with reducing the clearance volume was the reduction of exhaust gas temperature because of the increased expansion ratio of the combustion products. This increased fuel efficiency at the expense of exhaust gas energy. In this case, the expense was prohibitive. It became apparent that still another cam modification was in order to open the exhaust valve very early in the expansion stroke. Also, with decreased clearance volume, little overlap of exhaust and intake valves is required. The result was the choice of using a long duration exhaust lobe, and to avoid excess overlap (because the operation would likely require higher exhaust pressure than intake manifold pressure) use a short duration intake lobe.

To circumvent problems with overpressuring the small clearance volume, a pressure switch was installed in the intake manifold that would disconnect the ignition system if the manifold pressure rose above 1 psig (15.7 psia). Initial runs were very encouraging, showing volumetric efficiency at low speeds in excess of 90 percent. But at higher speeds, it was only 50 percent. A mechanical check revealed that the intake lobe was providing less than one-half the lift it was built for. Modification of the intake lobe required a broader tappet. The modified tappet had failed and worn the cam excessively and the weld material used to reconfigure the cam separated. In any case, this caused the low flow. The cam was reworked to the same configuration and testing proceeded.

Surprisingly, the flow continued to be low at high speeds. Volumetric efficiency in the range of 60 percent produced mass flow along the lower limit of the established requirement (see fig. 32). The manifold pressure limit held the mass flow even lower than in the unmodified runs where the manifold pressure was allowed to go to 20 psia (see fig. 32). At this point probably the most significant observation made in the project was apparent. At the low manifold pressure imposed by the pressure switch, the engine performed unpredictably. It

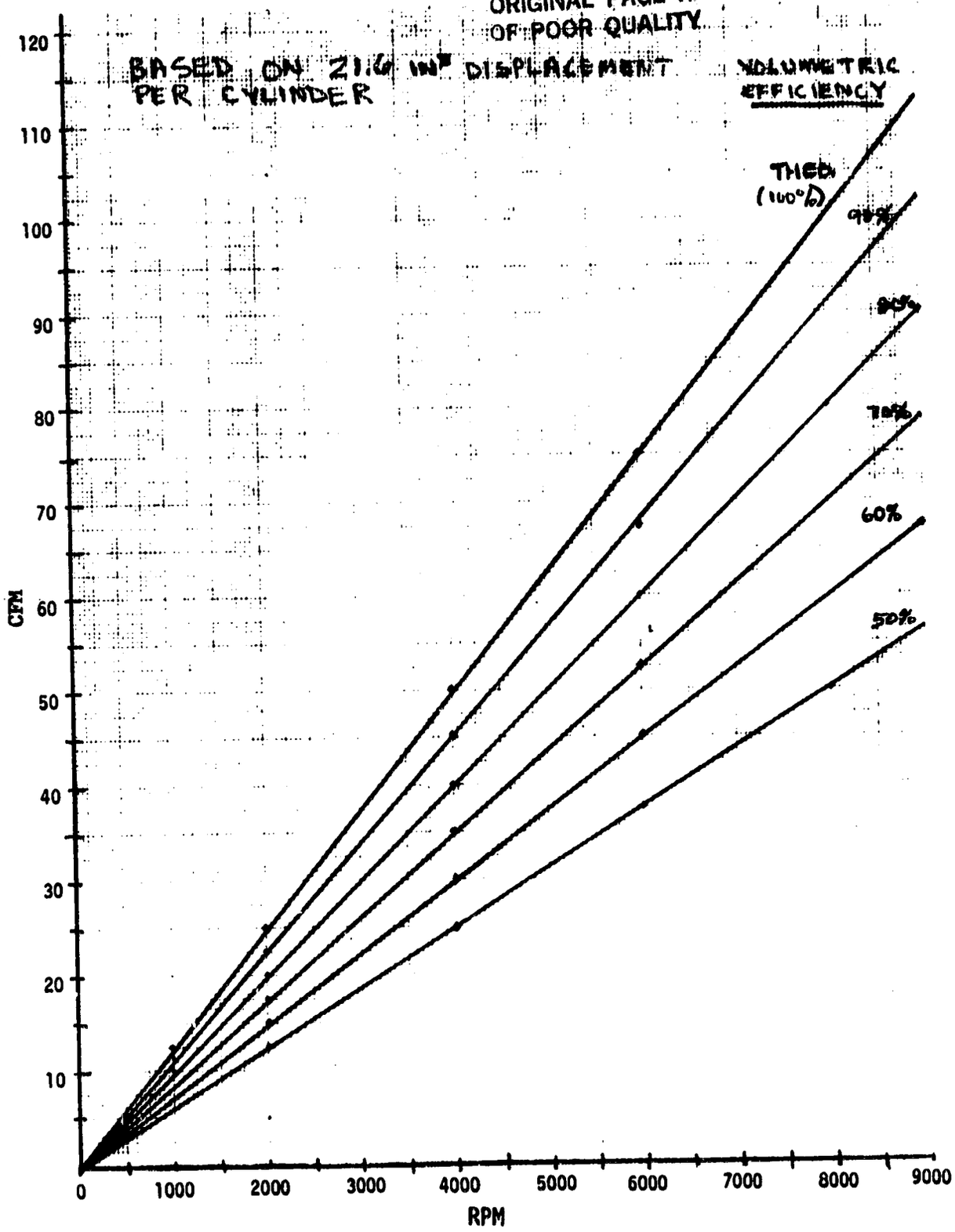

Figure 33. - Flow volume vs RPM.

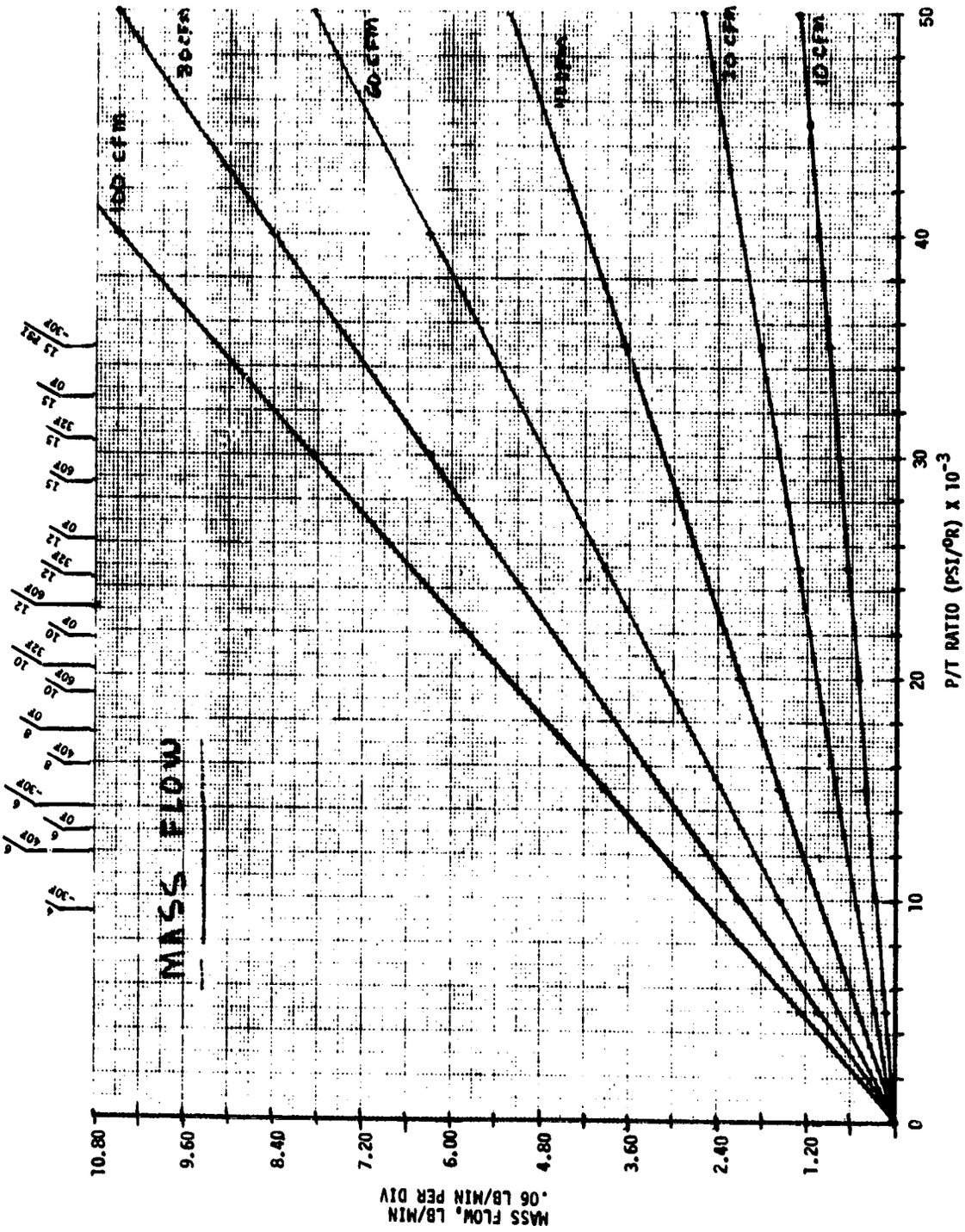

Figure 34 - Mass flow.

seemed to have a mind of its own. On occasion it would run very well, only to be followed by a period of extremely low-power operation - all on a 1- to 2-minute cycle. The ignition system seemed to be entirely functional. The engine/mechanical system was verified to be "as designed." The fuel/air flow system, however, showed unexplained pressure-time variations that previously were not considered carefully since most testing was done at higher manifold pressures. An exhaust gas analyzer was used to verify that the fuel and air mixture was not being delivered to the cylinder with a consistent mixture ratio. On more than one occasion, fuel was found puddling in various places - heat exchangers, accumulators, etc. This was disregarded because the system performed predictably in most cases (when the mass flow rate was high). However, when the mass flow rate was reduced by lowering the manifold pressure, the "puddles" apparently did not get "blown" along consistently, resulting in periodic "off mixture" operation. Review of the data indicates that in every case where the dynamic pressure of the flow is reduced, the system ceased to function properly. In early tests, this was caused by inadequate flow, giving inadequate turbine power. This was true, but not so much because of inadequate flow as low "quality" flow. A few moments of extremely rich or extremely lean fuel mixture would reduce turbine power enough to put the entire operation out of commission. The only way to get the system up and going again was to go back to sea level and start again. Consistently, whenever the manifold pressure got below 15 psia, the system would "die." This became apparent when the pressure switch was installed and all the operation was at the lower flow level. The system could not be coaxed to work, even with the turbochargers disconnected. It would run properly with the stock manifold, however, so the problem was narrowed to the aftercooler and the accumulators.

As a result, the carburetor was moved downstream of the aftercooler but upstream of the accumulator. Two carburetors were used - one in each side of the system. Operation was somewhat better, but cycling still occurred at a somewhat higher frequency - a few seconds instead of minutes. This indicated that the flow of fuel was possibly "hanging" on the walls of the induction system - and as the amount of area was reduced, the amount of fuel and the time involved were reduced. (The surface area was reduced by about one-half.) Finally, the two carburetors were moved to the cylinder interface downstream of all the plumbing. This gave steady engine operation at a reasonable specific fuel consumption. At last the engine would run steadily with less than one atmosphere in the manifold as it had in the tests G and H two years before.

The only problem was further flow reduction. With the carburetor upstream of the accumulators, the flow through the carburetors is essentially steady, allowing about four times the time for the flow to occur as in the case of the cylinder-mounted carburetor. Using the effective flow area of the carburetor throat, the volume that was required to go into the cylinder and the time available at 6000 rpm, it is clear that the flow in the carburetor throat was very close to sonic in the cylinder-mounted case.

At this point, part of the test facility being used was needed for another test project. The engine project was unfortunately terminated.

In event that someone will pickup the effort and continue, the following section, "Other Observations," outlines several of the "fringe" problems encountered and the solutions to them. Figure 35 shows a set of run data (run no. 44B). An analytically-derived set of operating conditions that should be

HAAP POWERPLANT TEST

RUN# 44B TIME 187:13:15:59 DATE 7/6/82 (Tuesday)

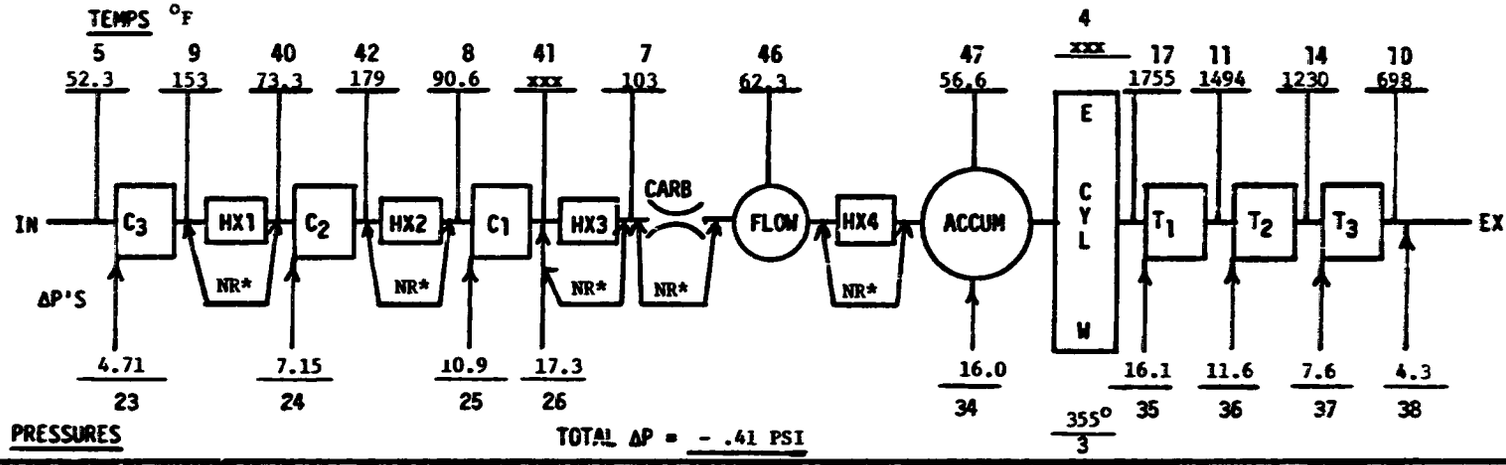

PRESSURES TOTAL ΔP = - .41 PSI

	DATA CHANNEL	
RPM =	1, 27	5800
FLOW =	39	49
MASS FLOW =		3.9 LB/MIN
LOAD PR =	21	894
TORQUE =	22	17.3
OIL TEMP =	2	248
OIL PR=	16	39.9
DENS. ALT. =		35,000 FT
HP =		
FUEL FLOW TIME =		
SFC =		
N_{VOL} =		

*NOT RECORDED

TURBOCHARGERS

COMP. RATIOS:

1 = 1.52

2 = 1.52

3 = 1.59

NET = 3.67

TURBINE RATIOS:

1 = 1.39

2 = 1.53

3 = 1.77

NET = 3.76

	TURBOCHARGER	HOUSING	COMPRESSOR
1.	RAYJAY	375	E
2.	SCHWEITZER	.7	S6
3.	IHI	P9	502

		DATA CHANNEL	
SPEEDS:	1 =	31	116,700
	2 =	32	76,400
	3 =	33	61,400
TURBO EFFICIENCY:	1 =		1.14
	2 =		.99
	3 =		.86
	NET =		.98

Figure 35.- Data sheet (44B)

demonstrable using the proper components is shown in figure 36. All the other run data are available if needed.

OTHER OBSERVATIONS

Several problems came about which were not entirely related to matching the turbochargers and the engine, but two deserving some mention are oil control and cooling.

The problems experienced with the oil were of three types:

1. Cavitation of the pump due to low feed pressure and high speed
2. Air/oil separation (foaming)
3. Inadequate return flow to the sump

In some cases, all three may have been occurring at the same time. The oil pump in the OMC engine begins to cavitate at the suction at about 4 psia when using SAE 10W oil at 250° F operating at 5000 rpm using the 5/8-inch I.D. 10-inch long suction tube as in the configuration. This was observed in the initial runs up to 40,000 feet with the crankcase vented. Later, in an effort to use oil cooling for the cylinder heads, an additional 3/8-inch I.D. suction line lowered this to about 3 psia. In most tests, the crankcase was connected to the discharge of the first compressor, keeping the crankcase pressure at or below the pressure in the compressors and turbines. This kept the oil from leaking past the compressor seals. However, there is evidence that air and exhaust leaked from the compressor into the crankcase cavity.

Oil consumption was a consistent problem during the entire altitude testing part of the project. In reflecting on the data, and after solving items 2 and 3 (air/oil separation and low return flow), it appears that the problem was with the crankcase vent. Mechanically it is arranged on the camshaft drive gear with the vented air passing inward through three radial holes in the cam gear and out through a passage cast in the crankcase adjacent to the cam bearing. The unit is designed to handle normal ring leakage, but it is possible that compressor and turbine seal leakage for three turbochargers was too much for this unit to handle and caused oil droplets to be blown through the vent mechanism. Future testing should include a clear line (tygon or glass) to verify this as a problem. The vent could be connected to an external supplementary tank through a relief valve (to maintain sufficient crankcase pressure to avoid pump cavitation, and stay below first-stage discharge pressure) to verify leakage. Removal of the turbochargers from the crankcase oil system to a separate supply eliminated the oil loss and verifies this hypothesis.

Power loss in early tests might have been caused by excess oil in the crankcase, but carburetor location and poor fuel mixture ratio control was the probable cause. The initial fix was to provide an air vent from the vapor space in the sump to the top of the crankcase. This allowed the oil to return to the sump along with whatever bubbles were entrained without the vapor going upstream in the return oil flow passage. The return oil flow passage from the crankcase to the unit is about 1 inch in diameter. It was surmised that the 5-gallon per minute oil flow was too slow if the gas from the accumulated bubbles was

HAAP POWERPLANT TEST

RUN# TIME DATE

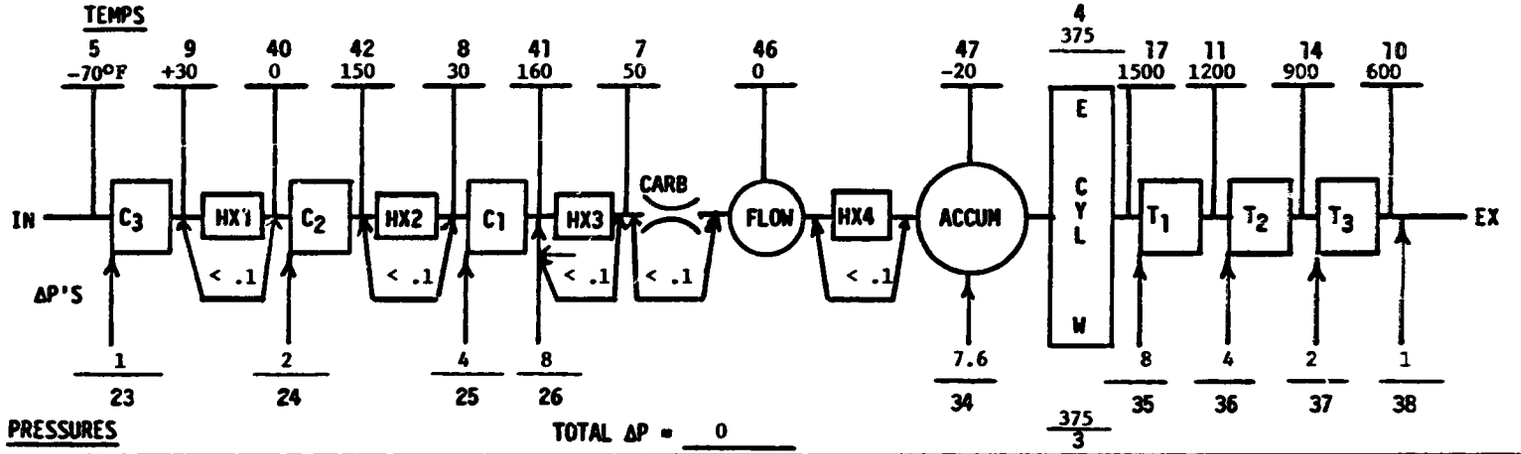

PRESSURES TOTAL ΔP = 0

	DATA CHANNEL	
RPM =	1, 27	5,000
FLOW =	39	60
MASS FLOW =		2.4 LB/MIN
LOAD PR =	21	500 PSI
TORQUE =	22	11 FT-LB
OIL TEMP =	2	275° F
OIL PR=	16	30 PSI
DENS. ALT. =		60,000 FT
HP =		12
FUEL FLOW TIME =		∿ 12 SEC
SFC =		.5
N_{VOL} =		88%

TURBOCHARGERS

COMP. RATIOS:

1 = 2

2 = 2

3 = 2

NET = 8

TURBINE RATIOS:

1 = 2

2 = 2

3 = 2

NET = 8

	TURBOCHARGER	HOUSING	COMPRESSOR
1.	IHI	P9	502
2.	?	?	?
3.	?	?	?

		DATA CHANNEL
SPEEDS:	1 =	31
	2 =	32
	3 =	33
TURBO EFFICIENCY:	1 =	1
	2 =	1
	3 =	1
	NET =	1

Figure 36.- Data sheet (predicted)

passing back upstream into the crankcase causing overfilling in the crankcase and a large power loss. The addition of the vent line seemed to fix the bogging problem at that time, but no specific tests were run to verify it. All later power loss was accounted for by lack of turbocharger performance.

Later, there continued to be problems with partial loss of oil pressure after long running - 10 minutes or more. The cause was surmised to be the long flow path in the sump oil cooler, allowing an accumulation of bubbles to become entrained with the oil. Thirteen 2-inch diameter holes were made in each of the 10 fins extending through the oil tank, and no further problems with oil pressure degradation were experienced.

In future testing, consideration might be given to using a separate oil pump operating at a very low speed to avoid cavitation at even 1 psia. This would allow venting of the crankcase to ambient air and would avoid reingesting the ring leakage and the exhaust leakage past the turbine seals into the intake system.

The other area of considerable consternation was cooling, or more generally thermal control. In some instances low temperature was a problem. This area will be greatly simplified when the environment is not artificial and when the power system behaves as designed. The overheat situations were always associated with high power tests to maintain sufficient flow for the desired boost pressures. The low temperature situations that gave problems were likewise cases with low power (idling) in a wait mode to achieve low cell temperature.

A notable exception is the problem with low oil temperature. This is the result of excessive fin area. The design was intended to be that way, with the plan to remove fin length as required when the system was functional. This low temperature did aggrevate pump cavitation, however, until much of the fin area was covered.

The addition of air intercoolers between the compressors appears to be an attractive feature. All the best turbocharger performance was recorded with cold air. This is a significant efficiency consideration in that the compression becomes closer to a constant temperature process. Also, with the denser air, the compressor gives higher pressure ratios with lower turbine speed requirements. The lowest temperature of operation was on run no. 18 at -8° F in the test cell. Operation at -70° F can be expected to be much improved - especially if effective intercoolers can be used between each stage. The bellows type tubing with a spiral turbulator, as seen in figure 16, yields an effective intercooler with low pressure loss. Mechanical vibration and fatigue cracking may be a problem with this design, however, so some life testing needs to be done.

CONCLUSIONS AND RECOMMENDATIONS

The only conclusion that can be reached here is that matching engines and turbochargers in the small size range, where only limited variations of sizes are available, is difficult. Limited published data on flow characteristics of the various elements makes it difficult to do analytically, thus requiring

experimentation. However, there seems to be no reason why the concept will not work.

After the concept is basically demonstrated, there will be a great need to establish the altitude limit of operation of the concept as it relates to the specific fuel consumption. Specifically, with reduced clearance volume (to the limit of power capacity for climb), the question becomes: "How early must the exhaust valve be opened to provide sufficient exhaust energy to run the turbochargers?" At higher altitude, more of the fuel energy must be used for gathering air, thus requiring a higher specific fuel consumption. This effect will likely begin to be a significant factor at about 50,000 feet. Above that altitude, the specific fuel consumption will go beyond the typical 0.5 pounds per horsepower hour feasible at the lower altitudes.

It is recommended that the project be continued with basically the identical configuration except with improved fuel control, possibly with a fuel injection system located at the cylinder inlet.

REFERENCES

1. Reed, Dale R.: High Flying Mini-Sniffer RPV: Mars Bound? Astronautics and Aeronautics, vol. 16, no. 6, June 1978, p 26.

2. Phillips, William H.: Some Design Considerations for Solar Powered Aircraft. NASA Technical Paper no. 1675, June 1980.

3. Turriziane, R. Victor: Sensitivity Study for A Remotely Piloted Microwave Powered Sailplane Used as a High Altitude Obeservation Platform. NASA Contractor Report 159089, June 1979.

4. Morris, C. E. K., Jr.; and Liu, Grace C.: Performance Evaluation of a High Altitude Airplane Platform with a Cryogenically Fueled Engine. NASA TM 83184, Dec. 1981.

5. Strganac, Thomas W.: Winds Study for High Altitude Platform Design. NASA Wallops Flight Facility RP-1044, Dec. 1979.

APPENDIX A

JSC-17268

COST SENSITIVITY ANALYSIS AND AERODYNAMIC PERFORMANCE
IMPROVEMENTS FOR A HIGH ALTITUDE AERODYNAMIC PLATFORM
PRELIMINARY DESIGN CONCEPT

Robert Zehentner
Program Development Office

Lyndon B. Johnson Space Center
Houston, Texas

March 17, 1981

CONTENTS

TABLES

FIGURES

ABSTRACT

A cost sensitivity analysis was conducted on a remotely-piloted High Altitude Aerodynamic Platform (HAAP) preliminary design concept. Using a single mission profile math model, all cost-affecting parameters were independently varied from a defined reference vehicle. The cost sensitivity of each performance, operations, and financing parameter was established by calculating the vehicle cost effectiveness change for $\pm$ 10 percent variation from the reference value of that parameter.

The results of the sensitivity study suggested further analysis to improve vehicle lift and drag coefficients. A higher performance airfoil and vehicle drag reduction resulted in greatly improved vehicle cost effectiveness as expected, while climb horsepower had very little influence on cost effectiveness.

INTRODUCTION

Geosynchronous earth orbit satellites have proven their effectiveness as communication relay systems for large area coverage. They are less cost-effective for small areas with relatively few users and for mobile receivers where antenna size is limited. More efficient limited area coverage may be accomplished by stationing of a High Altitude Aerodynamic Platform (HAAP) at an altitude where wind gust frequency and velocities are minimal and transmitter coverage adequate. Many possible communication relay applications include news media onsite coverage, county and state law enforcement stations and vehicles, and low usage telephone systems.

Piloted vehicles require limited flight duration resulting in an increased frequency of flights for continuous coverage and higher operations costs. A remotely-piloted vehicle does not have this constraint and makes lower vehicle costs possible by eliminating pilot weight and the need for cockpit environment.

The cost of a remotely-piloted HAAP must be competitive to replace existing communication relay systems and for other uses. This report describes a cost sensitivity analysis of a nominal HAAP.

COST SENSITIVITY ANALYSIS

The cost sensitivity analysis was performed on the HAAP preliminary design concept originating from the Systems Design Office in late 1979 (references 1 and 2). An evaluation of the vehicle concept was performed by Langley Research Center (ref. 3) which verified the feasibility of the HAAP project and suggested design improvements in airfoil selection and wing optimization. Table 1 compares the preliminary design aerodynamic parameters with evaluations of the same made by the Langley study and the Entry Aerodynamic Design Section at JSC (ref. 4). The consistency of parameter values is an indication of the validity of the original design concept. The last column in the table shows the values selected for the nominal vehicle used as a reference in the sensitivity analysis.

The configuration analyzed is illustrated in figure 1. It features outboard wing sections that are folded during takeoff and low altitude climb for reduced sensitivity to atmospheric turbulence. The outboard sections are deployed to the cruise configuration on reaching the altitude at which the full wing area is required for continued climb.

The first step in conducting the analysis was the design of an analytical model simulating a single HAAP mission profile: climb to 40,000 feet, deployment of the folded outboard section, and climb to 60,000 feet where the mission is completed in cruise as the fuel supply is depleted. The math model includes all mission parameters affecting flight cost and hence vehicle cost effectiveness. Aerodynamic and engine performance parameters examined were cruise lift and drag coefficients, propeller and drive train efficiencies, wing area, vehicle dry weight, engine power available and specific fuel consumption. Operations and mission profile parameters included in the model were cruise altitude, fuel and payload weights, operating costs per flight for man-assisted launches and facility cost per hour for hangar storage. A computer program coupled the mission profile math model to vehicle lifetime and cost, percentage of vehicle life spent in cruise, and an overhead cost factor by which all cost inputs are multiplied. The program calculated vehicle cost effectiveness in dollars per pound of payload per hour of cruise at 60,000 feet ($\$/lb_{PL}$-hr). Other outputs

of the program include a cost distribution breakdown for vehicle, operations, fuel, and facility as percentages of total mission cost, along with wing loading, fuel-to-payload-weight ratio, and usefulness factor (defined as the ratio of fuel plus payload weight to total takeoff weight). These outputs were desired to help simplify recognition of cost effectiveness patterns among combinations of original input parameters.

If any further analyses are carried out, some minor refinements in the computer program are suggested. Outputs of total single mission cost and total lifetime cost would be helpful in evaluating results. Also, the analytic mission model assumed a static rate of climb definition where all excess power available over power required went into raising the vehicle, assuming the aircraft held a constant velocity. A dynamic rate of climb definition would slightly decrease rate of climb performance and would be more appropriate. Climb power available, however, had little effect on cost effectiveness; therefore, the validity of the sensitivity analysis would be unchanged as long as the overall concept does not change a great deal.

To determine cost effectiveness sensitivity to individual parameter changes, a reference vehicle was first defined. The analysis was conducted by varying a single cost-affecting parameter while holding all other parameters at their reference vehicle values to determine the independent cost effect. Mission profile computer runs were made with parameter values both above and below the reference values to generate cost effectiveness vs. parameter curves for each parameter. These plots are displayed in figure 2.

Results

Figure 3 shows the relative independent effects of various parameters on reference vehicle cost effectiveness. The reference vehicle had a cost effectiveness value of $.103 per pound of payload-hour on-station. This value is based on a vehicle of nominal performance parameters with a 5-year vehicle lifetime cost of $50,000, an operations cost of $150 per flight, a facility cost of $.25 per hour of vehicle on-station time, and fuel cost of $30 per flight. The $50,000 aircraft cost was an estimate based on the cost of similar vehicles. A 50 percent utilization factor gives an on-station lifetime of 2.5 years at 60,000 feet with the other half of its life spent largely in the hangar, since climb is only 6.5 percent of total time aloft. With low turbulence

and gusts in the on-station cruise configuration, a 5-year lifetime seems reasonable. The $150 operations cost per flight represents an estimated three man-hours for preparation, launch, and recovery at $50 an hour. The $.25 facility cost per hour on-station is equivalent to $180 monthly rent for a hangar shared by two vehicles. Fuel cost of $30 per flight is based on 150 pounds of gasoline at $.20 per pound. An overhead factor of 2.0 doubles all cost parameters to account for financing and insurance, and results in a cost per flight of $535.90 and a total lifetime cost of $338,000 per airplane. The cost distribution is: operations 56.0%, vehicle cost 29.6%, facility cost 3.2%, and fuel cost 11.2% of total cost before inclusion of the overhead factor.

From figure 3, it is seen that reference vehicle cost effectiveness is more sensitive to the time-weighted average lift coefficient than any other parameter. Since the vehicle spends approximately 95 percent of the reference mission profile in the cruise configuration, the time-weighted average effectively becomes the cruise lift coefficient. The figure displays the change in cost effectiveness for 10 percent variations from the reference value for each of the parameters. A 10 percent change in cruise lift coefficient (0.1) yielded a cost effectiveness difference of $.009 per pound payload hour, or a 9.23 percent change in the base vehicle cost effectiveness of $.103. Table 2 gives the dollar value of this 10 percent parameter design improvement based on one reference vehicle lifetime as already described. In practical terms, then, a 10 percent design improvement in cruise lift coefficient (from C_L = 1.0 to 1.1) on the reference vehicle would yield a savings of $31,200 or 9.23 percent of the total lifetime system cost of $338,000. Over the lifetime of one hundred HAAP vehicles, the design improvement would save $3.12 million, well worth using the most efficient airfoil section design available. This great improvement in cost effectiveness is largely due to the large increase in endurance time on-station.

Lift coefficient is followed by cruise altitude in cost sensitivity. A 10 percent cruise altitude change yields an 8.75 percent change in cost effectiveness. The cruise altitude parameter does, however, have limitations of smaller area coverage and greater high gust frequency at lower altitudes, but these problems are minimal at the 54,000 foot level, a 10 percent decrease in the reference vehicle cruise altitude of 60,000 feet. Single vehicle lifetime

savings would amount to $29,600, largely resulting from an extended cruise duration made possible with additional fuel not used in the last 6,000-foot climb increment. Fuel saved is substantial because the climb mode becomes relatively inefficient as the aircraft ceiling is approached.

Lowering the reference vehicle empty weight by 10 percent (54 pounds) improves cost effectiveness by 8.26 percent for a vehicle lifetime savings of $27,900.

It must be remembered that the sensitivity analysis is restricted to a parameter range within $\pm$ 10 percent of the reference vehicle base value. Outside that range, sensitivities would not be the same, so that a larger variation in parameter value would not necessarily have proportionately the same effect on cost effectiveness. It should also be noted that the 10 percent variation used in this analysis is arbitrary and may not represent the probable ranges of parameters, which are discussed below.

Usefulness factor, defined as

$$U.F. = \frac{\text{FUEL WEIGHT + PAYLOAD WEIGHT}}{\text{TOTAL WEIGHT}}$$

is plotted vs. cost effectiveness in figure 4. Cost effectiveness improves rapidly as usefulness factor increases up to about 0.5, but very little thereafter. This suggests that fuel, fuel tank, and payload should comprise at least 50 percent of the total takeoff weight to achieve the most cost-effective flights. Figure 5, fuel weight/payload weight ratio vs. cost effectiveness, shows minimum cost when fuel and payload weights are about equal. Therefore, a general rule of thumb for best cost-effectiveness is to plan for fuel and payload each to represent 25 percent of the total weight.

A final observation, noted throughout the analysis process, is that climb performance has negligible effect on cost effectiveness. This is true if the 40,000 foot wing deployment altitude and 60,000 foot cruise altitude are both attainable. As long as these altitudes can be reached, climb lift and drag coefficients, time to climb, and fuel used in climb have little effect on the total mission since climb time is generally only 5 to 10 percent of time aloft. For this reason, design improvement efforts discussed in the second part of this report were concentrated on the vehicle cruise configuration with later checking back for adverse effects caused by the climb configuration performance.

To establish a credible base for comparison with other types of limited area communication relay systems, a realistic cost effectiveness band of performance should be defined. By estimating the most optimistic and pessimistic values for each of the cost-affecting parameters, a worst to best case vehicle cost effectiveness range is determined. Table 3 gives the parameter values for the worst and best case vehicles as well as for the reference vehicle. The cost effectiveness value ranges from $.668 per pound payload-hour for the worst case vehicle to $.021 per pound payload-hour for the best case vehicle. The reference vehicle has a cost effectiveness of $.103 per pound payload-hour, much closer to the optimistic performance vehicle than the pessimistic. With this cost effectiveness range definition, a comparison of the HAAP vehicle with present methods of communication relay including short wave radio, helicopters, hot-air balloons, and geosynchronous satellites could later be performed.

To get a feel for the upper performance limits of a HAAP system derivative, a special high altitude, high performance vehicle was evaluated for feasibility with little regard to cost effectiveness. Performance parameters are given in table 3 and show a vehicle takeoff weight of 300 pounds carrying 110 pounds of hydrogen fuel and a 5 pound payload to a 90,000 foot altitude, where cruise lasts for slightly over a week (175 hours). The cost was $2.80 per pound payload-hour, over four times that of the worst case performance vehicle.

AERODYNAMIC DESIGN IMPROVEMENTS

The cost sensitivity analysis illustrated those areas where design improvement would be most productive in improving HAAP cost effectiveness. As a result, aerodynamic design efforts were concentrated in the vehicle cruise configuration.

Airfoil Selection

An airfoil design for use on the HAAP vehicle must satisfy many requirements for efficient flight through its greatly varied regime. It must maintain effective performance through a Reynolds number range of 500,000 to 2,000,000. Since extended cruise duration is highly desirable, the endurance ratio, $C_L^{3/2}/C_D$, should be maximized. Low parasite drag at high angles of attack is also necessary. To achieve these characteristics, the airfoil must have minimum skin friction drag and flow separation on the airfoil upper surface. Separation results from adverse pressure gradient regions where the upper surface flow decelerates to achieve pressure recovery. Laminar (low skin friction) flows have minimal energy to maintain attachment through these regions. State-of-the-art airfoil technology deals with this problem by controlling the airfoil velocity profile and, hence, pressure distribution. The upper surface pressure distribution desired is relatively flat (constant velocity) back to about 40 percent of chord, where controlled transition from laminar to turbulent flow takes place and an abrupt pressure rise (adverse pressure gradient) occurs. The increasing pressure region develops a continuously decreasing pressure gradient. This has a favorable effect on the turbulent boundary layer development necessary for pressure recovery. The adverse pressure gradient reduces as the trailing edge is approached. For best performance and highest lift, the optimal pressure distribution is one in which a nearly separated turbulent boundary layer exists everywhere behind flow transition from laminar to turbulent on the upper surface. The lower surface profile should be nearly flat, producing a gradual flow acceleration once past the leading edge. Laminar flow is easily maintained since the pressure gradient is favorable. In summary, a high performance airfoil for the HAAP vehicle should have a pressure distribution described by a laminar region back to about 40 percent of chord where transition occurs and where a turbulent boundary develops from the rapidly decreasing adverse pressure gradient.

Of all the airfoils considered, two fit the above description exceptionally well. The Wortmann FX74-CL5-140 (reference 5) and the Liebeck L1003M (reference 6) had comparable maximum lift coefficients of 2.2 at a Reynolds number (Re) = 1 X 10^6. The Liebeck airfoil was selected over the Wortmann for several reasons. First, the L1003M was designed for high aspect ratio application and so has a higher maximum thickness-to-chord ratio of 18 percent. This enables use of a more substantial spar to handle span-wise wing loadings. Secondly, the Wortmann airfoil was optimized for high lift and large glide (C_L/C_D) ratios whereas the Liebeck was developed for long duration sailplane applications with an emphasis on high endurance ($C_L^{3/2}/C_D$) ratios. The design criteria for both airfoils evidence themselves in their drag polars. For the Liebeck L1003M, C_D remains about constant up to the stall angle of attack (ref. 6, figure 12) whereas the drag polar for the FL74-CL5-140 (ref. 5, figure 5) shows a large increase in C_D at higher C_L's. Therefore, the L1003M airfoil will give better cruise duration for the HAAP vehicle.

Design conditions for the Liebeck L1003M at Re = 1.0 X 10^6 include C_L = 1.8 and C_D = 0.009 at an 11.2° angle of attack. These values give an airfoil glide ratio (C_L/C_D) of 200 and an endurance ratio ($C_L^{3/2}/C_D$) of 268 -- ideal for the HAAP vehicle cruise configuration. An entire wing with the Liebeck L1003M airfoil section at the design condition should develop an estimated three-dimensional lift coefficient (C_L) = 1.6. With a 540 square foot wing area and an approximate 750 pound total vehicle weight at the start of cruise, the vehicle's air speed would be about 90 ft/sec or 53 knots. Based on a mean aerodynamic chord of 5.24 feet, Reynolds number is 4.0 X 10^5.

Aircraft Parasite Drag Reduction

Parasite drag reduction efforts were concentrated on the wing and the 520 feet of strut guy wire running perpendicularly to the free stream velocity. Since cruise performance greatly affected vehicle cost effectiveness, all analysis was done assuming cruise configuration at 60,000 feet.

Reference 3 calculated HAAP vehicle wing parasite drag coefficient (C_{D_p}) = 0.0113. The wing evaluated consisted of a high camber Miley airfoil (reference 7) for the inboard wing and a symmetric section for the outboard folding span. The Miley airfoil is much like the Wortmann FX74-CL5-140 already discussed. The Liebeck airfoil with C_{D_p} = .009 has 20.4 percent less wing

parasite drag. At design cruise conditions, this results in a drag decrease from 5.5 lb_f to 4.38 lb_f.

Parasite drag reduction for the HAAP vehicle's structural support guy wires has great potential largely due to the high drag associated with the wire's circular cylinder shape. With a 0.036 inch diameter, the wire has a cruise Reynolds number of 200. Reference 3 reports C_D for a cylindrical wire = 1.25, due largely to pressure differences between front and rear surfaces. Adding 20 percent for wing-guy wire interference effects results in C_D = 1.5. With this relatively high drag coefficient for the 520 feet of wire, a drag force of 2.11 lb_f results. Streamlined wire similar to that used in biplane applications offers substantial drag reduction. A streamlined wire with a fineness ratio (chord to maximum thickness) of 3.0 has C_D = .25 (ref. 8). Typical cross section profiles are shown in the reference. A streamlined wire will also have a smaller frontal thickness than the diameter of the original cylindrical wire. In addition, it may be possible to reduce the number of wing supporting wires, due to the large maximum thickness of the Liebeck airfoil which allows for the use of a torsionally stiffer wing spar. The preliminary HAAP design concept included two wing support wires above and two below each span. The high number of wires was originally felt necessary to control the torsional stiffness of the wing. With the stronger wing spar, four out of eight of these 26-foot wires could be eliminated, about a 20 percent reduction in total wire length.

The result of these design improvements is a substantial parasite drag reduction. With a drag coefficient of .30 (.25 plus 20% for interference effects), a streamlined wire frontal thickness of 0.03 inches (reduced 16.67 percent from 0.036 inch circular cylinder diameter), and the 20 percent reduction in total wire length, the resulting wire parasite drag = 0.279 lb_f (86.8% reduction). Together, the wing and strut drag reduction analysis lowered the vehicle drag 2.95 lb_f, from 7.61 lb_f to 4.66 lb_f. This increased aerodynamic efficiency represents a 25.5 percent reduction in the total vehicle parasite drag, and lowers the airplane's zero lift drag coefficient (C_{D_o}) from 0.0238 (ref. 3) to 0.01773.

Induced Drag and Wing Optimization Analysis

With the higher lift capability of the Liebeck L1003M airfoil, the addition drag induced by the wing at high C_L's must be considered in determining the best lift coefficient in cruise. Simply put, are the benefits of higher lift outweighed by the large increase in induced drag (proportional to the square of lift) that results? For best vehicle range, the L/D ratio is optimized. Figure 6, a plot of L/D vs. C_L, shows a C_L of 1.0 to 1.1 to be optimal for best range performance with a maximized L/D ratio. L/D falls off rapidly at higher C_L's, showing the effects of greater induced drag. The HAAP vehicle, however, sees improved cost effectiveness with endurance or maximum time in cruise optimization. Range is unimportant in its mission since it will be flying a stationary pattern over its relay area. A plot of the endurance ratio, $C_L^{3/2}/C_D$, vs. C_L in figure 7 shows a maximum endurance ratio of about 34 asymptotically approached at maximum C_L. This effectively says that for maximum endurance and minimum power, the wing should be flown at its highest design lift coefficient. For the airfoil selected, the maximum three-dimensional C_L possible is about 1.6.

However, to fly the HAAP vehicle at a cruise C_L of 1.6 requires the entire wing to be of the high performance Liebeck wing section. This presents a potential problem in the climb configuration, since the outboard wing is folded over and flying in an inverted position until deployment at 40,000 feet. Flying at the same angle of attack as the inboard section, but in the upside down position, the section would produce a high negative lift that might make the 40,000 foot deployment altitude unreachable. A solution exists in turning the outboard wing section at the inboard/outboard hinge point as the section is folded over and inverted. This is mechanized by appropriately choosing the hinge line. This turning or twist at the hinge line would result in the inverted section seeing lower angles of attack, resulting in lower negative lift forces. The inboard wing could still fly at its design angle of attack and high C_L with a less deleterious effect on climb performance from the inverted outboard section. For best climb performance, negative lift effects need to be minimized; however, reference 6 shows dramatic increases in airfoil parasite drag below C_L's = 55. The optimum hinge line angle would result in a low enough negative lift coefficient without large parasite drag increased. Figure 8 determines this optimum turn angle to be about 10 degrees of twist where the endurance ratio is maximized at 11.66.

A larger turn angle would result in great increases in parasite drag while a smaller angle would allow too high a negative lift coefficient. The inverted outboard wing section would fly at an effective C_L = -.55 with a resulting total wing effective C_L between .65 and .725 and L/D = 13.7. These values compare favorably with the climb performance of the cost sensitivity analysis reference vehicle. It climbed at C_L = 0.8 and L/D = 14.

Effect of Aero Efficiency Improvements on Cost Effectiveness

To determine the influence of improved aerodynamic performance on the baseline reference vehicle's cost effectiveness, a mission was flown changing only the aero parameters. The aero-improved reference standard incorporated a climb C_L = .65, climb L/D = 10.35, and a cruise C_L and 32 percent higher cruise L/D. All other parameters remained unchanged. Cost effectiveness for this model improved 25 percent, from $.103 to $.077 per pound payload-hour on station.

With the improved aerodynamic efficiency of the vehicle, greater weight-carrying potential is realized. A second aero-improved model was flown with 200 pounds additional weight and an increased mean aerodynamic wing chord of 7.0 feet. The increased chord created more wing area, keeping wing loading nearly constant, and helped maintain Reynolds number flow closer to the airfoil design condition. The 100 pounds each in additional fuel and payload resulted in a further improvement of the cost effectiveness to $.041 per pound payload-hour, a 60 percent improvement from the $.103 value of the reference vehicle.

RECOMMENDATIONS

Through the course of this analysis, many areas of additional needed research and study were identified. A larger vehicle may prove to be more cost-effective. Higher Reynolds number flow for better airfoil performance, increased engine efficiency, and lower operating costs per payload pound-hour are all advantages of a larger system that should be traded against higher weight and cost. In addition, much work can be done to improve the efficiency of propellers for this application.

REFERENCES

1. Akkerman, J. W. and Taub, W. M. Data Package for Airborne Experiment Program Vehicle, Johnson Space Center, December 1979 through February 1980.

2. Taub, W. M. and Akkerman J. W. HAAP-2 (High Altitude Airplane Platform), Johnson Space Center Drawing, January 1980.

3. Turriziani, R. V. Evaluation of an Airborne Experiment Program Vehicle Concept and Designed by the Johnson Space Center (W.O. J327), Hampton Technical Center Memorandum V-19100/OLTR-132, May 23, 1980.

4. Perez, L. F. HAAP-2 Aerodynamic Evaluation, Entry Aerodynamic Design Section, Johnson Space Center, June 2, 1980.

5. Wortmann, F. X. "The Quest for High Lift," AIAA Paper 74-1018, September 1974.

6. Liebeck, R. H. "On the Design of Subsonic Airfoils for High Lift," AIAA Paper 76-406, July 1976.

7. Miley, S. J. "An Analysis of the Design of Airfoil Sections for Low Reynolds Numbers," Mississippi State College, January 1972.

8. Mises, R. V. Theory of Flight, Dover Publications, Inc., New York, 1959.

BIBLIOGRAPHY

Ayers, T. C. "Supercritical Aerodynamics Worthwhile Over a Range of Speeds," Astronautics and Aeronautics, August 1972, pp. 32-36.

Heyson, H. H. "Initial Feasibility Study of a Microwave-Powered Sailplane as a High-Altitude Observation Platform," NASA TM-78809, Langley Research Center, December 1978.

Kuethe, A. M., and Chow, C. Y. Foundations of Aerodynamics: Bases of Aerodynamic Design. 3rd Edition. New York; Wiley and Sons, 1976.

Liebeck, R. H. "A Class of Airfoils Designed for High Lift in Incompressible Flow," AIAA Paper 73-86, January 1973.

McCormick, B. W. Aerodynamics, Aeronautics, and Flight Mechanics. New York; Wiley and Sons, 1979.

McMasters, J. H., and Palmer, C. M. "Possible Applications of Soaring Technology to Drag Reduction in Powered General Aviation Aircraft," NASA CR-145627, Proceedings of the NASA, Industry, University General Aviation Drag Reduction Workshop, July 14-16, 1975.

Miley, S. J. "On the Design of Airfoils for Low Reynolds Numbers," AIAA Paper 74-1017, September 1974.

Patrick, T. J. "Aerofoils Down to Critical Reynolds Numbers and the Performance of Remotely-Controlled Gliders," Department of Physics, University College London, U.K.

Pope, A., and Harper, J. J. Low Speed Wind Tunnel Testing. New York; Wiley and Sons, 1966.

Phillips, W. H. "Some Design Considerations for Solar-Powered Aircraft," NASA Technical Paper 1675, June 1980.

Pick, G. S., and Lien, D. A. "The Development of a two-Dimensional, High Endurance Airfoil with Given Thickness Distribution and Reynolds Number," Naval Ship Research and Development Center Report 4670, June 1975.

Sivier, K. R., Ormsbee, A. I., and Awker, R. W. "Low Speed Aerodynamic Characteristics of a 13.1% Thick, High Lift Airfoil," SAE Business Aircraft Meeting, Wichita, Kansas, April 2-5, 1974.

Strganac, T. W. "Wind Study for High Altitude Platform Design," NASA Reference Publication 1044, December 1979.

Turriziani, R. V. "Sensitivity Study for a Remotely Piloted Microwave-Powered Sailplane Used as a High Altitude Observation Platform," NASA CR-159089, Kentron International Inc. for Langley Research Center, June 1979.

Whitcomb, R. T. "Review of NASA Supercritical Airfoils," ICAS Paper 74-10, August 1974.

Wortmann, F. X. "A Critical Review of the Physical Aspects of Airfoil Design at Low Mach Number," NASA CR-2315, Motorless Flight Research Final Report, Massachusetts Institute of Technology, 1972.

Wortmann, F. X. "Airfoils with High Lift/Drag Ratio at a Reynolds Number of About One Million," NASA CR-2315, Motorless Flight Research Final Report, Massachusetts Institute of Technology, 1972.

Wortmann, F. X. "Drag Reduction for Gliders," NASA TM-75293, May 1978.

Table 1. Aerodynamics/Performance

Aerodynamics/Performance	JSC EW4	Langley	JSC EX3	Base Vehicle
Airfoil Section				
Inboard	Miley Cambered Low-Speed	Miley		
Outboard (Folded to 40K FT)	"	Symmetrical w/20% Flap		
Lift Coefficients				
Inboard, Cruise		1.22		
Outboard, Cruise		0.9		
Overall Optimum Cruise	1.1	1.1	1.1	1.0
Climb				0.8
Lift/Drag Ratio				
Climb	20	11.5		14
Cruise	20	$25_{60,000}$	17.6	20
Maximum		$27.6_{S.L.}$	18.1	
Propeller Efficiency				
Sea Level	.85	.57		.7
40,000 FT	.85	.67		.8
60,000 FT - Cruise	.85	.77		.8
Cruise Endurance - 60,000 FT	20.3 HR.	24.9 HR.		34.72 HR.

Table 2. Cost Sensitivity

Basic Vehicle Cost - $50,000
Vehicle Life: 5 years, 20,000 Hrs. Operation
Total Operations Cost: $86,000
Total Lifetime Cost: $338,000

Parameter	10% Delta	Vehicle Lifetime Cost Savings (compared to Reference)
Lift Coefficient	+0.1	$31,200
Cruise Altitude	-6,000 Feet	29,600
Vehicle Empty Weight	-54 Lb.	27,900
Fuel Specific Energy	+1,800 BTU/Lb. Fuel	25,300
Specific Fuel Consumption	-0.04 Lb. Fuel/Hp-Hr.	23,000
Drag Coefficient	-0.005	21,400
Propeller Efficiency	+8%	21,400
Operations Cost	-$15.00/Flight	18,700
Wing Area	+54 Ft^2	9,900
Fuel Cost	-$.02/Lb. Fuel	3,300
Climb Horsepower	+2.1 Hp	3,300

Dollar Value of 10% Parameter Design Improvement over One Base Vehicle Lifetime

Table 3. Design Features

PARAMETER	WORST	REFERENCE	BEST	MILITARY	MacCREADY
Fuel Cost $/Lb	.20	.20	.20	5.00 (H2)	.20
Fuel Weight Lb	81	150 (250)	350	110 (TK+H2)	36
Payload Weight Lb	81	150 (250)	350	5	1
Total Weight Lb	540	775 (975)	1400	300	237
Cruise Power HP	11	15	17.5	20 (20 KPT)	11
Cruise Altitude Ft	60,000	60,000	60,000	90,000	60,000
Wing Area Ft^2	540	540 (720)	540	540	260
C_{lift} (Cruise)	.8	1.0 (1.6)	1.3	1.3	1.0
L/D	15	20 (26.4)	25	25	25
η Propeller	.7	.8	.85	.85	.75
η Drive	.85	.9	.96	.96	.9
S.F.C. Lb/Hp	.360	.394	.45	.14 (H2)	.36
Climb Time Hr	7.04	2.40	5.06	1.39	.787
Cruise Time Hr	12.66	34.72	49.06	174.52	34.78
Operating Cost, $ Per Flight	200	150	100	250	150
Facility Cost, $/Hr	.30	.25	.20	.25	.25
Overhead Factor	2.5	2.0	1.5	2.0	2.0
% Life On-Station	40	50	80	50	-
Vehicle Life, Years	4	5	6	5	-
Cost Effectiveness, $/Lb-Hr	.668	.103	.021	2.80	-

ORIGINAL PAGE IS
OF POOR QUALITY

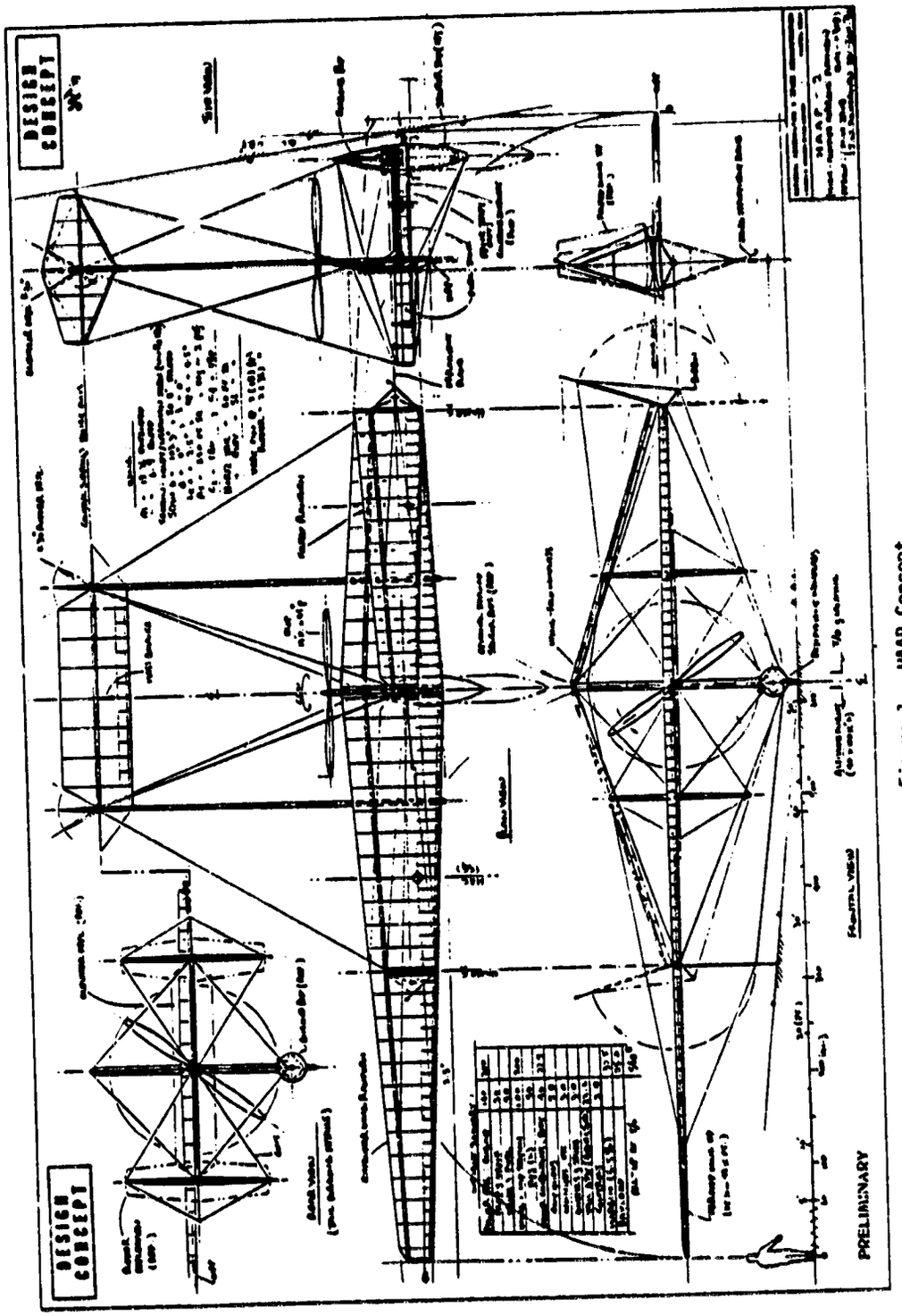

Figure 1. HAAP Concept

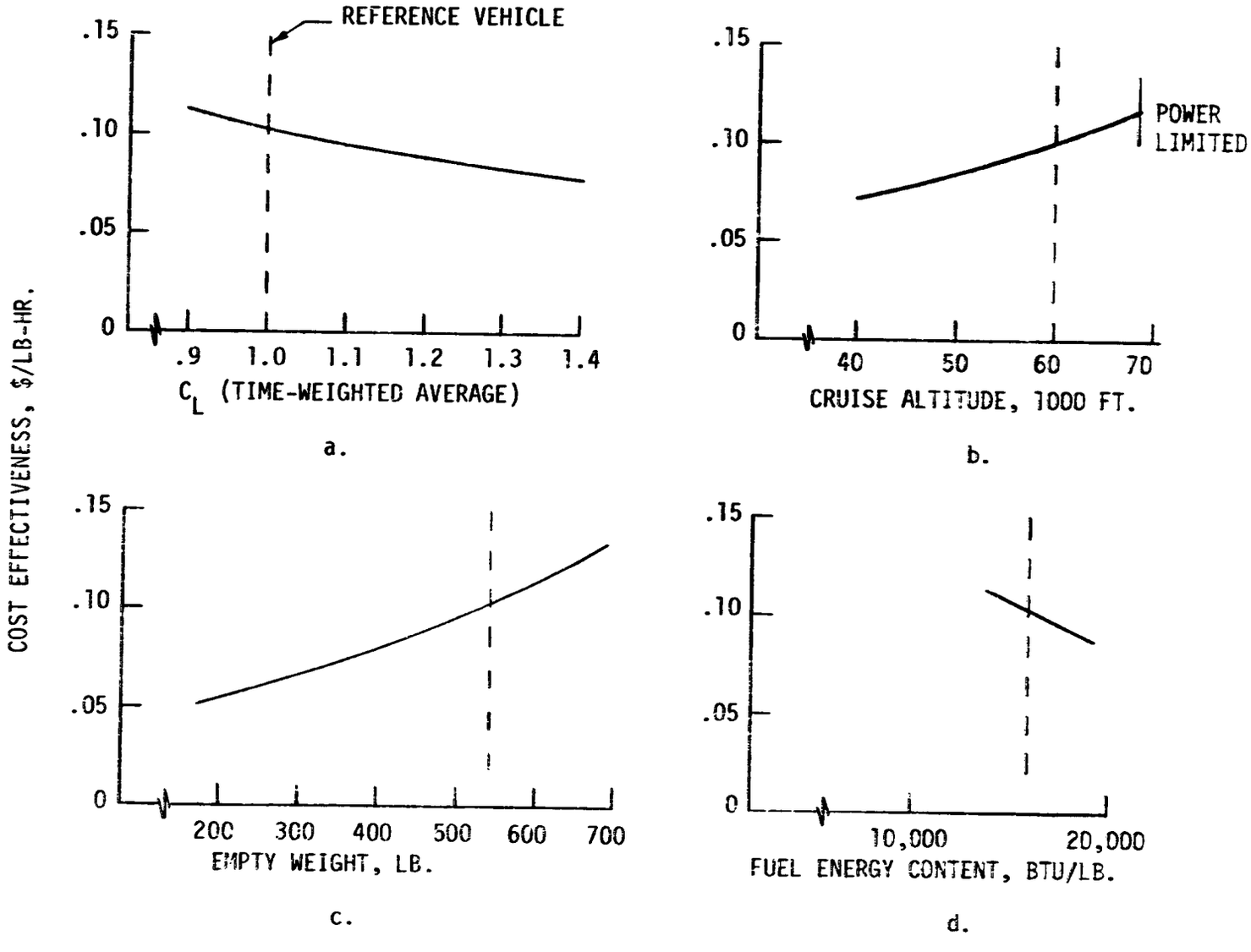

Figure 2. Cost Effectiveness vs. Parameters

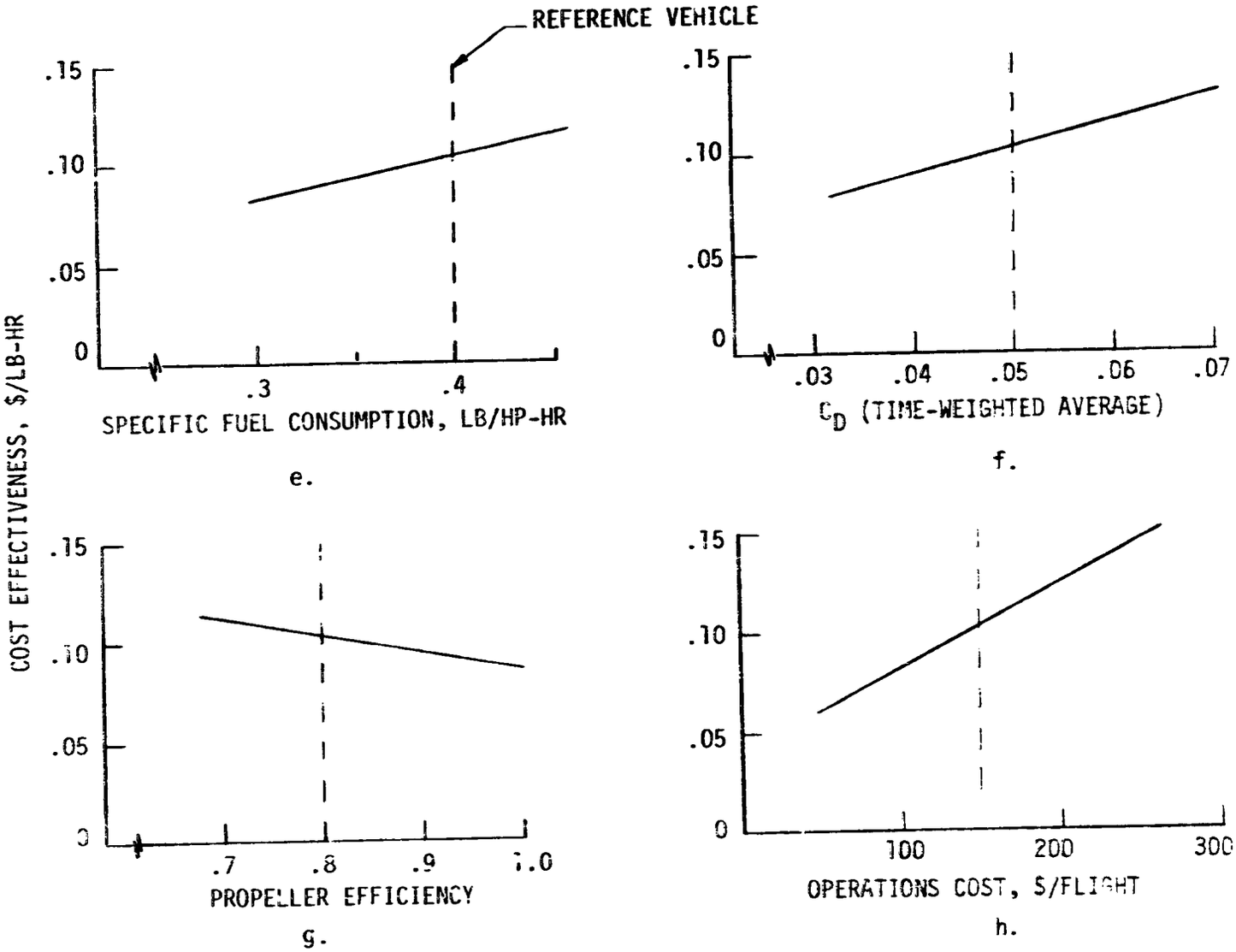

Figure 2.- Continued

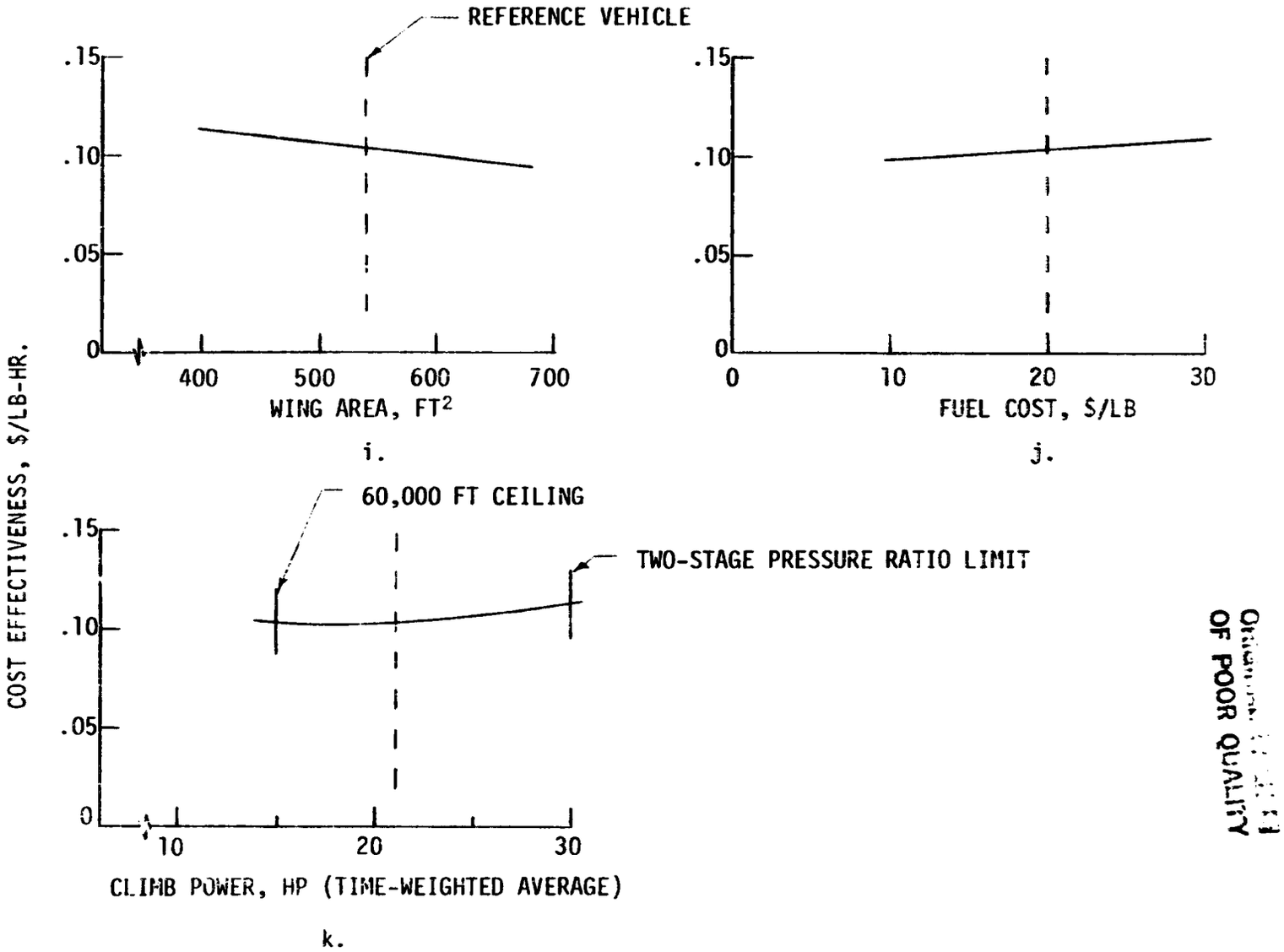

Figure 2.- Concluded

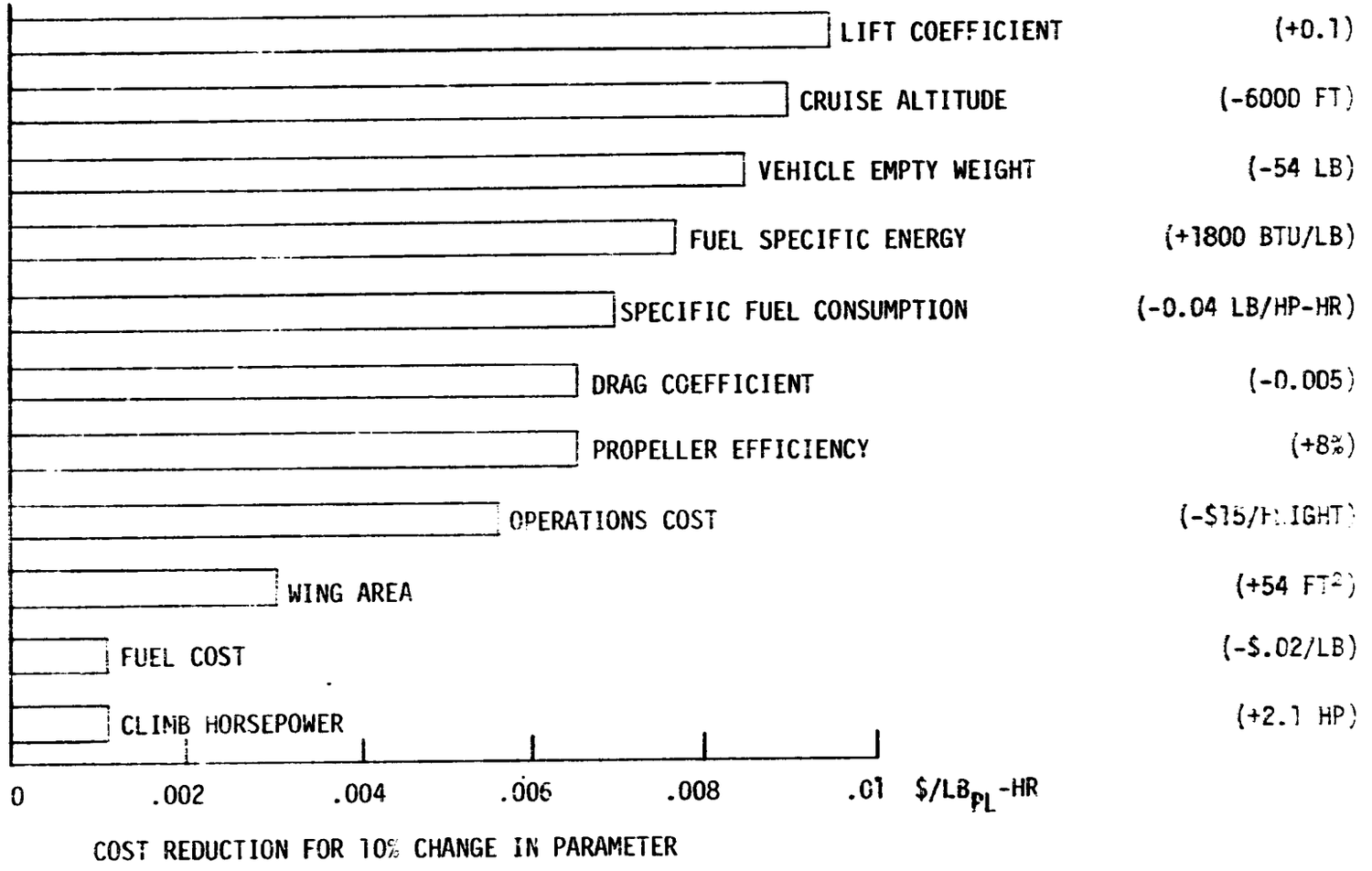

Figure 3. Cost Sensitivities

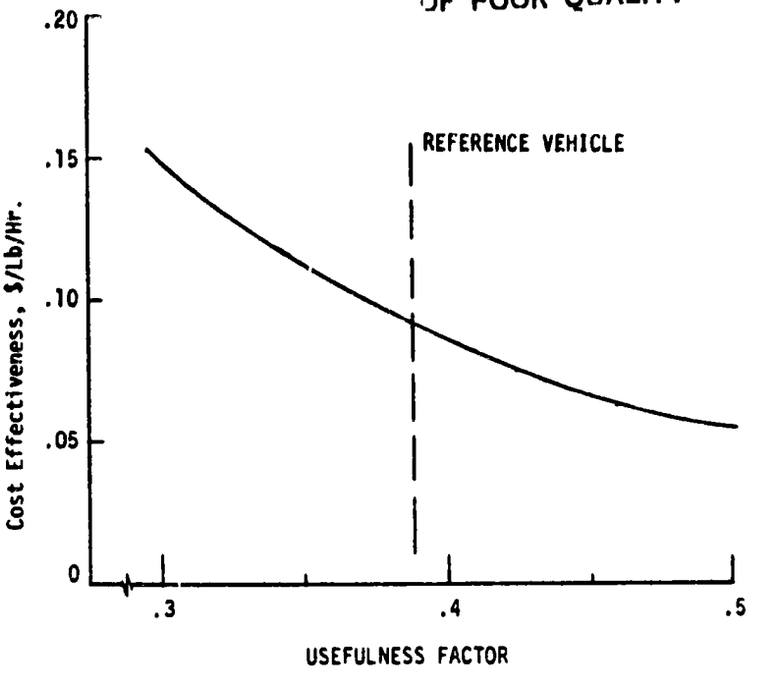

Figure 4. Cost Effectiveness vs. Usefulness Factor

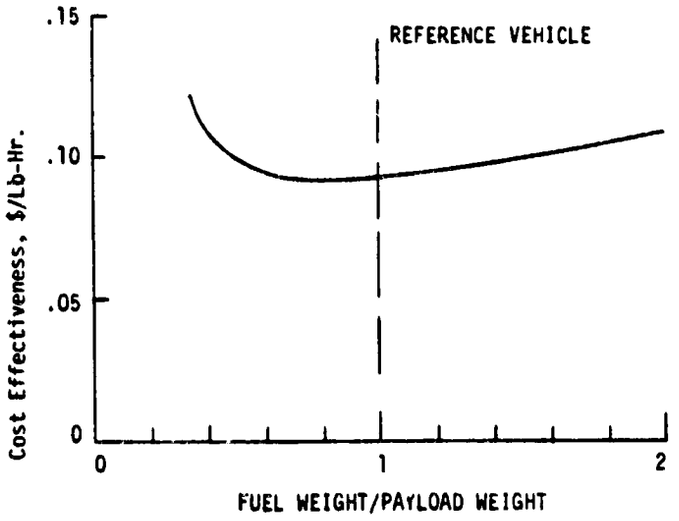

Figure 5. Cost Effectiveness vs. Fuel/Payload Ratio

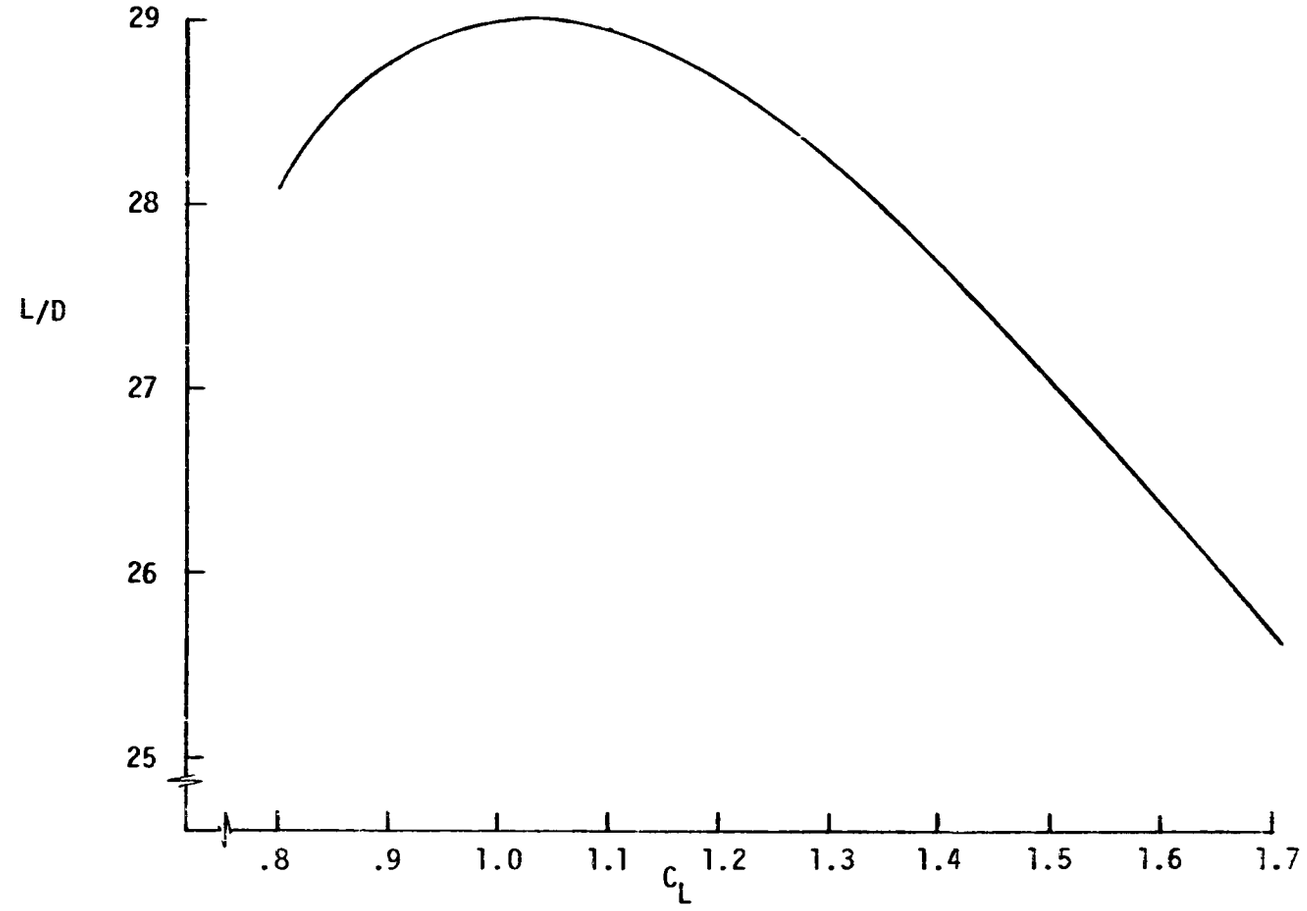

Figure 6. Range Optimization of Lift Coefficient

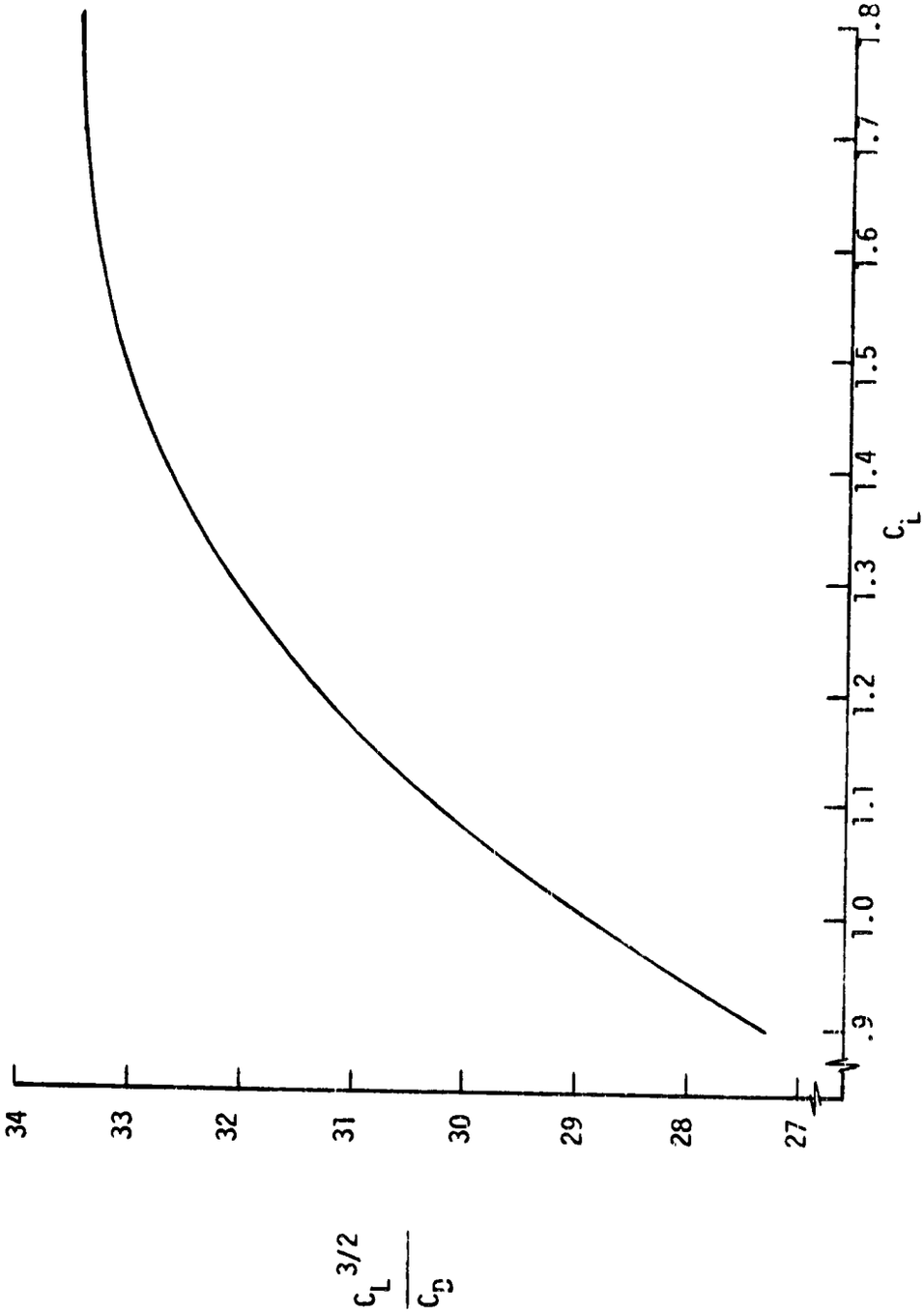

Figure 7. Endurance Optimization of Lift Coefficient

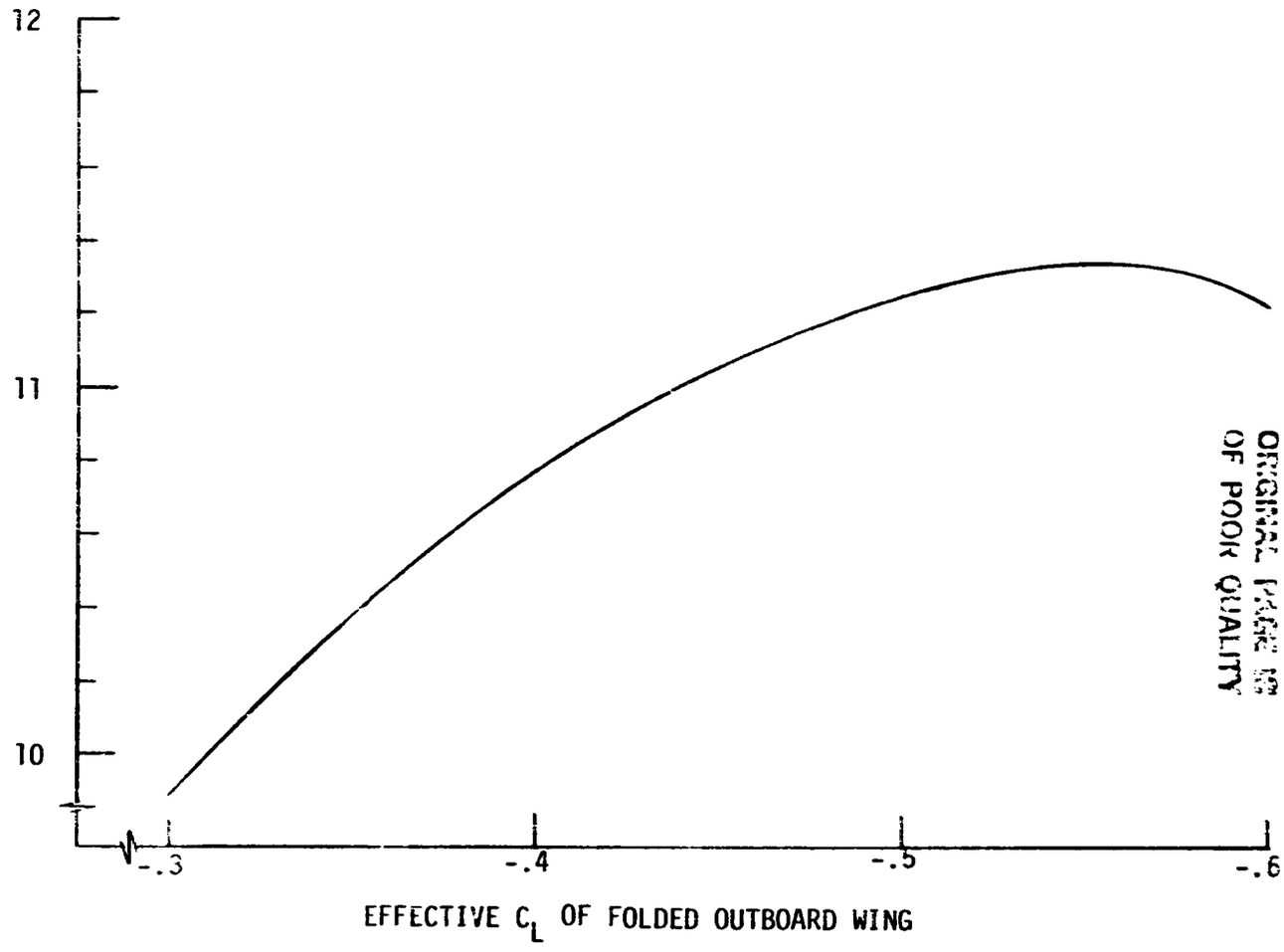

Figure 8. Wing Optimization - Climb Configuration

APPENDIX B

THE HAAP OPERATING PROCEDURE

DOC. NO. TTA-T-2P558 DATE 1/6/83

PREPARED BY:	James W. Akkerman 1/7/83
APPROVED BY:	(SECTION) Paul A. Svejkovsky 1/11/83
APPROVED BY:	(BRANCH OFFICE)
APPROVED BY:	(DIVISION)
APPROVED BY:	

1.0 Verify connection of system per the attached schematics (12 each):

1. Test article air/exhaust
2. Test article oil
3. Test article fuel
4. Dynamometer
5. Cooling air control
6. Throttle/choke
7. Turbocharger backpressure control
8. Facility vacuum/inbleed/dehumidifier
9. Facility safety
10. Cooling water
11. Facility cooling
12. Instrumentation/ignition/auto shutdown

2.0 Verify the following:

1. Oil level in engine reservoir at top fin ±1/2".
2. Dyno oil level within 5" of top of drum.
3. LN_2 supply to facility cooling shroud at 20" level or more.
4. LEL's calibrated for alarm at 0.25 LEL (alarm funct.)
5. Both vacuum pumps operating but valved "OFF"
6. Gasoline full to within 2" of top of sight glass used for volume measurement (100 to 130 octane) aviation fuel.
7. All instrumentation calibrated and in date, zero, span and functional.
8. Air control in "OPEN" position (schematic 5).
9. Backpressure control in "OPEN" position (schematic 8).
10. Throttle closed, choke open (schematic 6).
11. Dyno control valves (#4 & 5) closed (schematic 4).
12. Air inbleed valves (#6 & 7) open (schematic 8).
13. LN_2 main shut off valve 733 closed (schematic 11).
14. LN_2 control valve (#10) dehumidifier closed (schematic 8).
15. Battery charged and charger "ON".
16. Cooling water "ON" and flowing 5 gpm minimum (schematic 11).
17. Cooling fans connected and running (6 blowers, 1 fan; schematic 11).
18. Verify fan current 12±1 amps.
19. Verify safety chain for chamber door available (schematic 9).
20. Verify CO_2 fire extinguisher nearby.
21. Verify manifold pressure switch functional at 2 psig maximum.

3.0 Open fuel valves 12, 13, and 14 at bottom of measurement sight glass to allow fuel to fill carburator (schematic 3).

4.0 Open valve POV 1004 to small vacuum pump (schematic 8).

5.0 Open dyno load valve 4 (needle valve) about 2 turns (schematic 4).

6.0 Open throtle about 2 turns, pull choke momentarily, and push "START" button. Choke as necessary until smooth running is achieved. Verify oil pressure and set rpm at about 2,000 with about 400 psi on load gage (schematic 4).

7.0 Close chamber door and place safety chain across the face of the door.

8.0 Close inbleed valve HV7 to chamber (the one to the cold box). The altitude should go to about 5,000 ft (10 psia) (schematic 8).

9.0 Open the LN_2 supply valve 733 and the valve to the cold box HV10 (schematic 8).

10.0 Reverify instrumentation ready, all safety items checked, chain in place, LEL's not over 5%, and fire extinguisher handy.

11.0 Begin to add throttle, but control speed with load until wide-open throttle is achieved at 2500 rpm. This should be below the speed where any boost is achieved.

12.0 Close the air inbleed valve HV6 (ambient) to let about 8 psia in the chamber, reducing load to allow speed to increase to provide about one atmosphere (in the engine air receiver-manifold pressure).

13.0 As the chamber temperature drops, begin to close off the ambient air inbleed, HV6, and open the dehumidifier inbleed, HV7 to supply dry air.

14.0 Continue to close off air inbleed until about 5 psia where the large pump must be opened valve POV 1005 to the chamber, simultaneously opening the dry air inbleed (HV7) to hold 5 psia.

15.0 Continue to restrict the inbleed, holding the manifold pressure by reducing the load and allowing engine rpm to increase (maximum engine rpm is 8,000).

CAUTION:
- --Go slowly and watch cylinder heat temperature--it should not go over 425°F.
- --Also, oil temperature not over 375°F.
- --Control LN_2 flow to keep the cold wall at about -100°F.
- --Control the dehumidifier LH_2 to not waste LH_2 out the dump line.
- --If LEL gets to 0.25, stop and fix cause.

NOTE: If cylinder head temperature goes over 425°F, reduce manifold pressure by slowing engine rpm, or by going to lower chamber pressure without increasing engine rpm.

16.0 At some chamber pressure, hopefully 1 psia, the manifold pressure will reduce and the engine will stop. At this point, begin the inbleed (valve HV7), shut off the large pump, and allow the chamber to go to about 10 psia. Restart the engine and repeat as necessary to define the engine operating limits.

NOTE: The air control may have to be used to regulate cylinder head temperature in the range between 8 psia and 4 psia (schematic 5.)

The exhaust backpressure control will have to be used to balance the inlet air pressure (chamber pressure) and the exhaust pressure to equal levels (schematic 7).

17. Repeat runs as required to get data at various pressure levels (maximum and minimum power, SFC, etc.) i.e., 2, 1.5, 1, 0.75 psia, if possible. Keep the chamber as cold as possible without freezing the instrumentation lines.

18. After completion of test runs, shut off the LN_2 (valves 733 and HV10), open the inbleed valves HV6 and HV7 and allow the engine to idle at about 1800 rpm and 600 psi load until the temperature in the chamber returns to about 70°F.

19. Shut off the fuel (valves #12, 13, and 14) and allow the engine to deplete the supply in the plumbing before turning off the ignition. Let the instrumentation operate for a cycle or two after engine shutdown.

20. Secure the system as follows:

1. Turn off the cooling water.
2. Turn off GN_2 supply. See facility schematic.
3. Turn off vacuum pumps.
4. Turn off fans.
5. Disconnect chain door restraint.
6. Power down the instrumentation.
7. Close load valves HV4 and HV5.
8. Turn off battery charger.

21. Place catch pan under door joint and open door.

EMERGENCY PROCEDURE

A. In case of fire in chamber during run:

1. Close inbleed valves HV6 and HV7.
2. Shut off fuel (HV12, 13, and 14).
3. Monitor temperature.

B. In case of fire in facility area:

1. Call fire department x3333.
2. Use CO_2 fire extinguishers.
3. Terminate facility power.
4. Close all doors.
5. Avoid smoke inhalation.

22. For each test run (to altitude and back) designate a run number, date, etc.

23. Recheck data system calibration, etc. Record final "0" valves with the system "down" before instrumentation is shutdown.

24. Record on data sheet any observations which may need work before the next run.

25. In case a measurement of specific fuel consumption is to be made, close valve HV12 and open valve HV13 allowing engine to operate using fuel out of sight glass. Measure and record on Fluke print the time required to use the marked amount. reverse valves to resupply the sight glass.

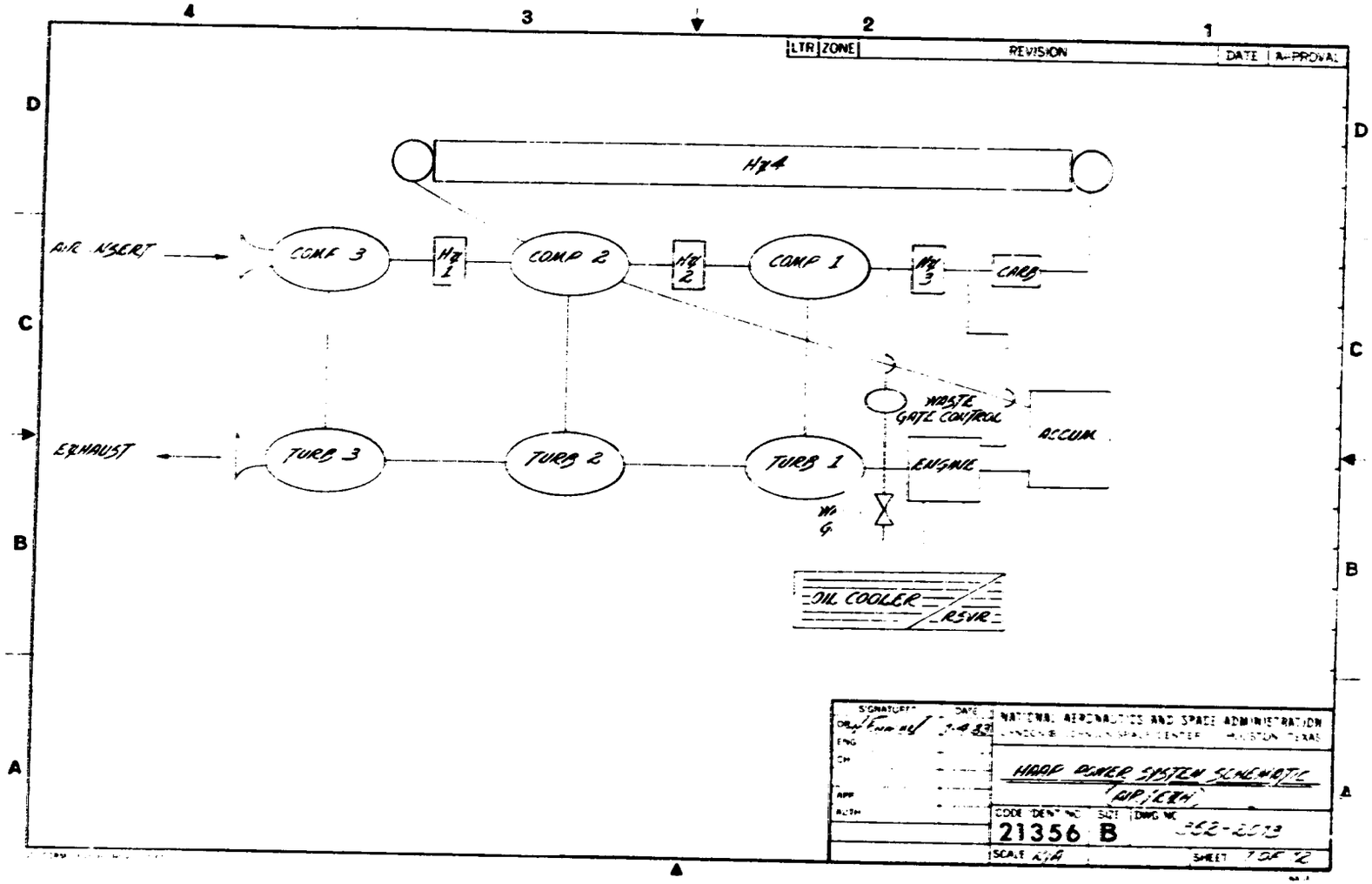

Figure 1.

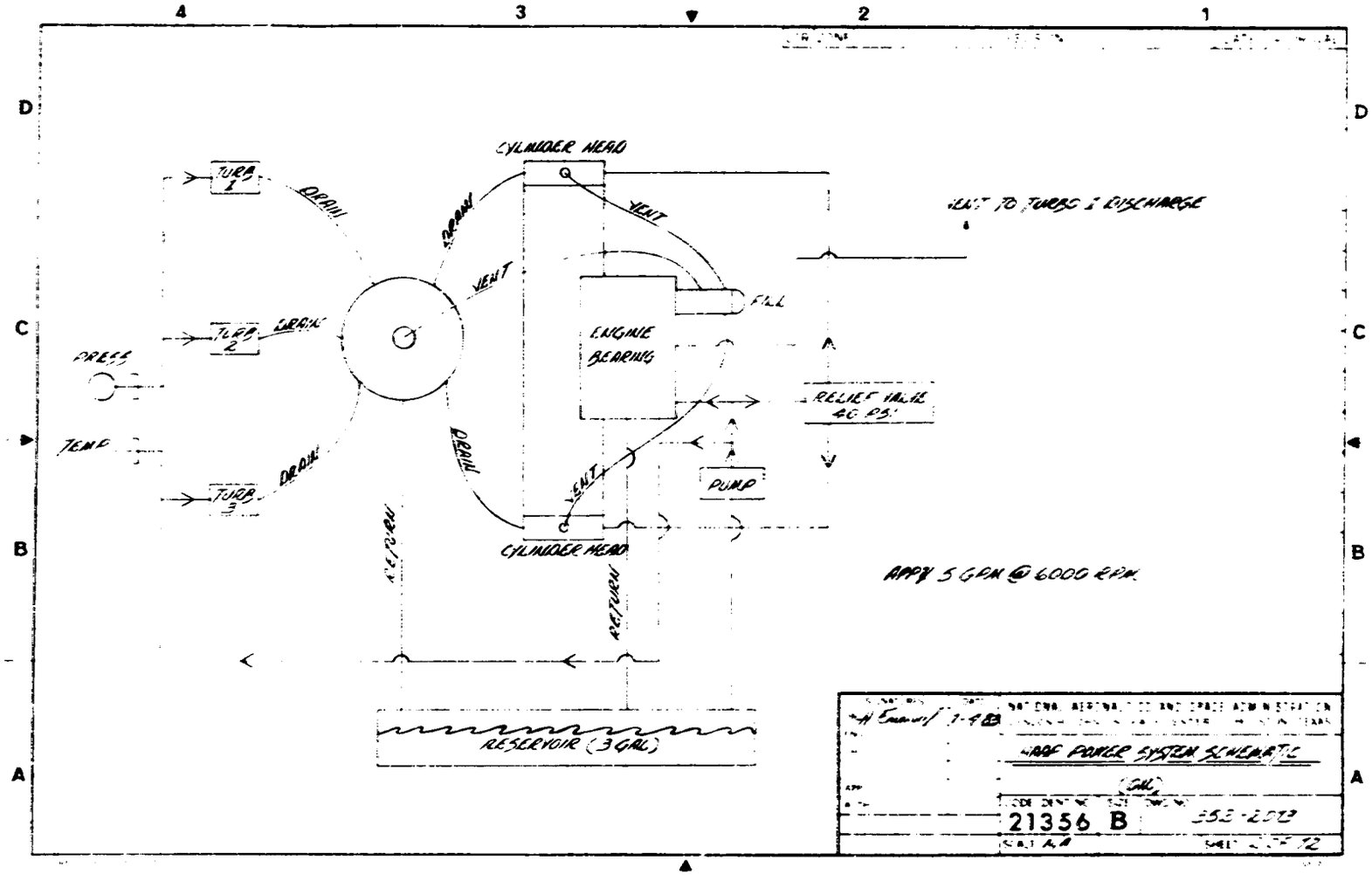
4
3
2
1
D
C
B
A
CYLINDER HEAD
TURB 1
DRAIN
TURB 2
DRAIN
PRESS
TEMP
TURB 3
DRAIN
DRAIN
VENT
ENGINE BEARING
FILL
VENT TO TURBO & DISCHARGE
RELIEF VALVE 40 PSI
PUMP
VENT
CYLINDER HEAD
RETURN
RETURN
APPX 5 GPM @ 6000 RPM
RESERVOIR (3 GAL)
HHF POWER SYSTEM SCHEMATIC
21356 B

Figure 2.

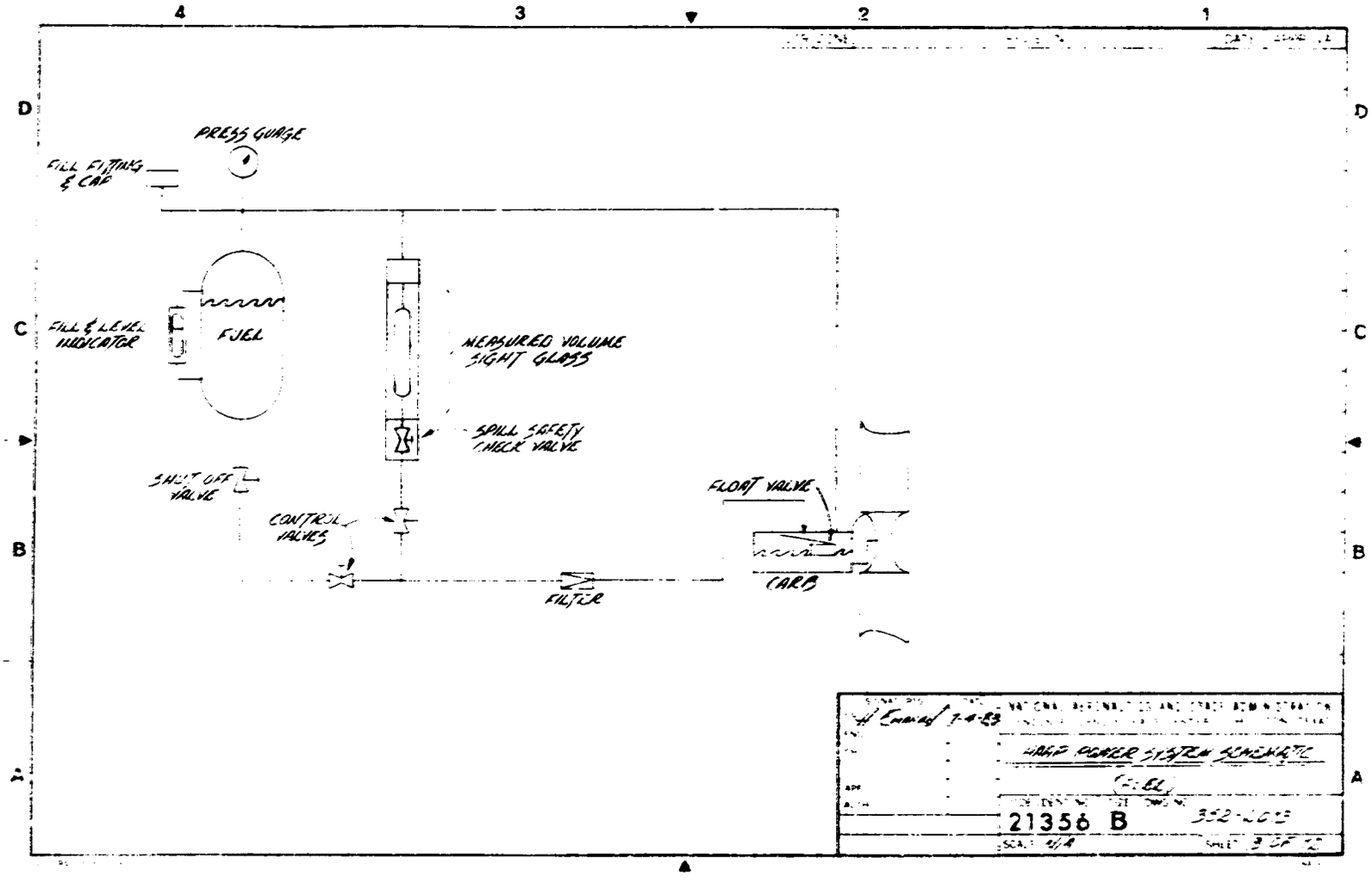

Figure 3.

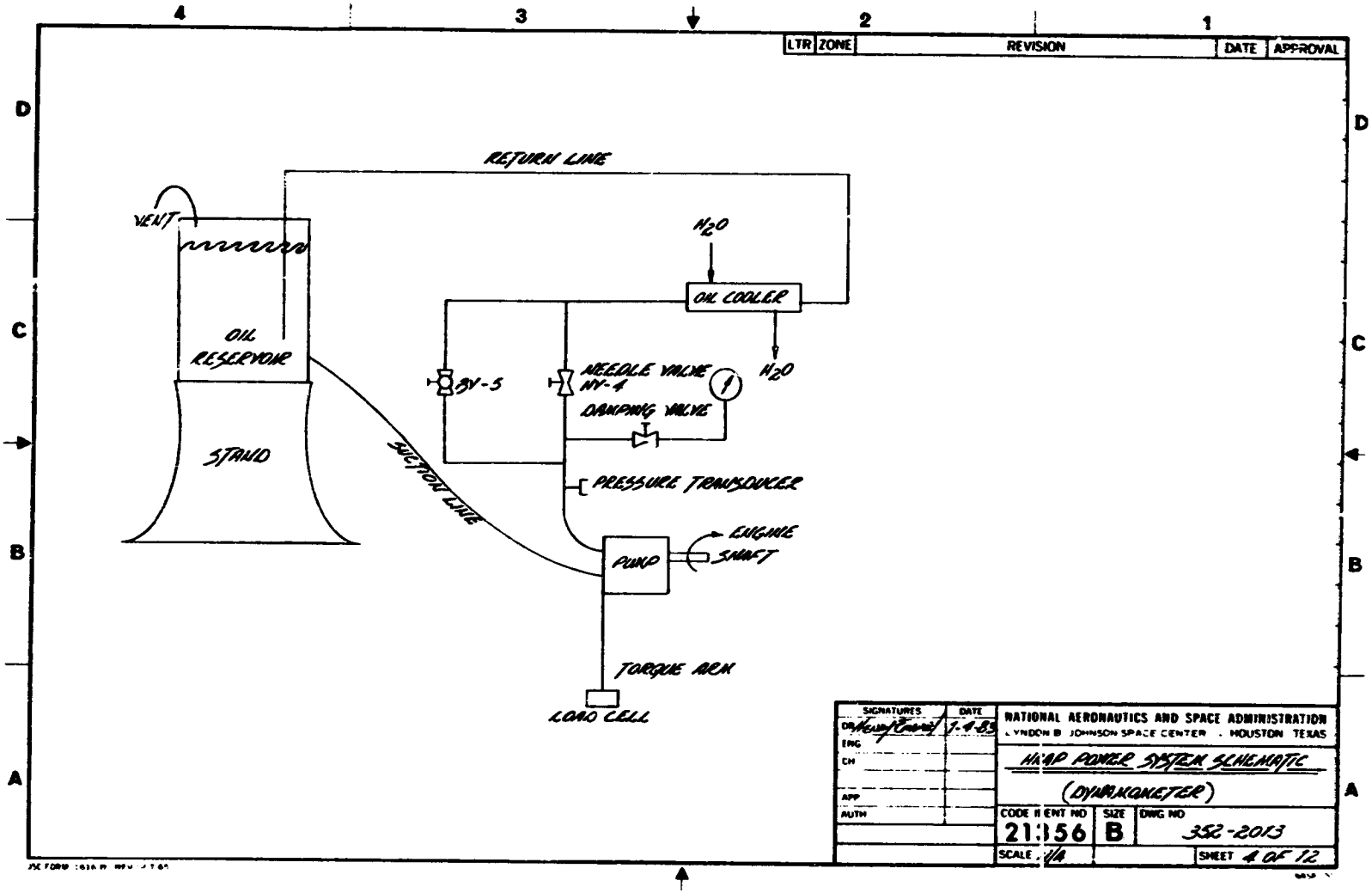

Figure 4.

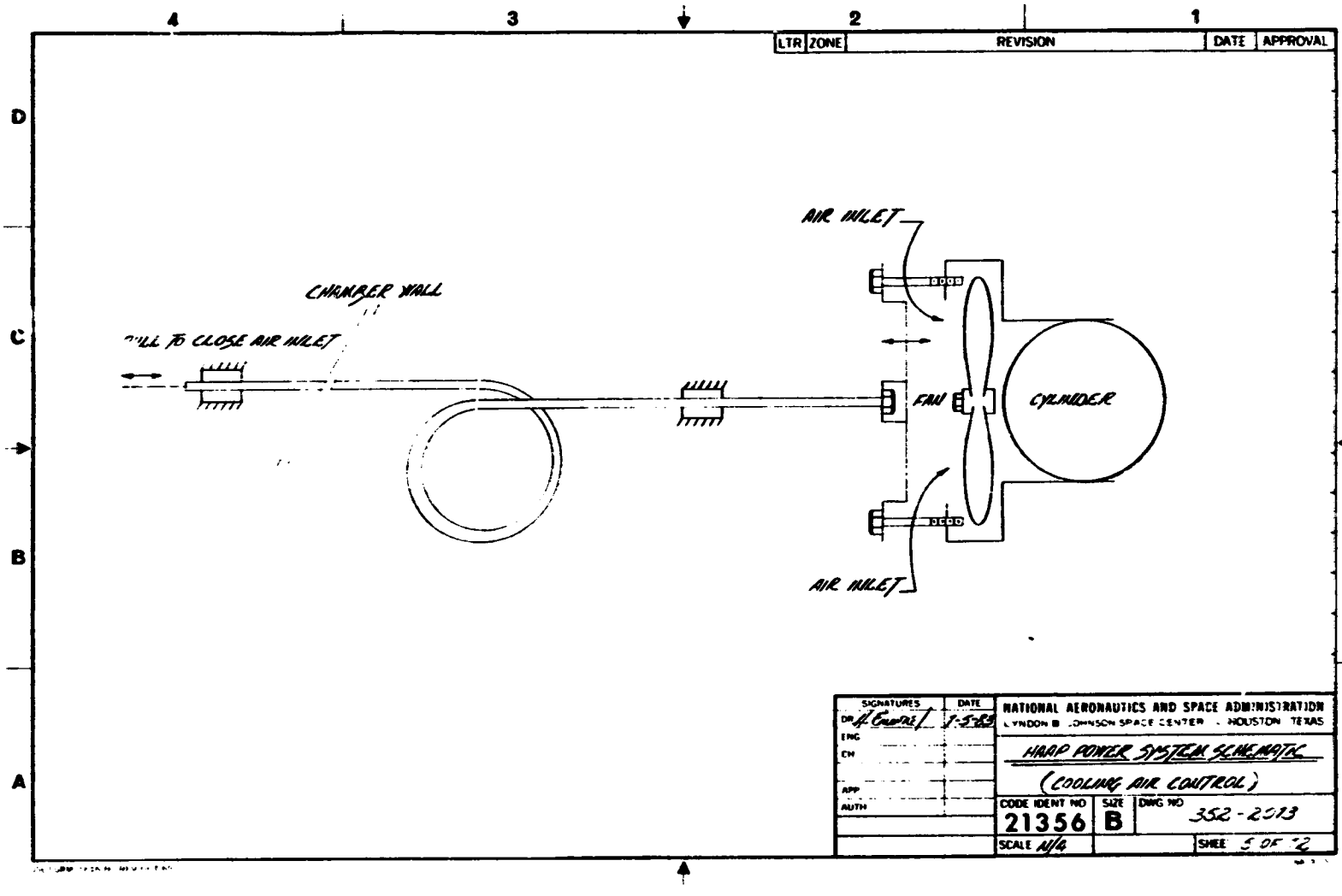

Figure 5.

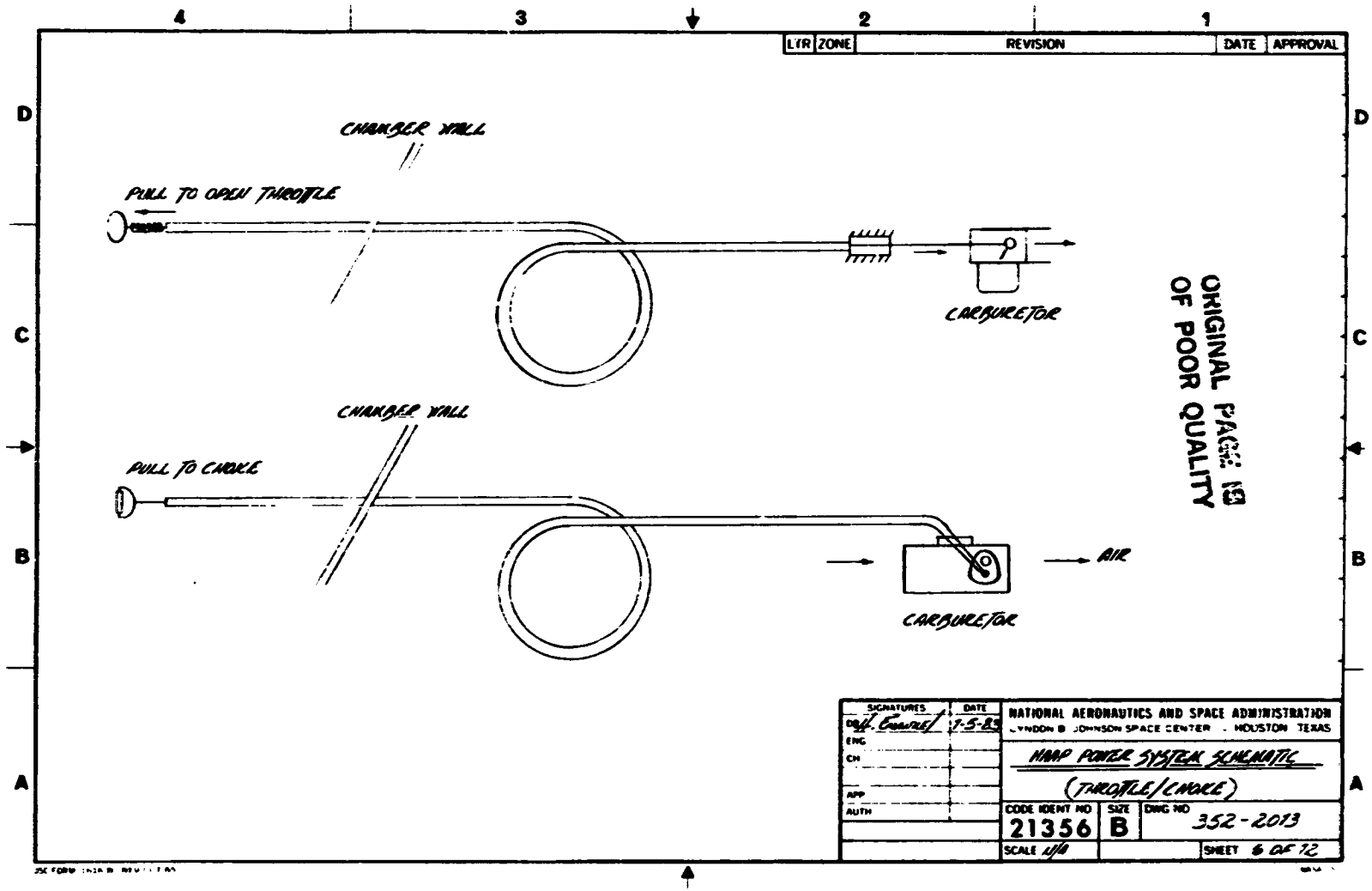
4
3
2
1
LTR
ZONE
REVISION
DATE
APPROVAL
D
C
B
A
CHAMBER WALL
PULL TO OPEN THROTTLE
CARBURETOR
CHAMBER WALL
PULL TO CHOKE
AIR
CARBURETOR
ORIGINAL PAGE IS OF POOR QUALITY
SIGNATURES
DRAWN
ENG
CH
APP
AUTH
DATE
NATIONAL AERONAUTICS AND SPACE ADMINISTRATION
LYNDON B JOHNSON SPACE CENTER - HOUSTON TEXAS
NIMP POWER SYSTEM SCHEMATIC
(THROTTLE/CHOKE)
CODE IDENT NO
21356
SIZE
B
DWG NO
352-2013
SCALE 1/1
SHEET 6 OF 12

Figure 6.

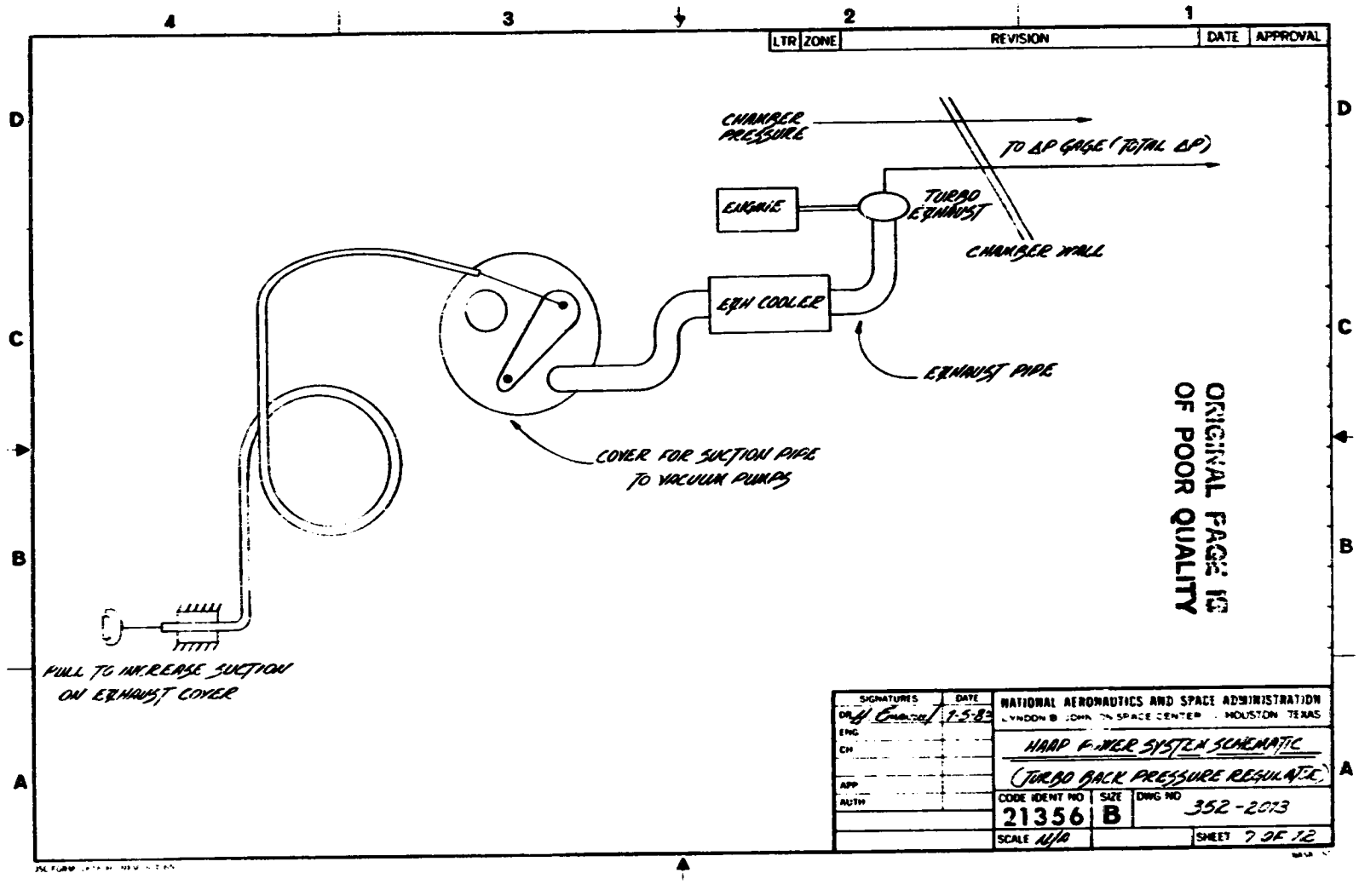
4
3
2
1
LTR
ZONE
REVISION
DATE
APPROVAL
D
C
B
A
CHAMBER PRESSURE
TO ΔP GAGE (TOTAL ΔP)
ENGINE
TURBO EXHAUST
CHAMBER WALL
EXH COOLER
EXHAUST PIPE
COVER FOR SUCTION PIPE TO VACUUM PUMPS
PULL TO INCREASE SUCTION ON EXHAUST COVER
ORIGINAL PAGE IS OF POOR QUALITY
SIGNATURES
DATE
DR
ENG
CH
APP
AUTH
1-5-83
NATIONAL AERONAUTICS AND SPACE ADMINISTRATION
LYNDON B. JOHNSON SPACE CENTER HOUSTON TEXAS
HARP POWER SYSTEM SCHEMATIC
(TURBO BACK PRESSURE REGULATED)
CODE IDENT NO
21356
SIZE
B
DWG NO
352-2073
SCALE 1/10
SHEET 7 OF 12

Figure 7.

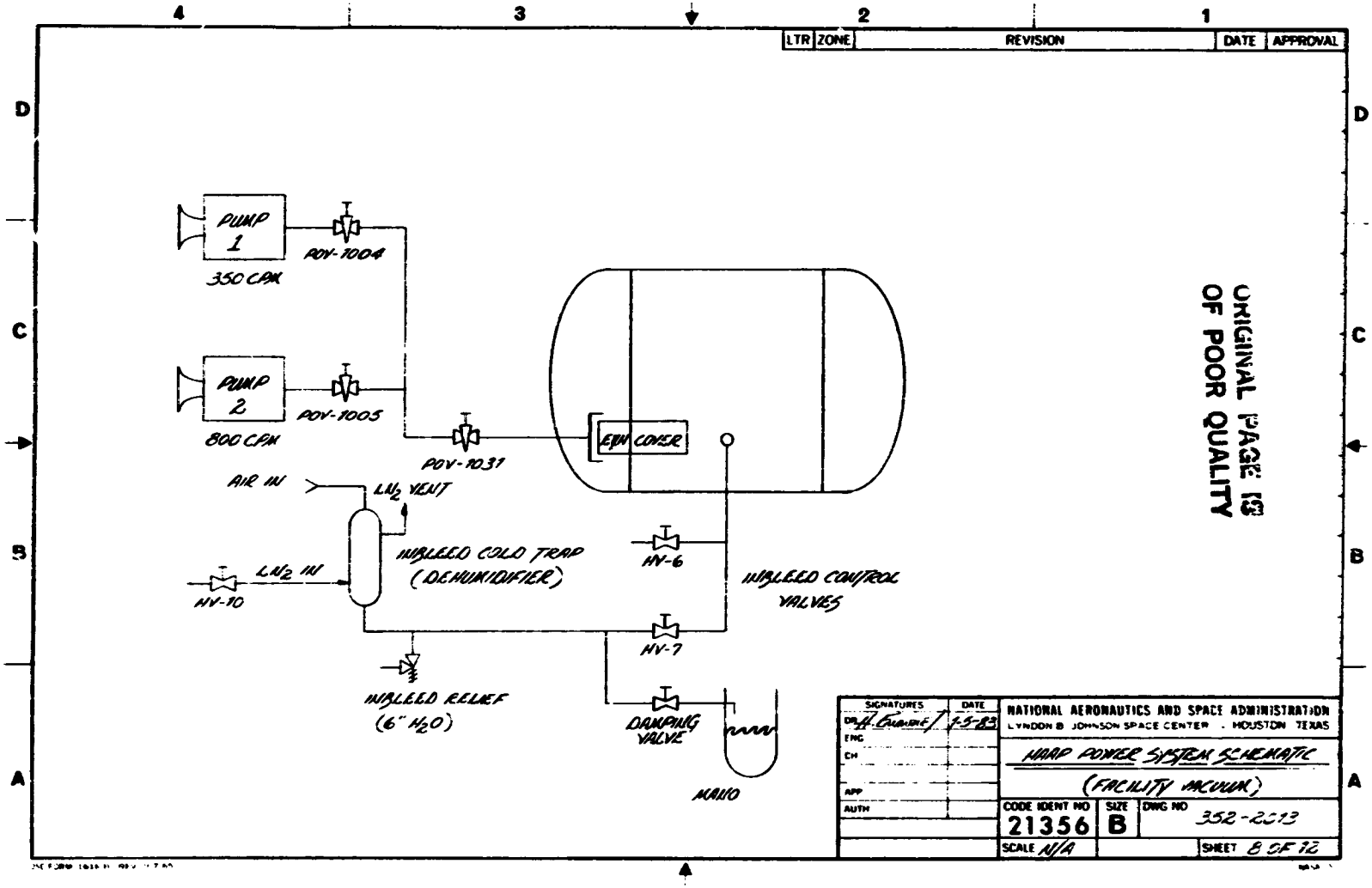
4
3
2
1
LTR
ZONE
REVISION
DATE
APPROVAL
D
C
B
A
PUMP 1
350 CFM
POV-1004
PUMP 2
800 CFM
POV-1005
POV-1031
EJM COVER
AIR IN
LN2 VENT
LN2 IN
HV-10
INBLEED COLD TRAP
(DEHUMIDIFIER)
HV-6
INBLEED CONTROL VALVES
HV-7
INBLEED RELIEF
(6" H2O)
DAMPING VALVE
MANO
ORIGINAL PAGE IS
OF POOR QUALITY
SIGNATURES
DATE
DR
ENG
CH
APP
AUTH
7-5-83
NATIONAL AERONAUTICS AND SPACE ADMINISTRATION
LYNDON B JOHNSON SPACE CENTER - HOUSTON TEXAS
HARP POWER SYSTEM SCHEMATIC
(FACILITY VACUUM)
CODE IDENT NO
21356
SIZE
B
DWG NO
352-2013
SCALE N/A
SHEET 8 OF 12

Figure 8.

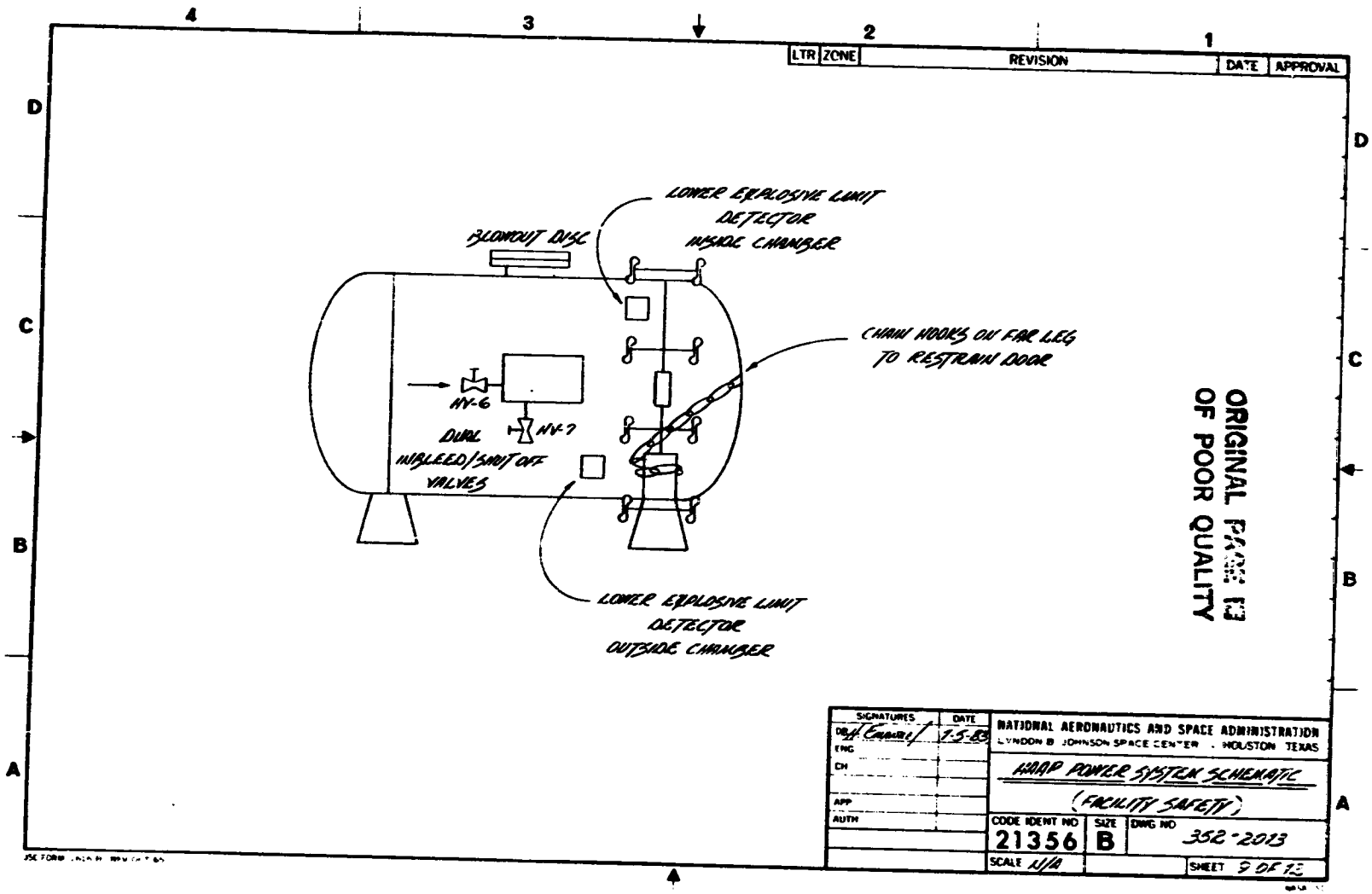
LTR
ZONE
REVISION
DATE
APPROVAL
LOWER EXPLOSIVE LIMIT DETECTOR INSIDE CHAMBER
BLOWOUT DISC
CHAIN HOOKS ON FAR LEG TO RESTRAIN DOOR
HV-6
HV-7
DUAL N2BLEED/SHUT OFF VALVES
LOWER EXPLOSIVE LIMIT DETECTOR OUTSIDE CHAMBER
ORIGINAL PAGE IS OF POOR QUALITY
SIGNATURES
DATE
DES
ENG
CH
APP
AUTH
NATIONAL AERONAUTICS AND SPACE ADMINISTRATION
LYNDON B JOHNSON SPACE CENTER . HOUSTON TEXAS
HRAP POWER SYSTEM SCHEMATIC
(FACILITY SAFETY)
CODE IDENT NO
21356
SIZE
B
DWG NO
352-2013
SCALE N/A
SHEET 9 OF 13

Figure 9.

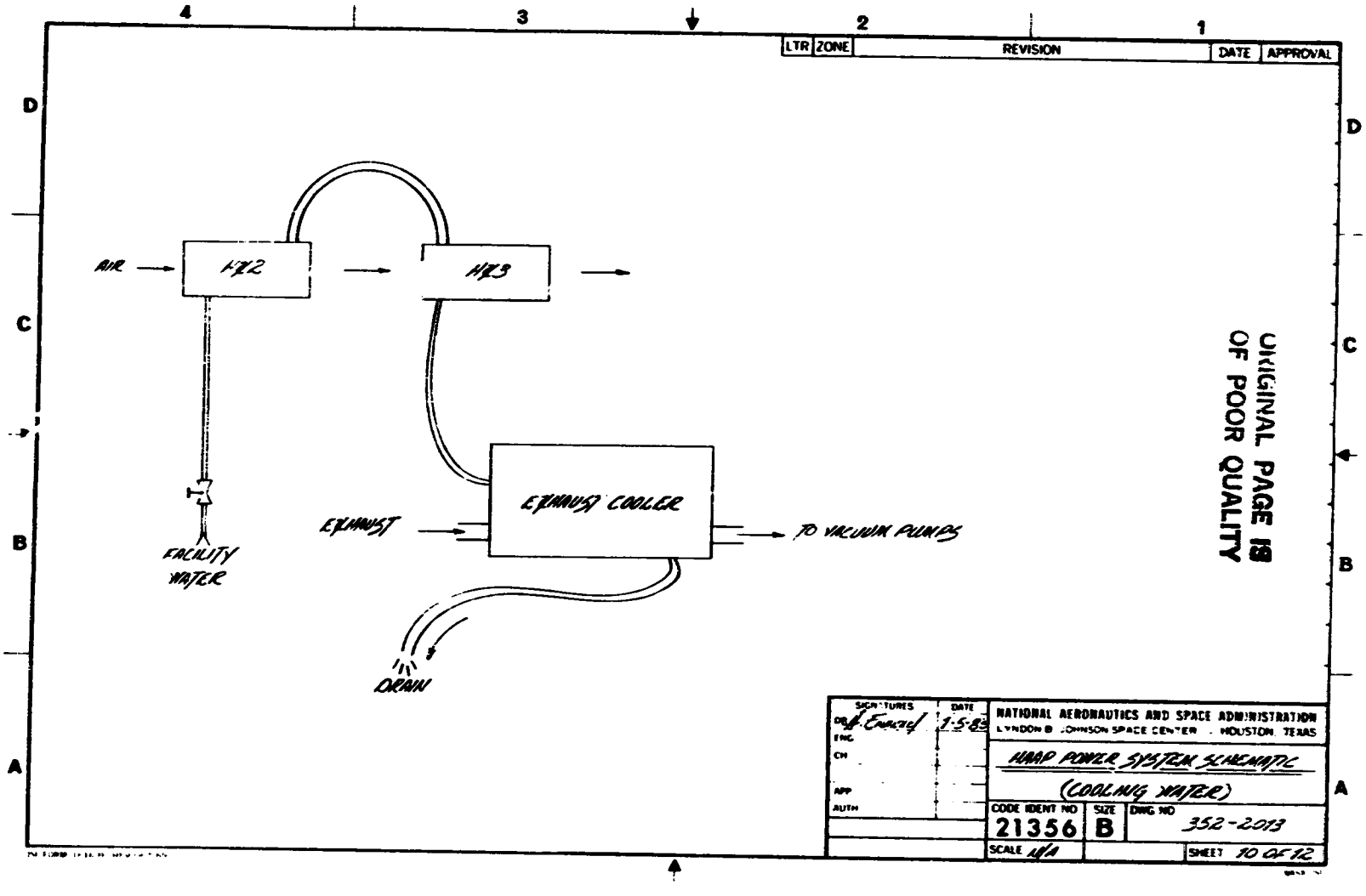
4
3
2
1
LTR
ZONE
REVISION
DATE
APPROVAL
D
C
B
A
AIR
HX2
HX3
EXHAUST COOLER
EXHAUST
TO VACUUM PUMPS
FACILITY WATER
DRAIN
ORIGINAL PAGE IS OF POOR QUALITY
SIGNATURES
DR
ENG
CH
APP
AUTH
DATE
1-5-88
NATIONAL AERONAUTICS AND SPACE ADMINISTRATION
LYNDON B. JOHNSON SPACE CENTER - HOUSTON, TEXAS
HHAP POWER SYSTEM SCHEMATIC
(COOLING WATER)
CODE IDENT NO
21356
SIZE
B
DWG NO
352-2013
SCALE 1/1
SHEET 10 OF 12

Figure 10.

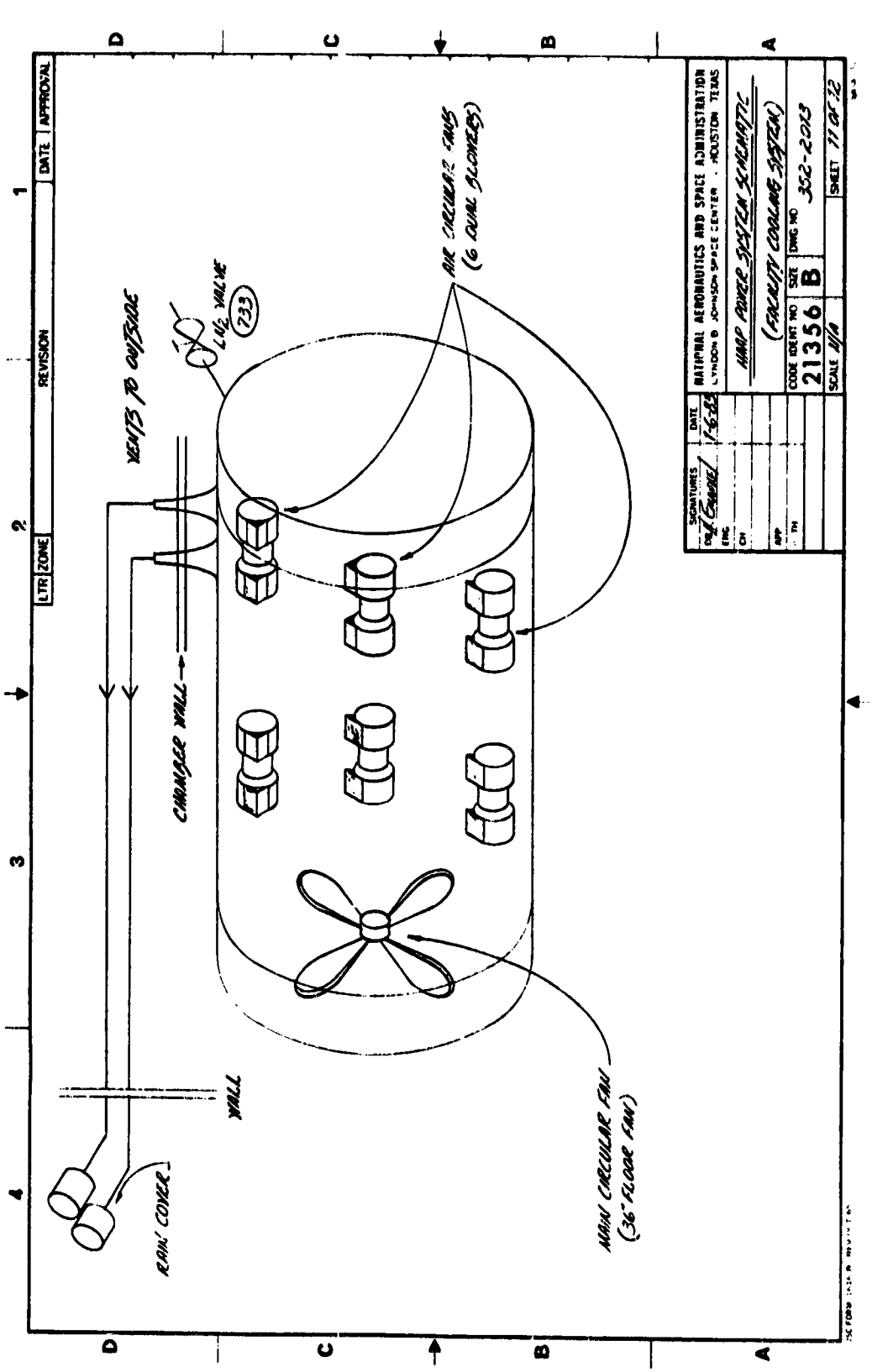

Figure 11.

HAAP POWERPLANT TEST

RUN# TIME DATE

TEMPS

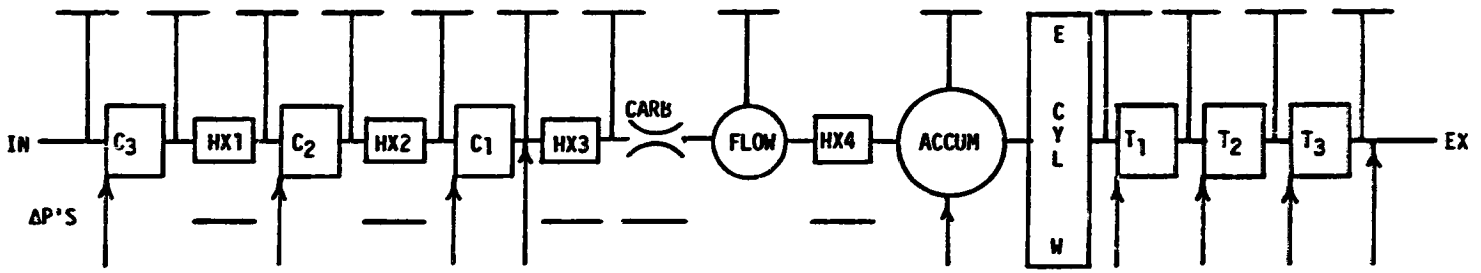

PRESSURES TOTAL ΔP = _____

RPM =

FLOW =

MASS FLOW =

LOAD PR =

TORQUE =

OIL TEMP =

OIL PR=

T. OIL TEMP =

T. OIL PR =

DENS. ALT. =

TURBOS

COMP. RATIOS:

1 =

2 =

3 =

NET =

TURBINE RATIOS:

1 =

2 =

3 =

NET =

1.

2.

3.

SPEEDS: 1 =

2 =

3 =

EFFICIENCY: 1 =

2 =

3 =

NET =

Figure 12.- HAAP powerplant test form.

APPENDIX C

EVENT CHRONOLOGY

HIGH ALTITUDE AERODYNAMIC PLATFORM
CONCEPT EVALUATION AND PROTOTYPE ENGINE TESTING
EVENT CHRONOLOGY

YEAR 1979

M.	WK.	CODE	EVENT
4	1		
APRIL	2		
	3	C	RTOP PROPOSED BY JIM WOOD FOR CONCEPT STUDY
		A	ANALYSIS OF RANKINE CYCLE SYSTEM PERFORMANCE
	4		
5	1		
	2		
MAY	3		
	4		
6	1	A	RANKINE CYCLE SYSTEM DESIGN
	2		
JUNE	3		
	4		

HIGH ALTITUDE AERODYNAMIC PLATFORM
CONCEPT EVALUATION AND PROTOTYPE ENGINE TESTING
EVENT CHRONOLOGY

YEAR 1979

M.	WK.	CODE	EVENT
7	1		
JULY	2		
	3		
	4		
8	1	M	PRESENTATION OF RANKINE CYCLE ANALYSES TO DR. KRAFT
AUGUST	2		
	3	C	DISCRETIONARY FUND ALLOCATION ($50,000)
	4		RTOP FOR RPV ENGINE DEVELOPMENT
9	1	C	P. R. FOR NSI ($30,000)
SEPTEMBER	2		
	3	C	DALE REED NOTE ON ENGINE PERFORMANCE ESTIMATES
		C	LANGLEY MEETING ANNOUNCEMENT (NOVEMBER)
	4	C	P. R. OMC ENGINE ($1,840)

HIGH ALTITUDE AERODYNAMIC PLATFORM
CONCEPT EVALUATION AND PROTOTYPE ENGINE TESTING
EVENT CHRONOLOGY

YEAR 1977

M.	WK.	CODE	EVENT
10	1	A	OTTO CYCLE PERFORMANCE ANALYSIS COMPLETION - COMPRESSION RATIO SEEN AS PRIMARY DRIVER ON PERFORMANCE AND ECONOMY
OCTOBER	2	C	P. R. OUT ON TURBOS
	3	C	JUSTIFICATION FOR NON-COMPETITIVE PROCUREMENT ON TURBOS
		C	INVITATION TO INTERCENTER MEETING ON HAAP AT LANGLEY
		C	NOTE TO DALE REED ON OTTO CYCLE ENGINE PERFORMANCE WITH VAR. COMPRESSION RATIO
	4	C	DELIVERY OF OMC ENGINE
		C	CONTRACT FOR TURBOS
11	1	C	PHONE CALL TO OMC - ASKED FOR ENGINE DRAWINGS
NOVEMBER		EC	COOLING SHROUD FOR ALT. CHAMBER
	2	M	LANGLEY MEETING PER HEADQUARTERS REQUEST
	3	C	P. R. FOR HONDA ENGINE FOR VAR. COMPRESSION RATIO TEST
		SD	CRANK MODIFICATION
	4	EC	ENGINE CHECKOUT
12	1		
DECEMBER	2	SD	CYLINDER HEAD MODIFICATION
	3		
	4		

HIGH ALTITUDE AERODYNAMIC PLATFORM
CONCEPT EVALUATION AND PROTOTYPE ENGINE TESTING
EVENT CHRONOLOGY

YEAR 1980

M.	WK.	CODE	EVENT
JANUARY 1	1	C	RTOP TO TEST VARIABLE COMPRESSION RATIO ENGINE
	2		
	3		
	4		
FEBRUARY 2	1	EO	PARTS MODIFICATION
		EO	PARTS MODIFICATION
	2	C	CALL FOR NEW DESCRETIONARY FUNDED ACTIVITIES
	3	C	LETTER TO OMC (THANKS FOR DRAWINGS)
	4		
MARCH 3	1		
	2	EO	BASEPLATE FAB.
	3		
	4		

HIGH ALTITUDE AERODYNAMIC PLATFORM
CONCEPT EVALUATION AND PROTOTYPE ENGINE TESTING
EVENT CHRONOLOGY

YEAR 1980

M.	WK.	CODE	EVENT
4			
APRIL	1		
	2	P1	CONTROL VALVE
		C	PHONE CALL TO OMC - ASK ABOUT PARTICULARS OF ENGINE & DRAWING
		C	TEST PLAN FOR TTA
	3	C	LETTER FROM OMC - CRANKCASE ASSY. DRAWING
		C	LETTER FROM FRANKLIN (TECH. SERV. TO SCHEDULE PARTS).
		EO	TURBO BLOCK
		C	LETTER TO OMC ASKING ABOUT ENGINE TESTING
	4	P2	MOLY COAT H
		P3	MOTOR OIL
		C	MINUTES OF MEETING WITH TTA - BASIC AGREEMENTS
		C	MEMO FROM J. D. WILLIAMS - (TECH. SERVICES TOO BUSY ON SHUTTLE)
5			
MAY	1	C	LETTER TO SCHWETZER ON TURBOS
	2		
	3	C	PROPSOSED LETTER FROM KRAFT TO DFRC
		P4	COPPER SHEET
	4	EO	DIP TUBE
		EO	EXHAUST COOLER
6			
JUNE	1	EO	TORQUE ARM
		D	HAAP - 2B DRAWING (TAPERED WING)
	2	T	A INST C/O
		T	B SYS C/O
		T	C IGNITION TIMING VS TORQUE
		T	D EXHAUST, AIR CLEANER, ON AND OFF
		T	E 10 W OIL PART THROTTLE, UPPER OIL LUBE
		T	F OVERSHEED
	3	C	PUBLISH SEA LEVEL STOCK ENGINE TEST DATA PLOT (TORQUE & POWER VS SPEED)
		C	MEMO FROM PEREZ ON HAAP AERO EVALUATION
	4	C	LETTER TO OMC DATA ON SEA LEVEL TESTS
		EO	FLANGE & GASKET

HIGH ALTITUDE AERODYNAMIC PLATFORM
CONCEPT EVALUATION AND PROTOTYPE ENGINE TESTING
EVENT CHRONOLOGY

YEAR 1980

M.	WK.	CODE	EVENT
7	1	C	LETTER FROM SCHWETZER (DATA FOR TURBO OVERHAUL ETC)
JULY	2		
	3	C	P. R. FOR HEAT EXCHANGER TUBING
		C	P. R. FOR NSI FUNDING
	4		
8	1	C	OAST REVIEW OF ENERGY PROJECTS
		T	G. STOCK ENGINE AT ALTITUDE
		T	H. STOCK ENGINE AT ATTITUDE
AUGUST	2	D	DRAWING OF AFTERCOOLER COMPLETE
		D	DRAWING OF OIL SUMP/COOLER COMPLETE
	3	C	MEMO TO HEADQUARTERS FROM COVINGTON ASKING SUPPORT
		D	DRAWING (3 VIEW) OF ENGINE INSTALLATION COMPLETE
	4	EO	TURBO INSTALLATION
		C	PUBLSIH ALTITUDE TEST DATA FOR STOCK ENGINE
9	1	EO	TURBO MOUNTING
SEPTEMBER	2	M	PROJECT REVIEW WITH DIRECTOR OF E & D
	3		
	4	D	DRAWING OF NAAP-3 COMPLETE STRAIGHT WING
		P5	O RINGS

HIGH ALTITUDE AERODYNAMIC PLATFORM
CONCEPT EVALUATION AND PROTOTYPE ENGINE TESTING
EVENT CHRONOLOGY

YEAR 1980

M.	WK.	CODE	EVENT
10 OCTOBER	1		
	2		
	3	EO	PUMP ADAPTER
		EO	EXHAUST FLANGE
	4	C	DELIVERY OF VARIABLE COMPRESSION RATIO PARTS
		EO	EXHAUST FLANGE
		EO	OIL COOLER
		EO	EXHAUST FLANGE
		EO	EXHAUST CONNECTOR
11 NOVEMBER	1	EO	AIR COOLER
		EO	HOLES IN BASEPLATE
	2	EO	WELD MANIF.
		EO	INT. MANIF. ADAPTER
		EO	OIL LINE CONNECTOR
	3		
	4		
12 DECEMBER	1		
	2	T	I. DATA SYSTEM C/O FOR ALTITUDE SYSTEM (2 TURBO)
		T	J. S. L. 2 TURBO SYSTEM & ALTITUDE
		T	K. S. L. 2 TURBO SYSTEM & ALTITUDE
			L. S. L. ? TURBO SYSTEM & ALTITUDE
	3	T	M. S. L. 2 TURBO SYSTEM & ALTITUDE (OIL PRESSURE INTERMITTANT)
		P6	BRASS TUBE
		T	N. S. L. 2 TURBO SYSTEM (TURBO SHEEDS WRONG)
		P7	PHOTOTRANSISTORS
	4		

HIGH ALTITUDE AERODYNAMIC PLATFORM
CONCEPT EVALUATION AND PROTOTYPE ENGINE TESTING
EVENT CHRONOLOGY

YEAR 1981

M.	WK.	CODE	EVENT
1 JANUARY	1		
	2		
	3		
	4	M	FORTUNE 500 PRESENTATION
2 FEBRUARY	1		
	2	P8 T T T	RADIATOR HOES 1. CHECKOUT RUN 2. LOAD CONTROL VALVE TOO SMALL, PUMP CAVITATION 3. SUCCESSFUL SEALEVEL RUN OF 2 STAGE TURBO SYSTEM
	3		
	4	T T EO	4. 20,000 FEET ALTITUDE 1/2 RATED POWER 5. 10,000 FEET SEALEVEL RATED POWER IGNITION TIMING CONTROL
3 MARCH	1	T C EO	6. IGNITION/.6 A/R (POOR RESULTS) LETTER TO SCHWETZER (20,000 FT MAXIMUM ALTITUDE ! COMPRESSION RATIO RAISER
	2	C	SENSITIVITY ANALYSIS REPORT BY ZEHENTNER OUT
	3		
	4	T C C	7. A/R= .75 OR TURBO 2 LETTER TO RAYJAY (HELP!) MEMO FORM HEADQUARTERS - MEETING HEADQUARTERS ON APRIL 17TH

HIGH ALTITUDE AERODYNAMIC PLATFORM
CONCEPT EVALUATION AND PROTOTYPE ENGINE TESTING
EVENT CHRONOLOGY

YEAR 1981

M.	WK.	CODE	EVENT
4	1		
	2	C	NSI P. R. 16571-F FOR IHI TURBO
APRIL		P9	TURBOCHARGER
		M	MEETING AT HEADQUARTERS ON HAAP. DICK KENNEDY ATTENDING
	3	EO	EXHAUST MANIF MOD
		EO	TURBO ADAPTER
		EO	DRAWING CONNECTOR
		EO	AIR DELIVERY
	4	EO	FLANGE
		EO	EXHAUST MANIF MOD
		EO	EXHAUST MANIF MOD
		T	8. FIRST IHI RUN. 36 HP. at S. L.
		EO	FIT & ASSEMBLY OF TURBOCHARGERS
5	1	C	LETTER FROM CUMMENS DIESEL. RE. FORTUNE 500 MTG & THEIR 2 STAGE SYSTEM
		EO	MOUNT BRACKET
		EO	TURBO SHEED PICKUP
	2	T	9. DEHUMMDIFUR CHECK
		T	10. 20,000 FEET-SEALEVEL RATED POWER
		C	SPHERCO TO GET SMALLER HOUSING FOR IHI TURBO
		P10	HOSE
		P11	GASKET MATERIAL
	3	T	11. 30,000 FEET ALTITUDE SEALEVEAL RATED POWER
MAY		P12	O RINGS
		P13	TURBOCHARGER
	4	C	MEMO FROM HEADQUARTERS - RESULTS OF HAAP MEETING ON APRIL 17TH (DISCOURAGING
		P14	OIL
		T	12. OIL HEATER CIRCUIT CHECKOUT
		T	13. COLD SOAK TEST
		T	14. ATTEMPT TO REPEAT #11- BLOWN GASKET
6	1	P15	BATTERYS (DIEHARDS)
		P16	PVC ADAPTERS
		P17	TURBINE HOUSING SWAP (UPS COST)
		P18	FITTINGS
	2	P19	GASKETS
		EO	TURBO ADAPTER FLANGE
		EO	WASTEGATE FLANGE
JUNE		EO	EXHAUST GASKET
	3	EO	INTERCOOLER ASSEMBLY
		EO	MAGNETIC WASHER ASSEMBLY
		EO	TURBO ADAPTER FITTING
		EO	TURBO FLANGE REINFORCEMENT
	4	EO	ADAPTER
		EO	OIL DIFUSER MOD.
		T	15. BIGGER HOUSING ON FIRST STAGE
		T	16. BIGGER HOUSING ON SECOND STAGE
		P20	BATTERY CONNECTORS

HIGH ALTITUDE AERODYNAMIC PLATFORM
CONCEPT EVALUATION AND PROTOTYPE ENGINE TESTING
EVENT CHRONOLOGY

YEAR 1981

M.	WK.	CODE	EVENT
7 JULY	1	T	17. CAVITATE OIL PUMP
		P21	HARDWARE CLOTH
	2	T	18. 40,000 FEET ALTITUDE SEALEVEL RATED POWER 4.6:1 COMP. RATIO IN TURBOS
		T	19. CRACKED EXH MANIF. OIL FOAMING
		T	20. TRY AGAIN-NEW CRACK IN EXHAUST MANIFOLD
	3		
	4	L	TO McCREADY - ASKING FOR LOOK AT VEHICLE
		LO	EXHAUST MANIF MOD.
8 AUGUST	1	C	HAROLD BENSEN'S NOTES ON HAAP CONTACTS
	2		
	3	T	21 WEST CYLINDER RICH (HOT 407°)
	4	T	22. WEST CYLINDER HOTTER (412°)
			23. WEST CYLINDER HOTTER (440°)
			24. WEST CYLINDER HOTTER (STOPPED)
			25. EXTRA FUEL PUMP
9 SEPTEMBER	1	LO	EXHAUST MANIFOLD
		T	26. TRY NEW EXHAUST MANIFOLD (LO FLO)
	2	T	27. INTAKE MANIF ELBO REINFORCEMENT
		T	28. EXCESS PRESSURE DROP IN AFTERCOOLER
		T	29. INSTRUMENTATION PROBLEMS
		T	30. 4.5 PSIA ALTITUDE - 19 PSIA IN MANIF.-GOOD-BUT NOT ENOUGH
	3	T	31, 32. RICH JETS-SLO SPARK LEAN JETS
		T	33. 40,000 FT. ALTITUDE-RATED SEALEVEL POWER IHI & RAYJAY
		P22	DURMAN BOLTS, HOSE
	4	T	34. 30,000 FEET-SMALL HOUSING ON BOTH TURBOS
		T	35. EXHAUST MANIF. BROKE
		T	36. EXHAUST MANIF. BROKE AGAIN

HIGH ALTITUDE AERODYNAMIC PLATFORM
CONCEPT EVALUATION AND PROTOTYPE ENGINE TESTING
EVENT CHRONOLOGY

YEAR 1981

M.	WK.	CODE	EVENT
10	1	C	P. R. FOR $15,000 to NSI
OCTOBER	2	M	REVIEW OF WORK TO DATE - PRESENTED REASONS FOR AND WAYS TO GET ADDITIONAL FLOW.
	3		
	4		
11	1		
NOVEMBER	2	P23	JOURNAL PINS
		P24	CYL STUDS
	3	C	STATUS REPORT OF 1000 CC ENGINE 50% COMPLETE
	4	P25	BOLTS
		P26	CAWSHAFT GRIND
		P27	OIL
		P28	MAGNETS
12	1	EO	PUSH ROD COVER MOD.
		EO	TURBO. INSTL.
		EO	EXHAUST ADAPTER
		EO	COWL MOD.
	2	EO	EXHAUST CONNECTOR
		EO	EXHAUST ADAPTER
DECEMBER		C	LANGLEY EVALUATION OF NOV. PROPOSAL ON HAAP TM #83184
	3	P29	TURBOCHARGER
	4		

HIGH ALTITUDE AERODYNAMIC PLATFORM
CONCEPT EVALUATION AND PROTOTYPE ENGINE TESTING
EVENT CHRONOLOGY

YEAR 1982

M.	WK.	CODE	EVENT
JANUARY 1	1	P30	BOLTS (4)
	2	P31	HEADER BOLTS & GASKET MAT.
	3		
	4	P32 P33	3/8" HOSE 3/8 COPPER ELBOS
FEBRUARY 2	1	15 EO'S	GROUP OF 15 EO'S SETTING UP NEW 1000 CC ENGINE 3 TURBOS
	2	P34 P35	INSULATION & FLEX HOSE CLAMPS
	3	EO EO	CATCH TANK FOR VAC. REF. LINES VAC. REF. MANIFOLD
	4	EO EO	HOSE ASSEMBLYS HOSE ASSEMBLYS
MARCH 3	1	P36 P37 T P38 P39	CLAMPS AVIATION GASOLINE 37 ROD BEARING FAILURE - 1000 CC CRANK PISTON PINS BUSHINGS
	2		
	3		
	4		

HIGH ALTITUDE AERODYNAMIC PLATFORM
CONCEPT EVALUATION AND PROTOTYPE ENGINE TESTING
EVENT CHRONOLOGY

YEAR 1982

M.	WK.	CODE	EVENT
4	1		
APRIL	2	T	38. CRANK FAILURE - 1000 CC CONFIG.
	3		
	4		
5	1	P40	CALIB CHAMBER
		P41	GASKETS, SEALS, O RINGS
		P42	OIL FILTER
MAY	2		
	3		
	4		
6	1		
JUNE	2	EO	NEW ACCUMULATOR
		EO	NEW ACCUMULATOR
	3	EO	COIL MOUNT
		P43	VALUE SPRINGS
		EO	PRESS PORT FILLING
		EO	ADAPTER UNION
		T	39. STOCK CRANK - MODIFIED CAMSHAFT (82) MIN. OVERLAP (LO FLO), (HI OIL US
	4	T	40, 41. STOCK INTAKE MANIFOLD (RATED POWER OK) ACOUSTIC PROBLEM?
		EO	EXHAUST MANIF
		P44	AIR MOTOR

HIGH ALTITUDE AERODYNAMIC PLATFORM
CONCEPT EVALUATION AND PROTOTYPE ENGINE TESTING
EVENT CHRONOLOGY

YEAR 1982

M.	WK.	CODE	EVENT
7 JULY	1	T	42. TURBO OIL, SEPARATE (NO OIL LOSS)
		T	43. 44. LOW BOOST
		EO	OIL INDUCTION TUBE MOD.
		EO	MOD. ACCUMULATION (2EA)
	2	T	45. STOCK CAM, BIG IHI .86 SCHWERTZER, 1.4 RAYJAY (LO FLO)
		T	46. LOW OIL
		T	47. TOOK OFF RAYJAY (STILL LO FLO)
		T	48. BROKE VALVE
		P45	CAMSHAFT REGRIND (MOD 3) SHORT EXHAUST DURATION, LONG INTAKE DURATION, LO OVERLAP
	3	EO	EXHAUST POST SURFACE
	4	P46	TURBINE SHAFT & HOUSING
		P47	VALVES (SATELLITE & GASKETS)
		P48	SOCKET HEAD SCREWS
		P49	SPARK PLUGS
8 AUGUST	1	P50	SPARK PLUGS
	2		
	3	EO	ACCUMULATOR MOD.
		EO	PISTON CAP. MACHINE
	4		
9 SEPTEMBER	1		
	2		
	3	EO	ACCUMULATOR MOD.
		EO	OIL MANIF
		EO	OIL CIRCUIT FITTINGS
	4	P51	REWELD & GRIND CAM
		P52	HOSE & FREEZE PLUGS
		P53	HEATER HOSE

HIGH ALTITUDE AERODYNAMIC PLATFORM
CONCEPT EVALUATION AND PROTOTYPE ENGINE TESTING
EVENT CHRONOLOGY

YEAR 1982

M.	WK.	CODE	EVENT
10 OCTOBER	1	EO C	OIL CIRCUIT FITTINGS LETTER TO BORG WARNER ASKING FOR BEST IHI COMBINATION
	2		
	3	P54 P55	FUEL HOSE FUEL HOSE & CLAMPS
	4	T T T T T	49. DATA SYS PROBLEM - CHANGED SPARK PLUG WIRE 50. LO BOOST (COOLING CIRCUIT ADDED) 51. LO BOOST N VOL 62% 5500 RPM 52. RETARD SPARK, LO EXHAUST GAS TAMP (LO FLO) 53. FOUND CAM "CHIPPED" & TAPPET BROKEN
11 NOVEMBER	1		
	2		
	3	P56	MOTOR OIL
	4		
12 DECEMBER	1		
	2		
	3		
	4		

HIGH ALTITUDE AERODYNAMIC PLATFORM
CONCEPT EVALUATION AND PROTOTYPE ENGINE TESTING
EVENT CHRONOLOGY

YEAR 1983

M.	WK.	CODE	EVENT
1	1	C	TEST PROCEDURE COMPLETE (FINAL VERSION)
JANUARY		T	54. PRESS SWITCH S/O CHECKOUT (15 PSIA)
	2	T	55. 56. SPECIFIC FUEL CONSUMPTION HI - CYCLIC OPERATION, LOW BOOST
		T	57. 58. SPECIFIC FUEL CONSUMPTION HI - WASTE GATE OPEN-CYCLIC OPERATION
	3	EO	DISC. TO CASTING (WELD AIR TRANSFER TUBES)
		EO	THROTTLE SHAFT
		EO	FAB ACCUMULATOR
		T	59, 60, 61. 2 CARBS DOWNSTREAM OF Hx4, UPSTREAM OF ACCUM. - HI FREQ. CYCLING, (LO FLO)
	4	T	62. CARBS ON CYLS. NO CYCLING - LO FLO - LO BOOST.
2	1		
FEBRUARY	2		
	3		
	4		
3	1		
MARCH	2		
	3	C	ACTIVITY REPORT- "END" OF TESTING AT TTA
		P57	CLAMPS (ACTUALLY PURCHASED IN JAN., BILL PAID HERE.)
	4		